การพัฒนาพื้นผิวไทเทเนียมเพื่อสนับสนุนการยึดเกาะและการแปรสภาพของเซลล์สร้างกระดูก

นางสาวธิดารัตน์ อังวราวงศ์

วิทยานิพนธ์นี้เป็นส่วนหนึ่งของการศึกษาตามหลักสูตรปริญญาวิทยาศาสตรดุษฎีบัณฑิต
สาขาวิชาชีววิทยาช่องปาก
คณะทันตแพทยศาสตร์ จุฬาลงกรณ์มหาวิทยาลัย
ปีการศึกษา 2554

MODIFICATION OF TITANIUM SURFACE FOR SUPPORTING OSTEOBLAST ADHESION AND DIFFERENTIATION

Miss Thidarat Angwarawong

A Dissertation Submitted in Partial Fulfillment of the Requirements

for the Degree of Doctor of Philosophy Program in Oral Biology

Faculty of Dentistry

Chulalongkorn University

Academic year 2011

Thesis Title	MODIFICATION OF TITANIUM SURFACE FOR SUPPORTING OSTEOBLAST ADHESION AND DIFFERENTIATION
By	Miss Thidarat Angwarawong
Field of Study	Oral Biology
Thesis Advisor	Professor Prasit Pavasant, D.D.S., Ph.D.
Thesis Co-advisor	Associate Professor Mansuang Arksornnukit, D.D.S., M.S., Ph.D.

Accepted by the Faculty of Dentistry, Chulalongkorn University in Partial Fulfillment of the Requirements for the Doctoral Degree

…….. Dean of the Faculty of Dentistry
(Associate Professor Wacharaporn Tasachan, D.D.S.)

THESIS COMMITTEE

…….. Chairman
(Associate Professor Neeracha Sanchavanakit, D.D.S., Ph.D.)

…….……. Thesis Advisor
(Professor Prasit Pavasant, D.D.S., Ph.D.)

…….. Thesis Co-advisor
(Associate Professor Mansuang Arksornnukit, D.D.S., M.S., Ph.D.)

…….. Examiner
(Assistant Professor Damrong Damrongsri, D.D.S., Ph.D.)

…….. Examiner
(Thanaphum Osathanon, D.D.S., Ph.D.)

…….. External Examiner
(Professor Hidekazu Takahashi, D.D.S., Ph.D.)

ธิดารัตน์ อังวราวงศ์ : การพัฒนาพื้นผิวไทเทเนียมเพื่อสนับสนุนการยึดเกาะและการแปรสภาพของเซลล์สร้างกระดูก. (MODIFICATION OF TITANIUM SURFACE FOR SUPPORTING OSTEOBLAST ADHESION AND DIFFERENTIATION) อ. ที่ปรึกษาวิทยานิพนธ์หลัก : ศ. ทพ. ดร. ประสิทธิ์ ภวสันต์, อ. ที่ปรึกษาวิทยานิพนธ์ร่วม : รศ. ทพ. ดร. แมนสรวง อักษรนุกิจ, 95 หน้า.

ฟิล์มบางหลายชั้นของพอลิอิเล็กโทรไลต์ หรือพีอีเอ็มฟิล์ม {polyelectrolyte multilayer (PEM) film)} ซึ่งเตรียมขึ้นด้วยเทคนิคเลเยอร์บายเลเยอร์สามารถนำมาใช้ปรับปรุงคุณสมบัติพื้นผิวของวัสดุเพื่อส่งเสริมการตอบสนองของเซลล์กับวัสดุ การศึกษาในครั้งนี้ใช้โพลิไดอัลลิวไดแมททิวแอมโมเนียมคลอไรด์ (พีดีเอดีเอ็มเอซี) โพลิโซเดียม-4-สไตรีนซัลโพเนท (พีเอสเอส) และโพลิ-4-สไตรีนซัลโพนิกแอซิดโคมาเลอิคแอซิดโซเดียมซอลล์ (พีเอสเอสโคเอ็มเอ) เพื่อทำให้เกิดพีอีเอ็มฟิล์ม {$(PDADMAC/PSS)_4$/PDADMAC+PSS-co-MA PEM film} บนกระจก ไทเทเนียม และแผ่นโพลิคาร์โพรแลคโตน (พีซีเอล) พบว่ากระจกและไทเทเนียมที่เคลือบด้วยพีเอสเอสโคเอ็มเอพีอีเอ็มฟิล์ม (PSS-co-MA PEM films) มีคุณสมบัติความชอบน้ำมากกว่าพื้นผิวปกติของกระจกและไทเทเนียม จากนั้นทำการทดสอบผลของพีเอสเอสโคเอ็มเอพีอีเอ็มฟิล์มต่อเซลล์สร้างกระดูกของหนู (เอ็มซีสามทีสาม-อีหนึ่ง) และเซลล์สร้างกระดูกที่ได้มาจากมนุษย์ พบว่ากระจกและไทเทเนียมที่เคลือบด้วยพีเอสเอสโคเอ็มเอพีอีเอ็มฟิล์มส่งเสริมการแปรสภาพของเซลล์สร้างกระดูก ในรูปแบบของการเพิ่มขึ้นของการทำงานของเอนไซม์อัลคาไลน์ฟอสฟาเทส การแสดงออกอาร์เอ็นเอนำรหัสที่เกี่ยวข้องกับการสร้างกระดูก ได้แก่ คอลลาเจนชนิดที่หนึ่ง ออสตีโอพอนทิน โบนไซอะโลโปรตีน ออสตีโอแคลซินเดนทีนเมทริกซ์โปรตีนชนิดที่หนึ่ง และเพิ่มการสร้างโปรตีนออสตีโอแคลซิน รวมถึงเร่งอัตราการตกตะกอนแคลเซียมเมื่อเปรียบเทียบกับพื้นผิวปกติของกระจกและไทเทเนียม สำหรับการศึกษาการสร้างกระดูกในสัตว์ทดลอง ทำการฝังพีเอสเอสโคเอ็มเอพีอีเอ็มฟิล์มที่เคลือบบนแผ่นพีซีเอลในความวิการของกระดูกที่ทำขึ้นในกะโหลกศีรษะของหนู พบว่ามีการเพิ่มขึ้นของปริมาณกระดูกที่สร้างใหม่รอบๆ พีเอสเอสโคเอ็มเอฟิล์มที่เคลือบบนแผ่นพีซีเอล เมื่อเปรียบเทียบกับแผ่นพีซีเอลที่ไม่ได้เคลือบ จากการศึกษาครั้งนี้แสดงให้เห็นว่าพีเอสเอสโคเอ็มเอพีอีเอ็มฟิล์มสนับสนุนการแปรสภาพของเซลล์สร้างกระดูก และสามารถนำมาใช้เพื่อส่งเสริมการพอกแร่ธาตุในงานวิศวกรรมเนื้อเยื่อกระดูก และปรับปรุงกระดูกเชื่อมประสานสำหรับรากเทียม

สาขาวิชา ชีววิทยาช่องปาก ลายมือชื่อนิสิต……..

ปีการศึกษา 2554 ลายมือชื่อ อ.ที่ปรึกษาวิทยานิพนธ์หลัก…….....

ลายมือชื่อ อ.ที่ปรึกษาวิทยานิพนธ์ร่วม ……...

5076452032 : MAJOR ORAL BIOLOGY

KEYWORDS : TITANIUM / POLY(4-STYRENESULFONIC ACID-CO-MALEIC ACID) SODIUM SALT / POLYELECTROLYTE MULTILAYER FILMS / OSTEOGENIC DIFFERENTIATION / MINERALIZATION

THIDARAT ANGWARAWONG : MODIFICATION OF TITANIUM SURFACE FOR SUPPORTING OSTEOBLAST ADHESION AND DIFFERENTIATION. ADVISOR : PROF. PRASIT PAVASANT, D.D.S., Ph.D., CO-ADVISOR : ASSOC. PROF. MANSUANG ARKSORNNUKIT, D.D.S., M.S., Ph.D., 95 pp.

Polyelectrolyte multilayer (PEM) film created via Layer-by-Layer deposition can be used to modify the surface properties of materials in order to improve cell-material interactions. In this study poly(diallyldimethylammonium chloride) (PDADMAC), poly(sodium 4-styrene sulfonate) (PSS) and poly(4-styrenesulfonic acid-co-maleic acid) sodium salt (PSS-co-MA) were assembled into PEM {$(PDADMAC/PSS)_4$/PDADMAC+PSS-co-MA} film on glasses, titanium (Ti) discs and polycaprolactone (PCL) films. PSS-co-MA PEM film coated substrates had better wettability property than uncoated substrates. The effects of PSS-co-MA PEM surface on murine pre-osteoblastic cells (MC3T3-E1) and human primary osteoblastic cells were examined. Results showed that PSS-co-MA PEM film coated substrates promoted osteoblast differentiation. In this regard, the increase of alkaline phosphatase activity, osteoblastic mRNA expressions (type I collagen, osteopontin, bone sialoprotein, osteocalcin and dentin matrix protein 1), osteocalcin protein secretion and calcium deposition rate were noted compared to uncoated substrates. To test bone induction ability *in vivo*, PSS-co-MA coated PCL films were implanted in murine calvarials defects. Result showed an increased amount of new bone formation around the PSS-co-MA coated PCL films compared to uncoated PCL. In conclusion, PSS-co-MA film enhanced osteoblast differentiation and could be used to promote mineralization in bone tissue engineering and to improve osseointegration for dental implants.

Field of Study : Oral Biology ..... Student's Signature .....

Academic Year : 2011 ..... Advisor's Signature .....

Co-advisor's Signature .....

ACKNOWLEDGEMENTS

First, I would like to express my deepest gratitude to my thesis advisor and co-advisor, Professor Dr. Prasit Pavasant and Associate Professor Dr. Mansuang Arksornnukit, who are my inspiration for working on research. They have given me valuable advice, guidance and kind assistance throughout the course. I have learnt a great deal from them and enjoyed working with both over my time at Faculty of Dentistry, Chulalongkron University. I also would like to extend my thanks to Dr. Stephan T. Dubas, who had been giving me scientific knowledge and technical supports.

I also would like to thank the thesis committee, Associate Profressor Dr. Neeracha Sanchavanakit, Assistant Professor Dr. Damrong Damrongsri, Dr. Thanaphum Osathanon and Professor Dr. Hidekazu Takahashi for their important comments, suggestions and kindness for my thesis.

I would not have been able to complete this thesis without helps and supports from the Research unit of Mineralized Tissue at Faculty of Dentistry, Chulalongkorn University and everyone in this Research unit. The research in this thesis would also have not been possible without funding from Chulalongkorn University Centenary Academic Development Project and Chulalongkorn University Dutsadi Phiphat Scholarship.

Finally and most importantly, this thesis would not have been possible without the love and support of my family. They have always been there for me and believed in me. I would especially like to thank my sister, Onauma Angvarawong, and my brother, Sorasak Angwarawong, for their love, spirit and encouragement in everything.

CONTENTS

Page

Page

LIST OF TABLES

LIST OF ILLUSTRATION

Page

LIST OF ABBREVIATIONS

ALB	Albumin
ALG	Alginate
ALP	Alkaline phosphatase
TGF-β1	Transforming growth factor β1
β-glycerophosphate	Glycerol-2-phosphate disodium salt hydrate
BSP	Bone sialoproteins
CaP	Calcium phosphate
CHI	Chitosan
ChS	Chondroitin 6-sulfate
Col I	Type I collagen
Col IV	Type IV collagen
cpTi	Commercially pure titanium
DMEM	Dulbecco's modified Eagle's medium
DMP1	Dentin matrix protein 1
DMSO	Dimethyl sulfoxide
ECM	Extracellular matrix
EDTA	Ethylenediaminetetraacetic acid
ELISA	Enzyme-linked immunosorbent assay
EMD	Enamel matrix derivative
ePTFE	Expanded poly(tetrafluoroethylene)
ERK1/2	Extracellular signal-regulated kinases
FN	Fibronectin
GAPDH	Glyceraldehyde-3-phosphate dehydrogenase
GEL	Gelatin
HA	Hyaluronan/hyaluronic acid
HCS-2/8 cells	Human chondrosarcoma-derived chondrocyte-like cell line
HEP	Heparin

HMDS	Hexamethyldisilazane
ICC	Inverted colloidal crystal
LbL	Layer-by-Layer
MA	Maleic acid
MTT	3-(4,5-Dimethylthiazol-2-yl)-2,5-dipheyl tetrazolium bromide
NG108-15 Hybrid Cells	Neuroblastoma x glioma hybrid culture cells
OC	Osteocalcin
OPG	Osteoprotegerin
OPN	Osteopontin
PA	Polyacrylamide
PAA	polyacrylic acid
PAH	Poly(allylamine hydrochloride)
PBS	Phosphate buffered saline
PCL	Poly-caprolactone
PDA	P-diazonium diphenyl amine polymer
PDADMAC	Poly(diallyldimethylammonium chloride)
PDL	Poly-D-lysine
PDL-LA	Poly(DL-lactide)
PDM	Poly(dimethacrylate)
PDMS	Poly(dimethylsiloxane)
PEI	Polyethyleneimine
PEM	Polyelectrolyte multilayer
PET	Poly(ethylene terephthalate)
PGA	Poly(L-glutamic acid)
PLL	Poly(L-lysine)
PMMA	Poly(methylmethacrylate)
PSS	Poly(sodium 4-styrene sulfonate)
PSS-co-MA	Poly(4-styrenesulfonic acid-co-maleic acid) sodium salt
qRT-PCR	Quantitative reverse-transcription polymerase chain reaction

RGD	Arginine-glycine-aspartic acid
SWNT	Single-walled carbon nanotubes
TCP	Tissue culture plate
Ti	Titanium
VEGF	Vascular endothelial growth factor
VPS	Vinylpolysiloxane
α-MSH	α-melanocyte-stimulation hormone

CHAPTER I

INTRODUCTION

Biomaterial used in the production of endosseous devices for dental, orthopedic, and maxillo-facial applications can be modified to improve the control and rapid wound healing or bone regeneration[1]. One of the factors playing an important role in determining cell responses at the cell-materials interface is the surface characteristics of biomaterials, such as microstructure, surface roughness, contact angle (wettability), surface energy, surface charge, topography, or surface chemistry[1-4]. Therefore, the modification of biomaterial surfaces may improve cellular functions and activities including cell adhesion, proliferation, and differentiation of osteoblasts[5].

Currently, a variety of strategies has been proposed to modify the surface of titanium (Ti)-based implants in order to enhance bone growth and initial implant stability. These strategies include immobilization of bioactive protein or peptides (such as fibronectin (FN)[6] and arginine-glycine-aspartic acid (RGD) peptides[7]), chemical treatment[8, 9], thermal treatment[10], coating with hydroxyapatite, electrochemical method (also known as anodization or anodic oxidation[11]), plasma surface treatment, micro-arc oxidation (MAO)[12], sol-gel process[13] and polyelectrolyte multilayer (PEM) film.

Polyelectrolyte multilayer film self assembly is a simple technique easily performed by simply dipping materials in polyelectrolyte solutions[14]. Sequential deposition of polyanions and polycations in a 'Layer-by-Layer' (LbL) fashion at the surface of materials results in a thin film on the material surface. The electrostatic attraction between oppositely charged polyelectrolytes is the main driving force for the multilayer build up[14]. Recently, PEM thin films have been proposed as a versatile, inexpensive, yet efficient technique to build biologically active surfaces for multiple purposes[15]. PEM films are currently being used to modify the surface properties of materials for clinical applications. For example, synthetic polyelectrolytes such as polyethyleneimine (PEI), poly(sodium 4-styrene sulfonate) (PSS), poly(allylamine hydrochloride) (PAH), poly(L-glutamic acid) (PGA) and poly(L-lysine) (PLL) were used in combination to create the $\{PEI\text{-}(PSS\text{-}PAH)_2\text{-}(PGA\text{-}PLL)_n\}$ PEM coating on the surface of oral

prostheses in order to increase wettability of the prosthesis bases[16]. The combination of polyelectrolytes such as PLL, PGA and functionalized-PGA was used with a synthetic analogue of natural peptide, α-melanocyte-stimulation hormone (α-MSH), to fabricate a PLL/$(PGA/PLL)_4$/PGA-αMSH PEM film with anti-inflammatory properties on the surface of tracheal prostheses[17]. In addition, fabricating PEM films, PEI-$(PSS\text{-}PAH)_2$-(PGA-PLL)-$(PGA\text{-defensin-PLL})_n$, have been introduced on implantable biomaterials in order to obtain anti-microbial property[18].

In term of endosseous implant materials, combinations of natural and synthetic polyelectrolytes have been generated on the Ti surface via the LbL technique to stimulate osteoblast behavior. These combined polyelectrolytes included the use of chitosan (CHI) with PEI/PSS {$PEI/(PSS/CHI)_5$}[19], gelatin (GEL)-PEI {$PEI/GEL/(CHI/GEL)_3$}[20], and heparin(HEP)-PAH {PAH/HEP}[21].

Poly(diallyldimethylammonium chloride) (PDADMAC) is a strong cationic polyelectrolyte, containing numerous positive charges along its backbone chain. In contrast, PSS, a strong anionic polyelectrolyte, possesses a number of negative charges along its backbone chain. Due to their strong ionic charges, both PDADMAC and PSS have been used as the polyelectrolytes for PEM preparation[22-25]. Since the hydrophobic ring structure of PDADMAC polycations is stiff and difficult to rotate both in water and air, the outer layer containing the quaternary ammonium end groups stays hydrophilic both in water and air. Thus, the hydrophilic property of the polycations helps the addition of the next PSS layer[26]. Another advantage of using strong polyelectrolytes is that their ionic charges are largely independent of the pH condition[27]. These characteristics support the advantage of using PDADMAC and PSS for PEM fabrication.

Poly(4-styrenesulfonic acid-co-maleic acid) sodium salt (PSS-co-MA) was selected for coating the final layer of PEM. PSS-co-MA is a copolymer of PSS and maleic acid. This copolymer contains both the strong sulfonate group in PSS and the weak carboxylic pendent group from maleic acid segments. The strongly charged group can generate electrostatic linkages thereby enhancing the film stability. Meanwhile, the weakly charged groups of maleic acid provide flexibility to the multilayer properties due to their ability to response to external pH

changes. For example, at high pH, the carboxylic acid group in maleic acid could be converted into a carboxylate group and become ionized, with the PSS-co-MA becoming a anionic polyelectrolyte[28]. Due to this property, PSS-co-MA has been used as a cation-exchange membrane. The maleic acid has two ion-exchangable sites and exhibits lower water uptake than sulfonic acid[29]. However, it was never been applied in order to influence osteoblast behavior.

In this study, the experiments were separated into three parts. The first part was to fabricate and characterize surface modified films using $(PDADMAC/PSS)_4$/PDADMAC+PSS-co-MA coated glass cover slips as well as to examine the function and behavior of osteoblasts grown on PSS-co-MA coated surface. The second part was to produce and analyze the $(PDADMAC/PSS)_4$/PDADMAC+PSS-co-MA coated Ti discs as well as to examine the function and behavior of osteoblasts grown on PSS-co-MA coated Ti surface. Finally, PSS-co-MA coated poly-caprolactone (PCL) films were used for evaluation of *in vivo* bone formation in murine calvarial defects.

RESEARCH QUESTIONS

1. Whether $(PDADMAC/PSS)_4$/PDADMAC+PSS-co-MA via PEM films support osteoblasts functions including cell adhesion, proliferation, differentiation and calcium deposition *in vitro*.

2. Whether $(PDADMAC/PSS)_4$/PDADMAC+PSS-co-MA PEM coated surfaces support new bone formation *in vivo*.

RESEARCH OBJECTIVES

1. To fabricate and characterize surface modified films using $(PDADMAC/PSS)_4$/PDADMAC+PSS-co-MA coated glass cover slips.

2. To examine the function and behavior of MC3T3-E1, osteoblast cell line, grown on PSS-co-MA coated glass cover slips.

3. To fabricate and characterize surface modified films using $(PDADMAC/PSS)_4$/PDADMAC+PSS-co-MA coated cpTi discs.

4. To examine the function and behavior of human primary bone cells grown on PSS-co-MA coated cpTi disc.

5. To examine *in vivo* bone formation in murine calvarial defects model.

RESEARCH HYPOTHESES

1. PSS-co-MA coating surface can enhance osteoblasts function *in vitro*.

2. PSS-co-MA coating surface can enhance bone formation *in vivo*.

EXPECTED BENEFITS

We anticipate that the result from this investigation would provide novel information regarding the Ti surface modification. PEM coated Ti may give a promising result as an alternative choice for metallic implants used in plastic and reconstructive surgery, orthopedic surgery, craniofacial surgery, and oral implantology. We hope that the use of this surface modification of Ti-based implant could accelerate osseointegration for endosseous implants and this outcome would allow faster recuperation for the patient, permit early or immediate loading of the device, decrease patient morbidity, improve patient psychology, and decrease health care costs.

CHAPTER II

REVIEW OF RELATED LITERATURE

Titanium and titanium alloys as implant materials

The research field of bone tissue engineering applies the principles of biology and engineering to develop functional substitutes for damaged bone tissue[30]. To restore, maintain and improve bone tissue function, three key elements are required: (1) a scaffold or carrier material combined with (2) cells and/or (3) bone stimulating molecules (e.g. growth factors). The scaffold provides mechanical support and serves as a substrate upon which cells attach, proliferate and undergo differentiation. In this respect, metallic implants used in plastic and reconstructive surgery, orthopedic surgery, craniofacial surgery, and oral implantology can be regarded as scaffolds for load-bearing, bone-replacing/contacting applications such as joint and tooth replacement, fracture healing, and reconstruction of congenital skeletal abnormalities [31]. For these implants, the ultimate goal is to obtain a life-long secure anchoring of the implant in the native surrounding bone. Commercially pure titanium (cpTi; > 99.9 % purity as defined by the American Society of Testing and Materials (ASTM)) and alloyed with other element (Ti6Al4V, Ti6Al7Nb), are the most commonly used metallic implant materials. Normally, cpTi has become the material of choice for dental implants[32]}, while orthopedic implants require the use of Ti alloys for higher load involved. Because of Ti and Ti alloys have superior bulk and surface properties compared to other metal biomedical implants. These properties are excellent mechanical properties, such as high strength and fatigue-resistance, with low modulus and extreme light weight[33, 34], with highly biocompatible materials and corrosion resistance. The biocompatibility and corrosion resistance of Ti or its alloys are based partly on its thin (2-8 nm) and chemically inert dense oxide layer spontaneously formed on Ti surface within milliseconds in air or physiological fluids[34-36]. This reaction prevents the formation of fibrous tissue around the implant, and created direct contact to osseous tissues. However, relatively poor surface hardness, wear resistance and metal release may cause some problems for clinical application[37].

The bone–implant interface

Bone[31]

Bone tissue is a living organ, which can be described as a natural composite tissue composed of an organic matrix strengthened by an inorganic calcium phosphate (CaP) phase. The extracellular matrix (ECM) of bone consists of 90% collagenous proteins {type I collagen (Col I) 97% and type V collagen (Col IV) 3%} and 10% non-collagenous proteins {osteocalcin (OC) 20%, osteonectin 20%, bone sialoproteins (BSP) 12%, proteoglycans 10%, osteopontin (OPN), FN, growth factors, etc.}. Regarding the inorganic component, the most abundant mineral phase in human bone is carbonate rich hydroxyapatite (with a carbonate content between 4% and 8%). The apatite in bone mineral is composed of small platelet-like crystals of just 2–4 nm in thickness, 25 nm in width, and 50 nm in length. This calcified matrix embeds bone cells, which participate in the maintenance and organization of bone. Bone is subject to constant remodeling by osteoblasts and osteoclasts. Osteoblasts are responsible for the synthesis, deposition, and mineralization of ECM. They are located at bone surfaces and form a continuous layer. Upon embedding in this matrix, osteoblasts finally transform into quiescent osteocytes. Osteoclasts are large multinuclear cells that are involved in bone resorption. A main feature of this bone cell type is its ruffled border, which acts as a high surface area interface for excretion of proteins and hydrochloric acid. The acid decreases the local pH and dissolves bone mineral. This dynamic process of bone formation and destruction accounts for its remodeling, thereby enabling bone regeneration.

Tissue responses to the implant materials following implant placement[31, 38]

A sequence of complex and strongly interrelated events takes place at the implant surface after implantation of the materials (Figure 2.1). Within a few nanoseconds following implantation, the tissue responds to the implant material surface by allowing water molecules to make contact with the implant surface and form a water mono- or bilayer surrounding the implant. Hydrated ions, such as Cl^-, Na^+, and Ca^{2+}, are subsequently incorporated into the surface water. The implant surface properties at atomic scale have a major influence on the extent and specific interaction pattern of the material surface with this hydration layer or the

arrangement of the water molecules, which in turn facilitate proteins and other molecules in the biological microenvironment to adsorb on material surface. In the second stage, from seconds to hours after implantation, blood proteins or tissue specific proteins (ECM protein) adsorb and desorb to and from the surface. This conformation, orientation and composition of adsorbed protein layer are also likely to be affected by the implant material surface features, such as its physicochemical, biochemical and topographic characteristics. The third stage involves the interaction of cells with the surface of the implant via the adsorbed protein layer. The cell-protein bound surface interface, occurring from as short as minutes after and up to days following implant placement, initiates cellular adhesion, migration and differentiation, which occurs from a few hours to several days after implantation. This surface specific adsorbed biofilm subsequently determines cell adhesion, since proteins act as contact for the attachment of cells. This adsorption stage is tightly regulated by numerous biological factors, including ECM proteins, cell surface-bound (or integrin) and cytoskeletal proteins (Figure 2.2), by chemical characteristics and topographies at the implant surface and by the released ions/products from the material. Inorganic, physicochemical stimuli, such as release of Ca^{2+} and PO^{3-}_{4} ions from calcium phosphates, can positively affect the cellular response. Additionally, implants biochemically modified with biomolecules immobilized on the surface, such as growth factors or cell adhesion motifs, induce certain cell responses in the physiological surrounding by specific cell signaling pathways. Next to that, implant surfaces that have protrusions, cavities, gullies, etc., on a micro- and/or nanoscale will induce biological interactions different from those with a flat surface. As a result, both the exact mixture of adsorbed proteins and their conformational state(s) are largely controlled by the implant surface. The final stage of the body responses to the implant, which can last up to several decades, is the continuing development of the earlier stages, eventually resulting in the formation of functionally active mineralized bone tissue surrounding the implant. However, adverse responses, such as pathological inflammation, fibrous capsule formation and implant failure, can also occur during this stage. The future development of modern implant biomaterials is therefore aimed to minimize such effects as well as to promote rapid wound healing and implant-to-bone integration for the long-term success of an implanted device in the body, which is significantly dependent on the tissue biocompatibility at the site of implantation as well as the physicochemical properties of the material.

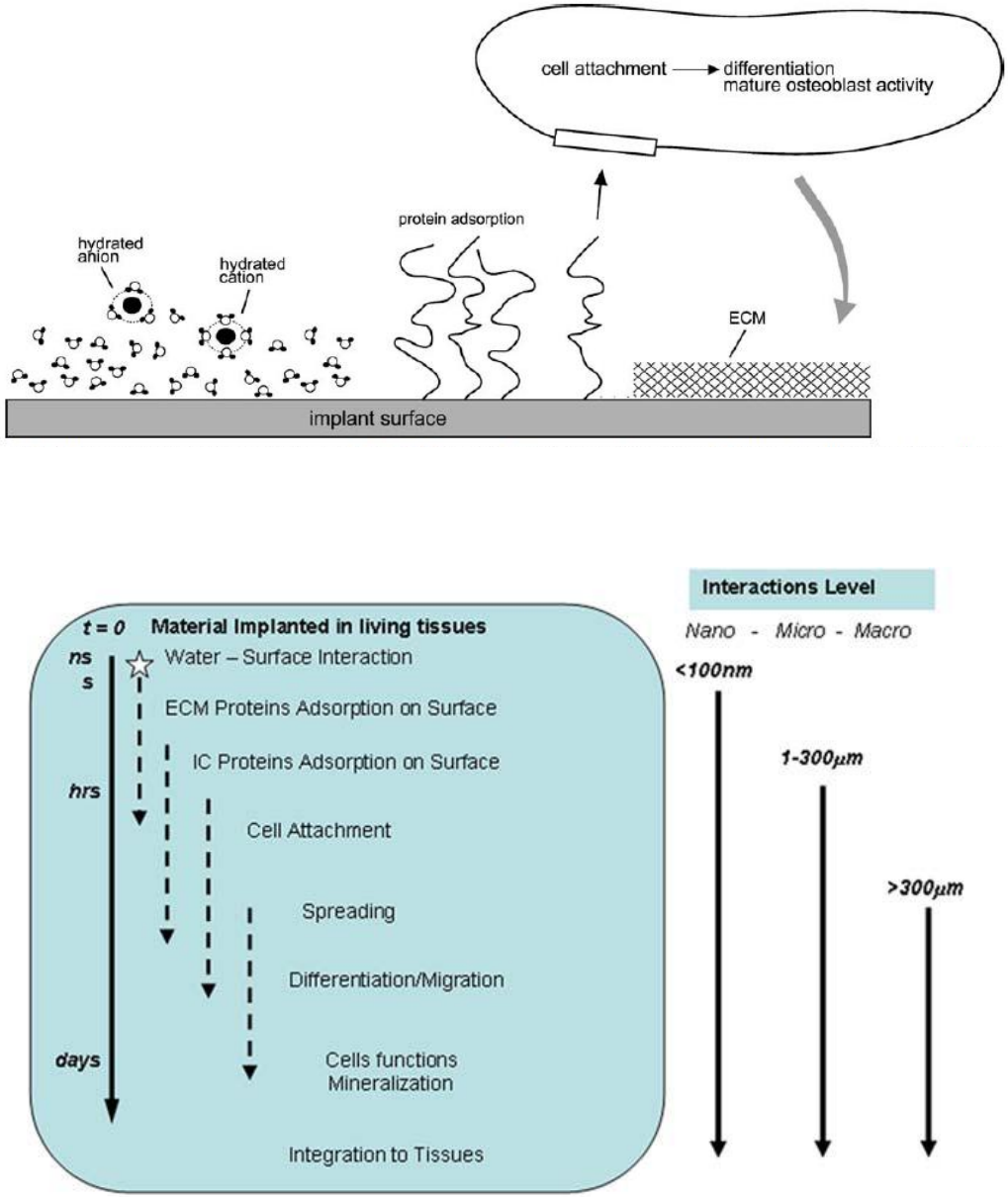

Figure 2.1 Schematic representation of events consecutively taking place at biomaterial surface after implantation into living bone tissue. Water binds to the surface, followed by incorporation of hydrated ions, adsorption and desorption of protein, eventually leading to cell attachment. After differentiation, mature osteoblasts produce the ECM and calcification.

Ref: de Jonge, L.T., *et al*. Organic–Inorganic Surface Modifications for Ti Implant Surfaces. Pharmaceutical Research 2008;25:2357-2369.[31]; Roach, P., *et al.* Modern biomaterials: a review—bulk properties and implications of surface modifications. J Mater Sci: Mater Med 2007;18:1263–1277.[39]

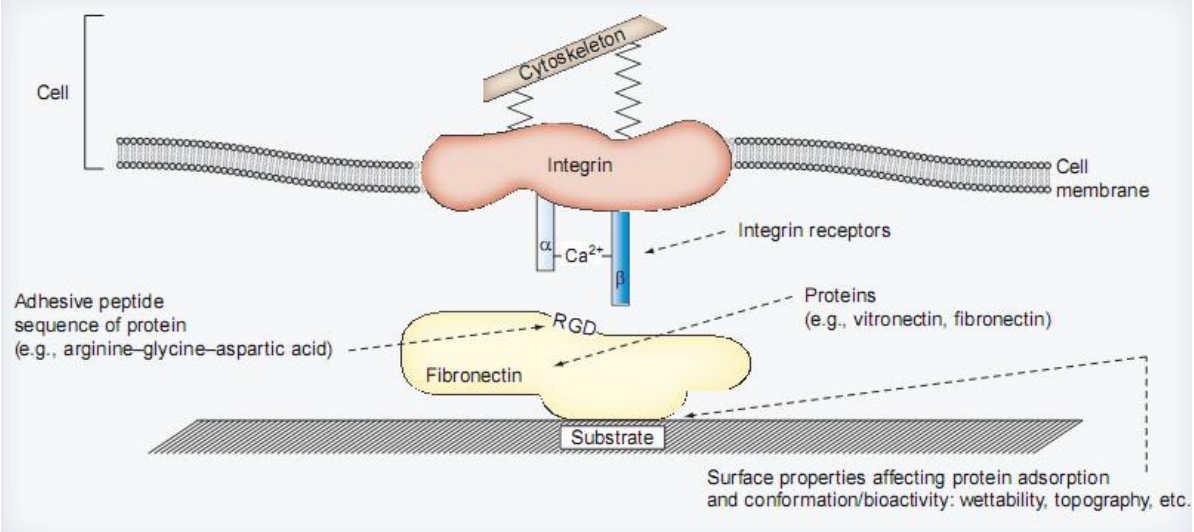

Figure 2.2 Initial protein interactions leading to cell recognition of implants.

Ref. Sato, M. and Webster, T.J. Nanobiotechnology: implications for the future of nanotechnology in orthopedic applications. Expert Rev Med Devices. 2004;1:105-14.[4]

Osseointegration

Osseointegration was first described by Brånemark *et al.* 1977 [40]. The term was first defined in a paper by Albrektsson *et al.* 1981 as direct contact (at the light microscope level) between living bone and implant[41]. Osseointegration is also histologically defined in Dorland's Illustrated Medical Dictionary as the direct anchorage of an implant by the formation of bony tissue around the implant without the growth of fibrous tissue at the bone–implant interface. Another more biomechanically oriented definition of osseointegration has been suggested: "A process whereby clinically asymptomatic rigid fixation of alloplastic materials is achieved, and maintained, in bone during functional loading"[42].

Around endosseous implants, osteogenic cells may lay down bone on the old bone surface or on the implant surface itself. This distinction was explored by Osborn and Newesley, who described the two phenomena, distance and contact osteogenesis, by which bone can become juxtaposed to an implant surface (Figure 2.3)[43].

I**n distance osteogenesis**, new bone is formed on the surfaces of old bone in the peri-implant site. The bone surfaces provide a population of osteogenic cells that lay down a new matrix that encroaches on the implant. Distance osteogenesis can be expected in cortical bone healing since vascular disruption of the cortex caused during implant site preparation is known to lead to death of the peri-implant cortical bone and its subsequent slow remodeling by osteoclast invasion from the underlying medullary compartment. In the latter, initiation of mineralization of the healing bone tissue did not occur on the implant surface, but bone grew towards the implant, subsequent to the death of the intervening tissue. In contrast, in the process of **contact osteogenesis**, new bone forms first on the implant surface and were called "*de novo* bone formation". It has been reported that the bone extending away from the implant forms at a rate about 30% faster than that moving toward the biomaterial[1].

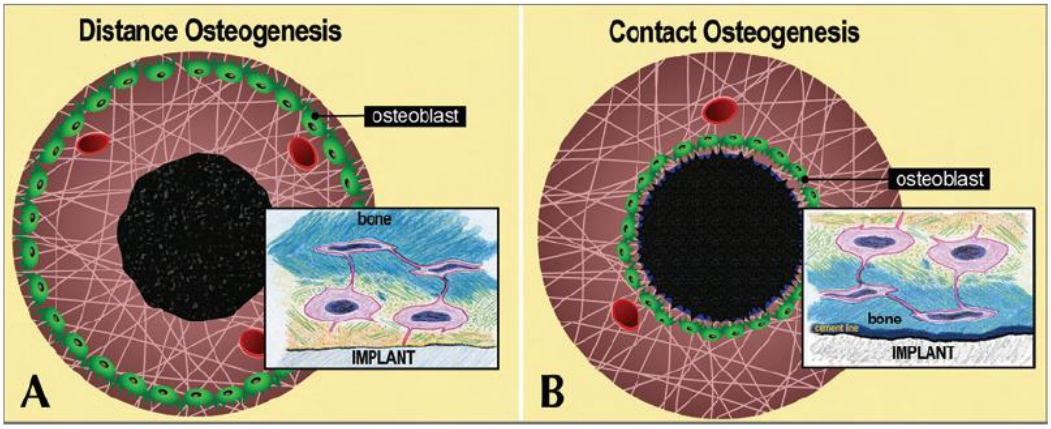

Figure 2.3 Drawings show the initiation of distance osteogenesis (A) and contact osteogenesis (B) where differentiating osteogenic cells line either the old bone or implant surface respectively. In the former the secretorily active osteoblasts, anchored into their ECM by their cell processes, become trapped between the bone they are forming and the surface of the implant. The only possible outcome is the death of these cells. On the contrary, in contact osteogenesis, *de novo* bone is formed directly on the implant surface.

Ref: Davies, J.E. Understanding peri-implant endosseous healing. J Dent Educ. 2003;67:932-49.[43]

Surface modification of titanium implants

Development of tissue-implant interface leading to osseointegration is complex and involves numerous factors including[1]

1. Surface properties of implant biomaterials such as material, shape, microstructure, surface roughness, contact angle or wettability, surface energy, surface charge, topography and surface chemistry or surface composition

2. Mechanical loading (magnitude & direction)

3. Surgical techniques

4. Patient variables such as bone quantity, bone quality and anatomical site

Nowadays, a large number of implant researches focus on the surface property of implants. This is because the initial cellular events at bone-implant interface are greatly affected by surface properties of implant materials. These initial interactions play a major role in healing process, bone cells behavior and later events such as adhesion, morphology change, functional alteration, proliferation, differentiation, ECM synthesis and its mineralization and differentiation[1-4].

An ultimate goal of current implantology research is to design bone implant materials that induce controlled, guided, and rapid healing which leads to the rapid integration of an implant into bone[1]. Osseointegration has been considered the most appropriate bone-implant interface[3]. These outcomes would allow not only faster recuperation for the patients, but also stable fixation between bone and implant that would permit early or immediate loading of the device. This latter point has great significance, in terms of decreased patient morbidity, improved patient psychology, and decreased health care costs[1].

For the improvement, the enhancement of cellular activities (cell adhesion, proliferation, and differentiation) of osteoblasts is needed. Surface modification is among one of the methods to improve osteoblast functions and activities.

To date, a variety of strategies have been implemented to modify the surface of Ti-based implants and enhance bone growth and their initial stability, including immobilization of bioactive protein or peptides (such as FN[6] and RGD peptides[7]), chemical treatment[8, 9], thermal treatment[10], hydroxyapatite coating, anodization or anodic oxidation[11], plasma surface treatment, micro-arc oxidation (MAO)[12], sol-gel process[15, 37, 44-46] and PEM film[1, 19-21].

Polyelectrolyte multilayer films (PEM)

Definition of polyelectrolytes

Polyelectrolytes are polymers that contain relatively high degree of ionizable groups along their backbone chains. Polyelectrolytes can be cationic, anionic or amphophilic (contain both cationic and anionic groups that are present in the same or different monomer units). Polyelectrolytes can be synthesized by polymerization of monomer units or by modification of the polymer to induce charges on the monomer repeating units. Polyelectrolytes can be found in nature i.e. proteins, polysaccharides and nucleic acids. The presence of ionic groups on the monomer repeat unit has a tremendous effect on the properties of polyelectrolytes. They generally exhibit higher water solubility, expanded hydrated dimensions and a higher sensitivity to ionic strength and pH than nonionic polymers[47].

Formation of polyelectrolyte multilayer films

Polyelectrolyte multilayer films were first introduced by Decher *et al.* over a decade ago[14]. The principle is based on an electrostatic LbL self- assembly process. PEM films were constructed by alternated adsorption of polyanions and polycations at the surface of materials[14]. Various depositing methods have already been proposed for LbL buildup, including dip coating, spin coating, and spraying. The most common to date is probably dip coating[48]. These polyelectrolyte based films are capable of self-assembly and self-organization. When a charged surface is exposed to a polyelectrolyte of the opposite charge, the polymer sticks to the surface physically leading to the formation of PEM. The driving forces behind

polyelectrolyte deposition using the LbL technique in order to form PEM have been already widely described and reviewed[49]. These include electrostatic interaction as well as non-electrostatic interactions, including short-range interactions such as hydrophobicity, hydrogen bonds, Van der Waals forces, charge transfer halogen interactions, and possibly covalent bonds formed by click chemistry. However, the electrostatic attraction is the main driving force for multilayer build up[14]. The binding is strong due to the several interaction points with the surface. Comparing to the classic chemical immobilization method, the LbL technique has the least demand for chemical bonds. The multilayers built by the LbL method offered a more stable coating than that prepared by physical adsorption because of the electrostatic attractions between layer to layer and layer to substrate. One important feature of this method is the adsorption at every step of polyanion/polycation assembly, which results in recharging of the outermost layer during the film fabrication process. The overcompensating adsorption, more than equal charge, allows for charge reversal on the surface, which has two important consequences: first, repulsion of equally charged molecules and thus self-regulation of the adsorption and restriction to a single layer; and second, the ability of an oppositely charged molecule to be adsorbed in a second step on top of the first one[14]. Films may be formed on virtually any biomaterial substrate and do not require intensive chemical processing.

In a typical process that is shown graphically in Figure 2.4, the process begins by properly charging a substrate. The charged substrate is dipped into the first oppositely charged polyelectrolyte solution for a certain period of time to allow the polyelectrolyte to adsorb to the surface. After being exposed to the oppositely charged polymer, the surface is then immersed in a rinse solution to wash off the loosely bound polymer as well as to prevent cross-contamination of the polyelectrolyte solutions. The substrate is then dipped into a polyelectrolyte solution of opposite charge. This second polyelectrolyte adsorbs to the surface due to electrostatic attraction and actually overcompensates for the surface charge resulting in a reversal of the surface charge. These simple steps complete the LbL deposition of the nanolayers. The substrate may be immersed and rinsed, in an alternating fashion, in the two polyelectrolyte solutions to form the multilayer layers. The process is repeated until the desired number of layers is deposited. Each step results in a reversal of surface charge allowing the next layer to be deposited.

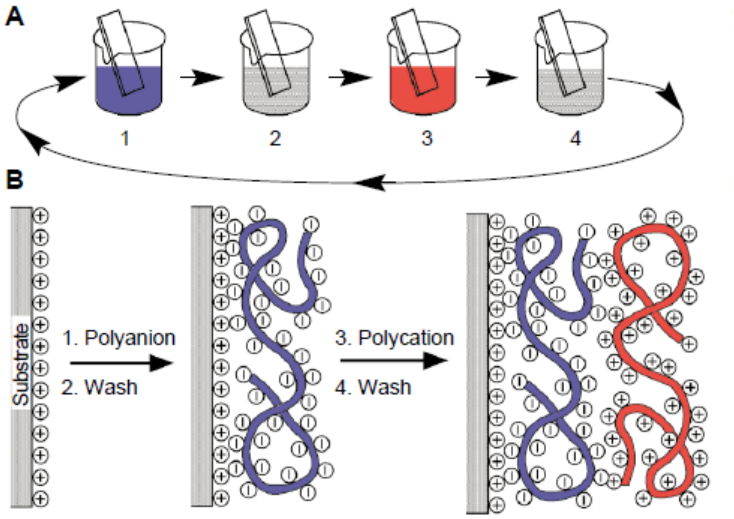

Figure 2.4 Assembly process for LbL PEM films formed by alternately dipping a substrate in a polycation and a polyanion solution.

(A) Schematic of the film deposition process using slides and beakers. Steps 1 and 3 represent the adsorption of a polyanion and polycation, respectively, and steps 2 and 4 are washing steps. The four steps are the basic buildup sequence for the simplest film architecture, (A/B)*n*. (B) Simplified molecular picture of the first two adsorption steps, depicting film deposition starting with a positively charged substrate. Counterions are omitted for clarity. The polyion conformation and layer interpenetration are an idealization of the surface charge reversalwith each adsorption step.

Ref: Decher, G. Fuzzy Nanoassemblies: Toward Layered Polymeric Multicomposites. Science 1997;277:1232 - 1237. [14]

In recent year, PEM thin films have emerged as a versatile, inexpensive yet efficient technique to “build” biologically active surfaces[15]. PEM has attracted an increasing number of researchers in recent years due to its wide range of advantages for biomedical applications: ease of preparation under ‘‘mild’’ conditions compatible with physiological media, capability of incorporating bioactive molecules, ECM components and biopolymers in the films, tunable mechanical properties, and spatio-temporal control over film organization[48].

PEM coating of biomaterials

For applications in the fields of implantable biomaterials and tissue engineering, films are used as surface coatings with the aim of providing an additional functionality for the original materials or engineered tissues. PEM films are currently used to modify the surface properties of materials for the coating of materials in different tissue engineering application which are classified according to the kind of application: bone morrow, vascular tissue, neuronal tissue, tracheal and oral prostheses, dental and general engineering applications as summarized in Table 2.1.

Table 2.1 PEM coating on materials for different tissue engineering applications

Application	Substrate	Film	Cells	Main findings	Ref.
Bone marrow	PDL-LA scaffold	$(PEI/GEL)_2$	MC3T3-E1	Increased adhesion and growth of osteoblast cells	[50]
	microfluidic PDMS bioreactors	$(PDADMAC/clay)_5/(Col\ IV/FN)_n$	Murine bone marrow stem cells	Automated microfluidic perfustion system Increased cell attachment and spreading	[51]
	PA hydrogel ICC scaffolds	$(PDADMAC/Clay\ platelets)_5$/clay platelets	Hematopoietic stem cells	Expansion of $CD34^+$ stem cells and B-lymphocyte differentiation	[52]
Vascular engineering	PET filaments, thread and prostheses	$(PSS/PAH)_{24}$, $(PLL/PGA)_{24}$, $(PLL/HA)_{24}$	-	Characterization of film deposition Good mechanical stability of the films under stretching	[53]
	Nitinol sheets	(PDA/ALG/PA/HEP)4	Fresh platelet-enriched plasma	Enhanced wettability Improve the blood compatibility by decreased thrombogenicity and strongly reduced platelet adhesion	[54]

Application	Substrate	Film	Cells	Main findings	Ref.
Vascular engineering	ePTFE	PEI-$(PSSPAH)_3$	Human umbilical vein endothelial cells	Enhanced adhesion and spreading of endothelial cells on the films	[55]
	NiTi for endovascular stent	PEI/HA$(CHI/HA)_n$	-	Film coated in situ in the artery in physiological conditions Prevention of platelet adhesion	[56]
	Cryopreserved artery	$(PAH/PSS)_3$-PAH	Human umbilical vein endothelial cells	Adhesion and spreading of endothelial cells Increased expression of Von Willebrand factor	[57]
	Stainless steel	$(ChS/HEP)_n$	Human umbilical vein endothelial cell Human normal aorta smooth muscle cell	Hemocompatibility , Longer blood clotting time than pure steel substrates. Control of releasing rate of Sirolimus by the number of layers Inhibition of smooth muscle cells growth	[58]
	Polyethersulfone foils	HEP/ALB	Whole human blood	Reduced activation of coagulation Reduction of the blood level of complement fragment C5a	[59]
	Aminolyzed PET films	$(HEP/CHI)_n$	E. *coli*	Decrease in the number of viable bacteria	[60]
Neuronal tissue	HYAFF 11® bioactivation	(PDADMAC/PSS)–(PDL/anti-TGFβ1)	-	Immunological activity of anti-TGFβ1 preserved	[61]
	Glass cover slips	PDADMAC$(SWNT/PAA)_n$	NG108-15 Hybrid Cells (neuroblastoma x glioma hybrid culture cells)	Good attachment and neuronal differentiation Guidance of neurites outgrowth	[62]

Application	Substrate	Film	Cells	Main findings	Ref.
Tracheal prostheses	Ti	PLL/$(PLL/PGA)_4$/PGA-αMSH, PLL/PGA/PLL/ PGA-αMSH/$(PLL/PGA)_3$	Blood samples from Wistar rats	Systemic anti-inflammatory IL-10 production was only detected in rats implanted with prostheses functionalized by αMSH	[17]
	3D porous Ti	PEI-(PSS-PAH)2-PSS, PEI-(PSS-PAH)2-PGA/PLL/PGA, PEI-(PSS-PAH)2-PGA/PLL	HCS-2/8 cells (a human chondrosarcoma-derived chondrocyte-like cell line)	More stable adhesion (focal contacts) on negatively charged (PSS, PGA) or uncoated surfaces In cells plated onto negatively charged or uncoated surfaces surfaces, phosphorylation of p44/42 MAPK/ERK was twofold increased	[63]
	3D porous Ti	(PAH/PSS)4/VEGF	Human umbilical vein endothelial cell (PromoCell)	Enhanced spreading and proliferation of endothelial cells via activation of VEGFR2 receptors and kinases (ERK1/2).	[64]
Oral prostheses/ devices	Heat-cured PMMA, cold-cured PDM. Cold-cured VPS	PEI-(PSS-PAH)2-(PGA-PLL)n	-	Increased surface wettability No coating films degradation in natural saliva, after 7 days *in vitro* and after 4 days *in vivo*	[16]
	PMMA	PEI-$(PSS-PAH)_2$-$(PGA-PLL)_{20}$-$(PGA\text{-chromofungin-}PLL)_{20}$	Yeast C. *albicans*, N. *crassa* Human gingival fibroblast Wistar rat's check	Inhibited the growth of yeast C. *albicans* and completely stop the proliferation of fungus N. *crassa* No cytotoxicity of fibroblast cell cultured on functionalized films No signs of a candidiasis at functionalized films *in vivo*	[65]

Application	Substrate	Film	Cells	Main findings	Ref.
Oral prostheses/ devices	Glass cover slips	PEI-(PSS-PAH)2-(PGA-PLL)-(PGA-defensin-PLL)n	M. *luteus*, E. *coli*	Increased anti-microbial activity	[18]
Dental Applications (the transmucosal part of the implant)	Porous Ti	$(PLL/PGA)_{5,6}$/ Laminin-5-derived peptide	Human oral epithelial cells	*In vitro*, the films enhance epithelial cell colonization and proliferation Specific formation of adhesive structures (hemidesmosomes) in the presence of the peptide	[66]
			Beagle dogs	*In vivo* experiment, a laminin-5 coated porous Ti-modified implant showing the colonisation of the material by cells of the peri-implant soft tissues	
	Ti	PEI-$(PSS/PAH)_{10}$, PEI-$(PSS/PAH)_{10}$-PSS, PEI-$(HA/PLL)_{10}$, PEI-$(HA/PLL)_{10}$-HA	Human fibroblasts	Fibroblast adhesion and proliferation was strongly dependent on film type. Films containing PSS/PAH generated a better cellular response than films containing cross-linked HA/PLL.	[67]

In terms of endosseous implant materials, many types of polyelectrolyte have been generated on the Ti surface via LbL technique for improving the osteoblasts response. Halthur *et al.*[68] successfully fabricated PLL/PGA multilayers on silica and titanium surfaces with immobilization of enamel matrix derivative (EMD) protein both on top and within PEM films. They suggested that polypeptide-EMD multilayer films could be able to trigger cell response and induce biomineralization and have potential application as bioactive and biodegradable coatings for future dental implants.

Cai *et al.*[19] used the combination of polyelectrolyte including PEI, PSS and CHI to fabricate PEI/$(PSS/CHI)_6$ PEM films on Ti surfaces. They found that osteoblast cultured on chitosan-modified Ti films displayed higher cell proliferation, DNA synthesis and alkaline phosphatase (ALP) activity than those cultured on Ti control. Moreover, Cai *et al.*[69] reported that silk fibroin (SF){PEI/(SF/CHI)5/SF} PEM films promoted cell proliferation, cell viability, DNA synthesis and ALP activity of osteoblast cells compared to Ti.

Another study of Cai *et al.*[20], CHI and GEL were employed to form PEI/GEL/$(CHI/GEL)_3$ PEM films. They reported that these PEM films have higher osteoblast cell proliferation than those of Ti surface. Moreover, this group fabricated hybrid multilayers composed of CHI/GEL pairs in between embedded with β-estradiol (E2) loading mesoporous silica nanoparticles, which coated with PEM of GEL/CHI, (E2-MSN@PEM) onto Ti substrates {PEI/$(GEL/CHI)_2$/GEL/(E2-MSN@PEM/GEL/$(CHI/GEL)_2)_2$} via the LbL assemble technique to investigate its potential for regulating osteoblast/osteoclast growth balance *in vitro* at molecular level. They found that it not only promotes the biological functions of osteoblasts (proliferation, ALP activity, *in vitro* mineralization) but also inhibits the proliferation of osteoclasts, via the induction of osteoclasts apoptosis through the up-regulating osteoprotegerin (OPG)[70].

Chua *et al.*[71] improved biocompatibility and confered long-lasting antibacterial properties on Ti via PEM of hyaluronic acid (HA) and CHI, coupled with surface-immobilized cell-adhesive RGD peptides. They found that the HA/CHI PEM-functionalized Ti was highly effective as an antibacterial surface but the adhesion of osteoblasts was poorer than on pristine Ti. However, when RGD peptide was immobilized on HA/CHI PEM film {$(HA/CHI)_5$-RGD PEM film), the osteoblast functions in term of cell adhesion, proliferation and ALP activity can be significantly improve compared to pristine Ti substrates while retaining high antibacterial efficacy. They proposed that the effect of osteobalst functions on RGD-conjugated HA/CHI PEM is dependent on the density of the peptide immobilized on the surface.

van den Beucken *et al*.[72] fabricated multilayered DNA coatings, consisting of either PDL or PAH as the cationic counterpart of anionic DNA. They found that multilayered DNA coatings increased its potential to nucleate CaP deposition from simulated body fluids (SBF) as compared to non-coated Ti control, and the deposition of CaP was dependent on the

type of cationic polyelectrolyte used in the build-up of the DNA coatings {$(PAH/DNA)_5$ > $(PDL/DNA)_5$}. Besides, Non-SBF-pretreated DNA coatings were found to have no effect on osteoblast-like cell behavior compared to Ti controls. On the other hand, SBF-pretreatment of DNA coatings affected the differentiation of rat bone marrow cell through an increased deposition of OC.

Kreke *et al.*[21] fabricated PAH/HEP bilayers films by varied PAH solution pH (pH 6.4, 7.4, 8.4, and 9.4). They found that PAH/HEP films with PAH pH 8.4 supported MC3T3-E1 cell adhesion and FN adsorption similar to glass control but more than HEP-containing electrostatic film with others PAH pH.

Titanium dioxide (TiO_2) films fabricated via LbL technique have been reported. Kommireddy *et al.*[73] constructed TiO_2 nanoparticle thin films {$(PDADMAC/PSS)_2$ /PDADMAC/$(PSS/TiO_2)_n$} on the glass substrate and further evaluate for murine mesenchymal stem cell attachment, proliferation, and spreading. They found that TiO_2 nanoparticle thin films had higher cell attachment and proliferation as well as faster cell spreading than that of glass substrate control. Moreover, the result showed that the higher number of TiO_2 layers (greater surface roughness/ surface area), the faster cells attachment and spreading on implant surface.

In present study, PDADMAC, PSS and PSS-co-MA, which are synthetic polyelectrolyte, were used to fabricate PEM films. PDADMAC, is one of a strong cationic polyelectrolyte, consists of numerous positive charges along the backbone chain. In contrast, PSS, a strong anionic polyelectrolyte, possesses a number of negative charges along the backbone chain. Due to their strong ionic charges, both PDADMAC and PSS were selected by a number of investigators to be used as the polyelectrolytes for PEM preparation[22-25]. Since the hydrophobic ring structure of PDADMAC polycations is stiff and difficult to rotate both in water and air. Therefore, the outer layer containing the quaternary ammonium end groups stays hydrophilic both in water and in the air. Hydrophilic property of the polycations supports the next dipping PSS layer[26]. Another advantage of using strong polyelectrolytes is that their ionic charges are largely independent of the pH condition[27]. All evidences support the advantages of using PDADMAC and PSS for PEM fabrication.

PSS-co-MA was selected for coating the final layer of PEM. PSS-co-MA is a copolymer of PSS and maleic acid. This copolymer contains both strong sulfonate group in PSS and weak carboxylic pendent group from maleic acid segments. The strongly charged group can generate the electrostatic linkages thereby enhancing the film stability. Meanwhile, the weakly charged groups of maleic acid provide the alteration to the multilayer properties due to their ability to response to external pH changes. For example, at high pH, the carboxylic acid group in maleic could be converted into carboxylate group and become ionized, therefore, the PSS-co-MA became an anionic polyelectrolyte[28]. Due to this unique properties, PSS-co-MA has been recently used as an cation-exchange membranes[29]. However, it has never been applied in order to influence osteoblast behavior.

The objective of this study was to fabricate PEM films using PSS-co-MA, PDADMAC and PSS. The characteristics of the surface modified films and their effects on osteoblast functions were investigated *in vitro* and *in vivo*.

CHAPTER III

RESEARCH METHODOLOGY

Part I: Fabrication and characterization of $(PDADMAC/PSS)_4$/PDADMAC+PSS-co-MA coated PEM film on glass surface and examination of the functions and behaviors of osteoblasts grown on PSS-co-MA coated surface

Selection of polyelectrolyte to be used in the study

In the pilot study**,** many polyelectrolytes such as PDADMAC, PSS, PSS-co-MA, polyacrylic acid (PAA), GEL, and silicon dioxide (SiO_2) were used to fabricate PEM film. Chemical structure of each polyelectrolyte used and the PEM fabrication method were shown in Appendix A (Figure A1, A2). Then each PEM coated surface was examined for its ability to support cell growth. The cell viability, cell morphology and ALP activity was performed. (The methods of cell viability, cell morphology, and ALP activity are showed in Appendix A).

According to the results of cell viability (Figure A3), cell morphology (Figure A4) and ALP activity (Figure A5), PDADMAC, PSS and PSS-co-MA were employed to fabricate bioactive coatings on glass cover slips.

Fabrication of $(PDADMAC/PSS)_4$/PDADMAC+PSS-co-MA PEM films

Glass cover slips (12 mm round or 22×22 mm^2 square) were pretreated with freshly prepared piranha solution, a 30:70 v/v mixture of 40% hydrogen peroxide and concentrated sulfuric acid, for 10 minutes followed by immerging in 1% ammonia solution for another 10 minutes. The pretreated glass surfaces were thoroughly rinsed three times with distilled water and air dried.

PEM films were constructed by forming 9 layers of PDADMAC and PSS with a final layer of PSS-co-MA {$(PDADMAC/PSS)_4$/PDADMAC+PSS-co-MA} on glass surfaces as described in Appendix A. Briefly, the pretreated cover slips were alternately immersed in 10 mM PDADMAC in 0.1 M NaCl or 10 mM PSS in 0.1 M NaCl for 5 minutes, respectively, with intermediate triple rinses with distilled water until the ninth layer was formed. For the final layer,

the glasses were immersed in 10 mM PSS-co-MA (pH 10) in 0.1 M NaCl for 30 minutes, rinsed three times with distilled water (pH 10) and air dried resulting in a polyanionic surface. PDADMAC, PSS and PSS-co-MA were purchased from Aldrich (St. Louis, MO, USA). Chemical structures of the polyelectrolytes used and the fabrication method diagram were showed in Figure 3.1.

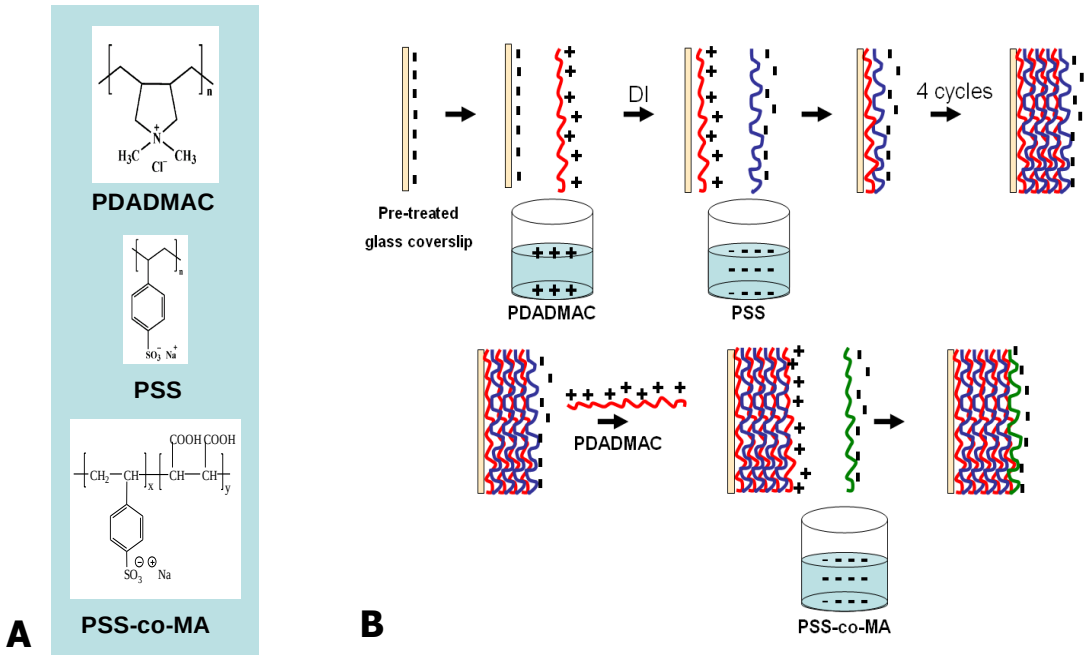

Figure 3.1 Fabrication of polyelectrolyte multilayer films

Chemical structures of the polyelectrolytes used in this study were shown in (A). Diagram of $(PDADMAC/PSS)_4$/PDADMAC+PSS-co-MA coated PEM films fabrication methods were shown in (B).

UV-vis spectroscopy

PEM films were assembled on fused quartz plates (2 mm thick, 1 inch diameter, GM Associates, Oakland, CA, USA) which are transparent to the UV-visible spectrum. The plates were pretreated with piranha solution, 1% ammonia and rinsed with distilled water. UV-vis absorption spectra were recorded using a UV-vis Spectrophotometer (SPECORD® S100, Analytik Jena AG, Jena, Germany). This method was used to measure the thickness of PDADMAC/PSS multilayer and PSS-co-MA adsorption onto PEM. PEM buildup can be monitored with this method since the amount of polymer deposited is proportional to the absorbance according to Beer's law: $A=\varepsilon.b.C$, where A is the absorbance, ε is the molar absorptivity ($Lmol^{-1}\ cm^{-1}$), b is the absorbing medium pathlength (cm) and C is the concentration (mol^{-1}).

Surface characterization analysis

Surface roughness was measured by atomic force microscopy (AFM; Nanoscope IV, Multimode, Veeco, Santa Barbara, CA, USA). Average surface roughness (R_a), the root mean square (rms) roughness (R_q) and thickness of the PSS-co-MA film were calculated from measurement of three independent samples. Surface morphology of the specimens was also examined using a scanning electron microscope (SEM; JSM-5410LV, JEOL, Tokyo, Japan) and atomic force microscope (Nanoscope IV, Multimode, Veeco, Santa Barbara, CA, USA).

Hydrophilicity

Static contact angle measurement was performed using a contact angle meter (DSA 10, Krüss, Hamburg, Germany) at room temperature to determine the existence of hydrophilic sites on both glass surfaces and PSS-co-MA-coated PEM surfaces. The samples were kept in the ambient environment for 15 minutes to set as a standard for contact angle measurement in this work. To perform this measurement, a 10 µl droplet of de-ionized water was dropped vertically on the specimen surface without any physical contacts with a micro-syringe onto the film surface. The contact angles were measured ten times and then averaged.

Cell culture

MC3T3-E1 cells (ATCC CRL-2593), an immortalized cell line derived from murine calvarial tissue, were maintained in minimum essential medium (HyQ® MEM/EBSS, Hycone, Logan, Utah, USA) supplemented with 10% fetal bovine serum (FBS, ICP biologicals, Henderson, Auckland, New Zealand), 2 mM L-glutamine, 100 unit ml^{-1} penicillin, 100 μg ml^{-1} streptomycin and 0.25 μg ml^{-1} amphotericin B (Gibco, Grand Island, NY, USA) under standard condition (at 37°C in 5% CO_2). Cell from passage 18 to 22 were used in the experiments. For MTT assay, SEM and ALP activity, quantitative reverse-transcription polymerase chain reaction (qRT-PCR), OC protein analysis, cells were seeded on glass cover slips (diameter 12 mm) in 24 well plates at a density of 40,000 cells per well. For Alizarin red staining, cells were seeded on 22×22 mm^2 glass cover slips in 6 well plates at a density of 200,000 cells per well. The cover slips were sterilized with 70% ethanol, rinsed with culture medium and air dried before use. The medium was changed every other day.

Scanning electron microscopy (SEM)

For SEM analysis, MC3T3-E1 cells were cultured on uncoated and PSS-co-MA coated PEM glass for 4 and 16 hours. Cells were rinsed twice with phosphate buffered saline (PBS) and fixed with 3% glutaraldehyde solution (Fluka, Milwaukee, WI, USA) dilute with 0.1 M PBS for 30 minutes. The samples were rinsed twice with 0.1 M PBS and dehydrated in a graded series of ethanol (30, 50, 70, 90 and 100%), and then critical point dried with 100% hexamethyldisilazane (HMDS; Fluka, Steinheim, Germany) for 5 minutes. Gold was sputter-coated on the surface and the samples were examined using a scanning electron microscope (JSM-5410LV, JEOL, Tokyo, Japan).

MTT assay

MC3T3-E1cells were seeded on glass cover slips (diameter 12 mm) in 24 well plates at a density of 40,000 cells per well. Cell number was determined by MTT (3-(4,5-Dimethylthiazol-2-yl)-2,5-dipheyl tetrazolium bromide) assay. MTT (USB Corporation, Cleveland, OH, USA) solution of 5 mg ml^{-1} was prepared by dissolving MTT in 10% serum culture medium without phenol red. At the end of culture periods (4 and 16 hours), cells were

washed with PBS prior to the addition of MTT solution into each well and incubated for 15 minutes at 37°C. At the end of the assay, the blue formazan reaction product was dissolved by 1 ml of glycine buffer (pH 10) (125 μl/well) and dimethyl sulfoxide (DMSO; Sigma-Aldrich Chemie GmbH, Steinheim, Germany) (900 μl/well). The optical density of this colored solution in each well, representing the number of viable cells, was measured using a spectrophotometer (Thermospectronic Genesis10 UV-vis, Madison, WI, USA) at a wavelength of 570 nm. Cell numbers were determined according to the standard curve of relative known cell number.

Quantitative reverse-transcription polymerase chain reaction (qRT-PCR) analysis

MC3T3-E1 cells were seeded on glass cover slip and PSS-co-MA coated glass and cultured for 13 days. Expressions of Col I, OPN, BSP, and OC messenger RNA (mRNA) were assessed using qRT-PCR. The MC3T3-E1 cells were detached from samples using 1 ml of 0.2% EDTA (ethylenediaminetetraacetic acid; Sigma, St. Louis, MO, USA) in PBS. A cell pellet was obtained by centrifugation at 12,000xg (14,000 rpm) for 10 minutes and the RNA was extracted with 1 ml of TriPure Isolation Reagent (Roche Diagnostics, Indianapolis, IN, USA) according to the manufacturer protocol. RNA yields were evaluated with a NanoDrop 2000 UV-Vis spectrophotometer (Thermo Fisher Scientific Inc., Wilmington, DE, USA) based on the absorbance ratio at 260/280 nm. First strand DNA was reverse transcribed from 1 μg of total RNA using reverse transcriptase enzyme (ImProm-II Reserve Transcription System, Promega, Madison, WI, USA).

qPCR was performed using the LightCycler 480 (Roche, Mannheim, Germany) and LightCycler® SYBR Green I Master (Roche, Mannheim, Germany) in a 10 μl reaction volume under the following cycling conditions: 95°C, 5 min, followed by 40 cycles of 95°C for 10 s; 60°C for 10 s: 72°C for 25s. PCR oligonucleotide sequences of the primers are followed: Col I sense 5′GGT GCC CCC GGT CTT CAG3′, antisense5′AGG GCC AGG GGG TCC AGC ATT TC3′, OPN sense 5′CCA ACG GCC GAG GTG ATA3’, antisense 5′CAG GCT GGC TTT GGA ACT TG3’, BSP sense 5′TGT CTG CTG AAA CCC GTT C3′, antisense 5′GGG GTC TTT AAG TAC CGG C3′,OC sense 5′CTT GGG TTC TGA CTG GGT GT3’, antisense 5′AGG GAG GAT CAA GTC CCG3′ and glyceraldehyde-3-phosphate dehydrogenase (GAPDH) sense 5′ACT TTG TCA AGC TCA TTT CC3′ and antisense 5′TGC AGC GAA CTT TAT TGA TG3′.

The primer was designed from the sequence in GenBank database (NM_007742.3, NM_009263.1, NM_008318.1, NM_001032298.2 and XM_001476723.1 for Col I, OPN, BSP, OC and GAPDH, respectively). All samples were performed in triplicates and the house keeping gene, GAPDH, was used as a reference control. The calculations of average Cp values and resulting expression ratios for each gene were performed using the Roche LightCycler 480 software version 1.5 (Roche, Mannheim, Germany).

Alkaline phosphatase activity (ALP activity)

Cells were rinsed with PBS and scraped in alkaline lysis buffer (10 mM Tris-HCl, 2 mM $MgCl_2$, 0.1% Triton-X100, pH 10) (100 µl/well). A half volume of each sample was mixed with ALP substrate solution containing 2mg/ml *p*-nitrophenyl phosphate (PNPP; Zymed, Invitrogen, Carlsbad, CA, USA) in 0.1 M 2-amino-2-methyl-1-propanol, 2mM $MgCl_2$, pH 10.5 for 10 minutes at 37°C. The reaction was stopped by the addition of 0.9 ml/well of 0.1 M NaOH, and the absorbance was read at 410 nm. The other half volume of each sample was used for protein quantification using a bicinchoninic acid protein assay (BCA™, Thermo Scientific, Rockford, IL, USA). The absorbance for the protein assay was read at 562 nm. The amount of ALP was calculated as nanomolar of *p*-nitrophenyl/µg protein/min.

Osteocalcin analysis using enzyme-linked immunosorbent assay (ELISA)

MC3T3-E1 cells were seeded on tissue culture plate (TCP), glass cover slip and PSS-co-MA coated glass and incubated for 13 days, using mouse osteocalcin EIA kit (Biomedical Technologies Inc., Stoughton, MA, USA). The culture medium was changed 1 day prior to sample collection. The supernatants of cell seeded on each sample were used to analyze osteocalcin protein according to manufacturer's instruction.

Alizarin red-S staining

Calcium deposition was quantified by Alizarin red-S staining (Alizarin Red S – certified, Sigma, St. Louis, MO, USA). MC3T3-E1 cells were cultured overnight on uncoated glass or PSS-co-MA-coated PEM surfaces until confluent. The media was changed to medium containing 5 mM glycerol-2-phosphate disodium salt hydrate (β-glycerophosphate; Sigma, St.

Louis, MO, USA) and 50 μg ml^{-1} l-ascorbic acid sodium salt (Sigma, St. Louis, MO, USA). Media was changed every other day. After culture for 15 days, the cells were rinsed with PBS and fixed with cold methanol for 10 minutes, washed with de-ionized water, followed by staining with 1% Alizarin Red in 1:100 (v/v) ammonium hydroxide/water (pH 4.2) into each well for 3 minutes. The amount of calcium deposition was quantified by destaining with 10% cetylpyridinium chloride monohydrate (Sigma, St. Louis, MO, USA) in 10 mM sodium phosphate at room temperature for 15 minutes. The absorbance was measured at 570 nm using the UV-vis spectrophotometer (Thermospectronic Genesis10 UV-vis, Madison, WI, USA).

Statistical analysis

Data were analyzed using stastical software (SPSS® 15.0 for Windows, SPSS, Chicago, IL, USA). A two-tailed students't-test was used to compare results from the PSS-co-MA-coated PEM films and the uncoated glass cover slips. Data were presented as the mean±SD. The *p*-values<0.05 were considered as a statistical significance.

Part II: Fabrication and analysis of the (PDADMAC/PSS)$_4$/PDADMAC+PSS-co-MA coated PEM films on cpTi discs and examination of the function and behavior of osteoblasts grown on PSS-co-MA coated on Ti surface

Titanium disc preparation

Ti discs (cpTi grade 2, Morita Company, Japan) were casted in disc shape, 12 mm in diameter and 2 mm thick. The specimens were polished using 1000-grit SiC paper in a polishing machine (DPS 3200, IMPTECH, South Africa), then ultrasonically cleaned with de-ionized water for 10 min and consequently rinsed with de-ionized water for two times.

Fabrication of (PDADMAC/PSS)$_4$/PDADMAC+PSS-co-MA films on cpTi discs

After the preparation specimens, Ti substrates were ultrasonically washed 10 min in ethanol followed by three times rinsing with de-ionized water and then dried at room temperature before dipping. PEM films were constructed by forming 9 layers of PDADMAC and PSS with a stop layer of PSS-co-MA {(PDADMAC/PSS)$_4$/PDADMAC+PSS-co-MA} on Ti surfaces as described in part I.

Surface characterization analysis

Surface roughness was measured by contact profilometry using a profilometer (Talyscan 150, Taylor Hobson, UK). Average surface roughness (R_a) measurements were randomly measured at nine different locations on each sample under the following conditions: measurement speed at 2.0 mm/s, one way direction measurement.

Hydrophilicity

Static contact angle measurement of glasses, Ti discs and PSS-co-MA-coated PEM on Ti discs was performed using contact angle meter (DSA 10, Krüss, Hamburg, Germany) as previously described.

Human primary bone cell culture

Human primary osteoblast cells were obtained form alveoloplasty, torus palatinus or torus mandibularis removal for prosthodontic reasons or residual iliac bone in procedure of cleft palate reconstruction. All patients gave informed consent and the protocol has been approved by the Ethical Committee, Faculty of Dentistry, Chulalongkorn University. Bone chip was washed extensively in PBS (pH 7.4) and cut into pieces of approximately 2x2 mm^2. The bone pieces were digested with 0.25% trypsin-EDTA to remove residual adipose and hematopoietic tissue. The bone pieces were harvested in 35 mm × 10 mm culture dish (Coring, NY, USA) and grown in Dulbecco's modified Eagle's medium (DMEM, GIBBCO, Grand Island, NY, USA), containing 15% FBS (ICP biologicals, Henderson, Auckland, New Zealand), 2mM L-glutamine, 100 units/ml penicillin, 100 µg/ml streptomycin, and 5 µg/ml amphotericin B (Gibco, Grand Island, New York, USA) in a humidified incubator at 37°C with 5% (v/v) CO_2. Human primary osteoblast cells were subcultured at a 1:3 ratio after cells become confluent. The expression of osteoblastic gene including Col I, ALP, OPN, BSP, OC and dentin matrix protein 1 (DMP1) was examined by RT-PCR and cells were also stained with ALP staining (TRACP & ALP double-stain kit; TAKARA BIO INC., Shiga, Japan) and Alizarin Red S staining (Alizarin Red S –certified, Sigma, St. Louis, MO, USA) to confirm the characteristic of osteoblast cells (Appendix B). The cell passages numbers from 3 to 6 were used in this study. All experiments were performed in triplicate using cells prepared from three different donors.

Prior to cell culture experiment, all specimens were sterilized by washed with 70% ethanol for 10 minutes and three times rinsing with de-ionized water and air dried. For all experiment, MTT assay, SEM and ALP activity analysis, RT-PCR, OC analysis and Alizarin red staining, cells were seeded on materials in 24 well plates at density of 40,000 cells per well. The medium was changed every other day.

In the present study, glass cover slips (12 mm round) were used to be as a control and to check on cell adhesion and proliferation during the experiment.

Cell morphology in scanning electron microscopy (SEM)

The morphology of cells cultured on glass coverslips, titanium discs and PSS-co-MA coating Ti discs for 1 hour incubation were evaluated by SEM as previously described.

MTT assay

Cell viability was determined by MTT assay after 4 and 24 hours of incubation as described in part I.

Reverse-transcription polymerase chain reaction (RT-PCR)

Expressions of BSP, OC and DMP1 mRNA were assessed using RT-PCR after 14 days of primary human osteoblast cell cultured on glass surfaces, Ti discs and PSS-co-MA coating Ti discs.

The human primary osteoblast cells were detached from samples using 1 ml of 0.2% EDTA (Sigma, St. Louis, MO, USA) in PBS. A cell pellet was obtained by centrifugation at 12,000xg (14,000 rpm) for 10 minutes and the RNA was extracted with 1 ml of TriPure Isolation Reagent (Roche Diagnostics, Indianapolis, IN, USA) according to the manufacturer protocol. RNA yields were evaluated with a NanoDrop 2000 UV-Vis spectrophotometer (Thermo Fisher Scientific Inc., Wilmington, DE, USA) based on the absorbance ratio at 260/280 nm. First strand DNA was reverse transcribed from 1 μg of total RNA using reverse transcriptase enzyme (ImProm-II Reserve Transcription System, Promega, Madison, WI, USA).

The PCR was performed with Tag DNA Polymerase (Tag DNA Polymerase, Recombinant, Invitrogen, Sao Paulo Brazil) using PCR oligonucleotide sequences of the primers are followed: BSP sense 5'GAT GAA GAC TCT GAG GCT GAG A3', antisense 5'TTG ACG CCC GTG TAT TCG TA 3', OC sense 5'ATG AGA GCC CTC ACA CTC CTC 3', antisense 5'GCC GTA GAA GCG CCG ATA GGC 3', DMP1 sense 5' CAG GAG CAC AGG AAA AGG AG 3', antisense 5' CTG GTG GTA TCT TGG GCA CT 3', and GAPDH sense 5′TGA AGG TCG GAG TCA ACG GAT 3′ and antisense 5′TCA CAC CCA TGA CGA ACA TGG 3′. The primer was designed from the sequence in GenBank database (NM_004967.3, MN_199173.3, NM 004407.3 and MN_002046.3 for BSP, OC, DMP1 and GAPDH, respectively). The PCR products were

analyzed by separation on 1.8% agarose (Usb, Cleveland, OH, USA) gel using electrophoresis (Power Pac Junior, Bio-Rad, Hercules, CA, USA) and visualized with ethidium bromide solution (EtBr; Bio-Rad, Hercules, CA, USA) staining. The stained bands were photographed under UV light, and the intensity was quantified with Scion Image Software (Scion Corporation, Walkersville, MD, USA).

Alkaline phosphatase activity

After 3, 5 and 7 days of incubation, ALP activity of cell seeded on glass, Ti discs and PSS-co-MA coated Ti discs was determined as previously described.

Osteocalcin analysis using enzyme-linked immunosorbent assay (ELISA)

To examine the OC protein synthesis, human primary osteobalsts were seed on each sample and incubated for 14 days, using intact human osteocalcin ELISA kit (Biomedical Technologies, MA, USA) as described in part I.

Alizarin red-S staining

Calcium deposition was quantified by Alizarin red-S staining (Alizarin Red S – certified, Sigma, St. Louis, MO, USA) after human primary bone cells cultured on uncoated glass, Ti discs or PSS-co-MA-coated PEM surfaces in osteogenic medium {containing 5 mM β-glycerophosphate (Sigma, St. Louis, MO, USA), 50 μg ml^{-1} l-ascorbic acid sodium salt (Sigma, St. Louis, MO, USA) and dexamethazole (Sigma, St. Louis, MO, USA)} for culture for 15 days. The amount of calcium deposition was quantified by destained with 10% cetylpyridinium chloride monohydrate (Sigma, St. Louis, MO, USA) in 10 mM sodium phosphate at room temperature for 15 minutes as previously described.

Statistical analysis

Data were analyzed using SPSS® 15.0 for Windows (SPSS, Chicago, IL, USA). One-way analysis of variance, followed by a multiple comparison using Scheffe or Tamhane was used to compare the results from PSS-co-MA-coated PEM, Ti disc and uncoated glasses. Data were presented as mean±SD. p-values < 0.05 were considered as a statistical significance.

Part III: Analysis of *in vivo* bone formation after implantation of PCL and PSS-co-MA coated PCL films in mouse model

Preparation of the PCL and PSS-co-MA coated PCL films for transplantation

The PCL film was prepared by simple solvent casting method. PCL (Aldrich, USA, M_w = 80,000 g/mol^{-1}) was dissolved in chloroform (Labscan; Asia, Thailand) (3.5g/mL) at room temperature. The mixture was stirred vigorously for 1 hour and poured into a glass plate. The PCL film was solidified by evaporating chloroform slowly at room temperature for 24 hours.

For PSS-co-MA coated PCL films, PEM films were constructed from 9 alternating layers of PDADMAC and PSS, with PSS-co-MA as a last layer {$(PDADMAC/PSS)_4$/PDADMAC+PSS-co-MA} onto PCL films as described above.

Before starting *in vivo* test, each film was cut into small pieces of 2 mm. in diameter, which is appropriate for surgical defect of mice. The film then placed in 70% ethanol for 30 minutes, washed with autoclaved de-ionized water and subsequently immersed in cell culture medium overnight at room temperature for sterilization.

Surgical procedure

Eight-week-old-male (ICR Mouse) mice (National Laboratory Animal Center, Mahidol University) were used. The protocol was approved by the Animal Care and Use Ethical Committee, Faculty of Dentistry, Chulalongkorn University. Mice were anesthetized with intraperitoneal injection of sodium pentobarbital. Lidocain hydrochloride was injected in subcutaneous tissue and subcutaneous surgery at the head of mice. Two circular calvarial defects (2 mm. in diameter) were created by trephine bur drilling with saline irrigation. A total of 6 mice were used and 12 calvarial defects were generated. The defects were implanted with PCL and PSS-co-MA coated PCL films by randomization. The wounds were closed with a 4-0 nylon suture. At 6 weeks after implantation, the mice were sacrificed and the calvarial bone was carefully excised, cleaned and fixed immediately with 4% formaline for 24 hours at 4ºC. Before decalcification, the harvested constructions were taken photo by using stereomicroscopy (SZH10 RESEARCH STEREO, OLYMPUS, Olympus Optical Co., Ltd., Shibuya-ku, Tokyo, Japan)

Masson's Trichrome staining

After 1 month decalcification in 0.5mM EDTA, specimens were dehydrated in serials of graded ethanol, followed by infiltration and embedded in paraffin wax. Harvested tissues were cut into 10 μm sections and stained with Masson's Trichrome. Digital images of sections were scanned by a visual slide microscope (Mirax desk, Carl Zeiss, GmbH, Gottingen, Germany).

CHAPTER IV

RESULTS

Part I: Fabrication and characterization of $(PDADMAC/PSS)_4$/PDADMAC+PSS-co-MA coated PEM film on glass surface and examination of the functions and behaviors of osteoblasts grown on PSS-co-MA coated surface

Formation of $(PDADMAC/PSS)_4$/PDADMAC+PSS-co-MA multilayer

The presence and growth of multilayers of PDADMAC, PSS and PSS-co-MA solutions in 0.1 M NaCl was monitored using UV-vis spectroscopy. The chemical structure of PDADMAC, PSS and PSS-co-MA was shown in Figure 4.1a. PSS and PSS-co-MA have an absorption peak at 226 nm due to the sulfonate phenyl ring in the PSS moiety, while PDADMAC showed no absorption in the UV-vis region. For the UV-vis measurement, the PSS absorption was monitored as a function of the layer number to obtain information on the absorbed amount of PSS at 226 nm. The absorbance of PSS was found to increase with increasing numbers of layers (Figure 4.1b). The PSS-co-MA absorbance increased rapidly after 30 seconds of dipping and became constant after 2 minutes (Figure 4.1c). These results indicated the success of PEM film construction with polyelectrolyte solutions.

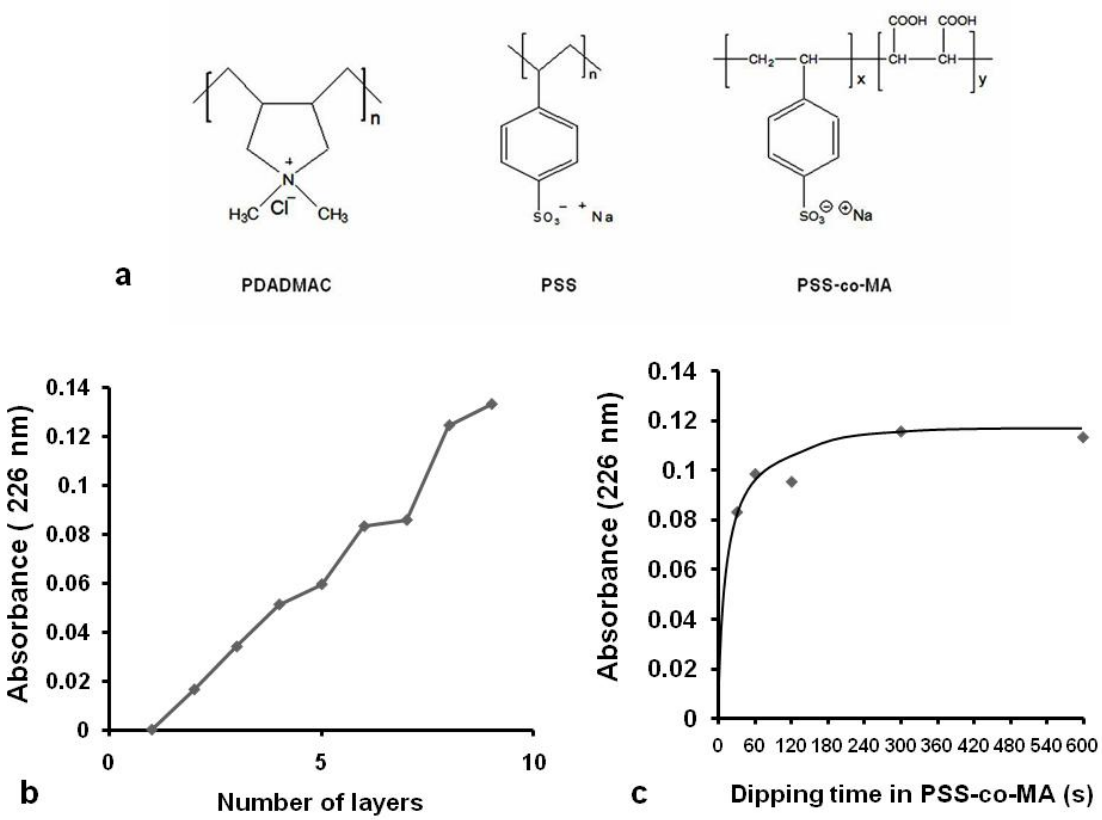

Figure 4.1 Formation of (PDADMAC/PSS)$_4$/PDADMAC+PSS-co-MA multilayer on glass cover slip surfaces

The chemical structure of polyelectrolyte used in this study (a). The thickness of PDADMAC/PSS multilayers was shown in (b). Odd layer numbers correspond to PDADMAC while the even layer numbers correspond to PSS. The kinetic adsorption of PSS-co-MA was shown in (c).

Hydrophilicity

The wettability of the surface was measured by dropping a drop of water onto the PSS-co-MA coated surfaces and uncoated glass. Results showed the water-drop spread more on PSS-co-MA coated surfaces than on uncoated glass as shown by the side view images (Figure 4.2a). The contact angle of a water-drop on PSS-co-MA coated surfaces was significantly lower (18.56°) than on uncoated glass (31.44°) (Figure 4.2b), indicating PSS-co-MA coated surfaces possessed a greater wettability than the glass surfaces.

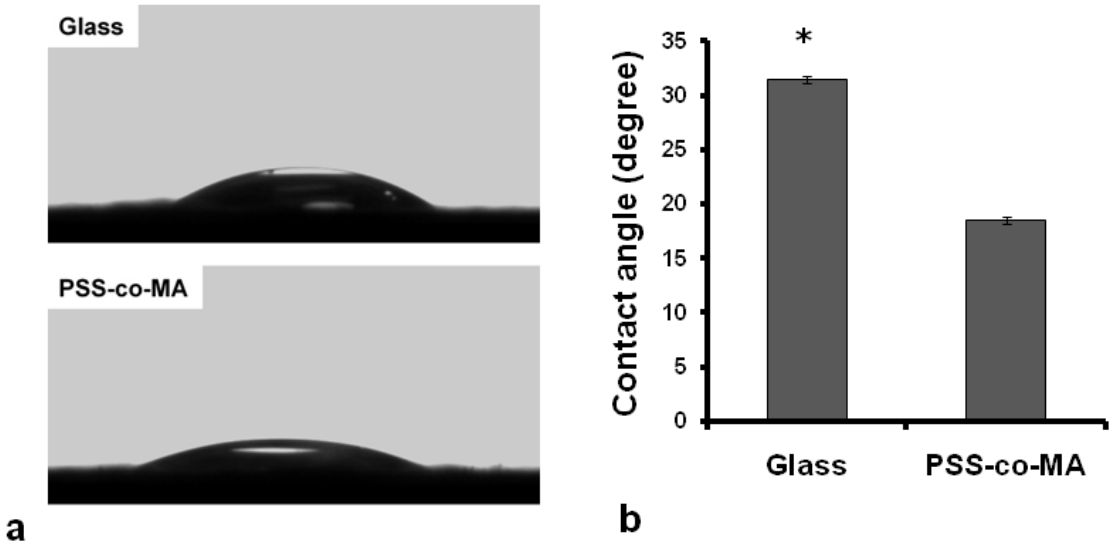

Figure 4.2 The wettability of glass and PSS-co-MA PEM surfaces

Photographs of water dropped on glass and PSS-co-MA coated surface were shown in (a). The water contact angle on glass and PSS-co-MA coated surfaces were shown in (b). Data was shown as the mean±SD. * denoted the statistically significant at $p<0.05$.

Surface characterization analysis

Results from AFM analysis revealed the significant difference between the glass and PSS-co-MA coated surfaces as showed in Table 4.1 ($p<0.01$ for both R_a and R_q). The R_a of glass and PSS-co-MA coated surfaces were 0.350±0.02 nm and 1.421±0.04 nm, respectively. The R_q values of glass and PSS-co-MA coated surfaces were 0.421±0.01 nm and 1.857±0.03 nm, respectively. In addition, AFM results also revealed that the average thickness of PSS-co-MA PEM film was 9.088±1.37 nm.

Table 4.1 Surface roughness determination of Glass surface and PSS-co-MA PEM surface

Materials	R_a (nm)	R_q (nm)
Glass surface	0.350 (0.02)	0.421 (0.01)
PSS-co-MA PEM surface	1.421 (0.04)*	1.857 (0.03)*

Data were shown as the mean (SD). * Statistically significant, $p<0.05$

The 3-dimensional images from AFM (Figure 4.3a1, 4.3a2) showed significant difference in surface topography between the glass and PSS-co-MA coated surfaces. PSS-co-MA coated films revealed the uniform and homogeneity. However, SEM examination showed that there was no significant difference in surface topography between the glass and PSS-co-MA coated surfaces (Figure 4.3a3, 4.3a4). This result demonstrated that SEM analysis failed to represent true nanoscale feature of PSS-co-MA coated films.

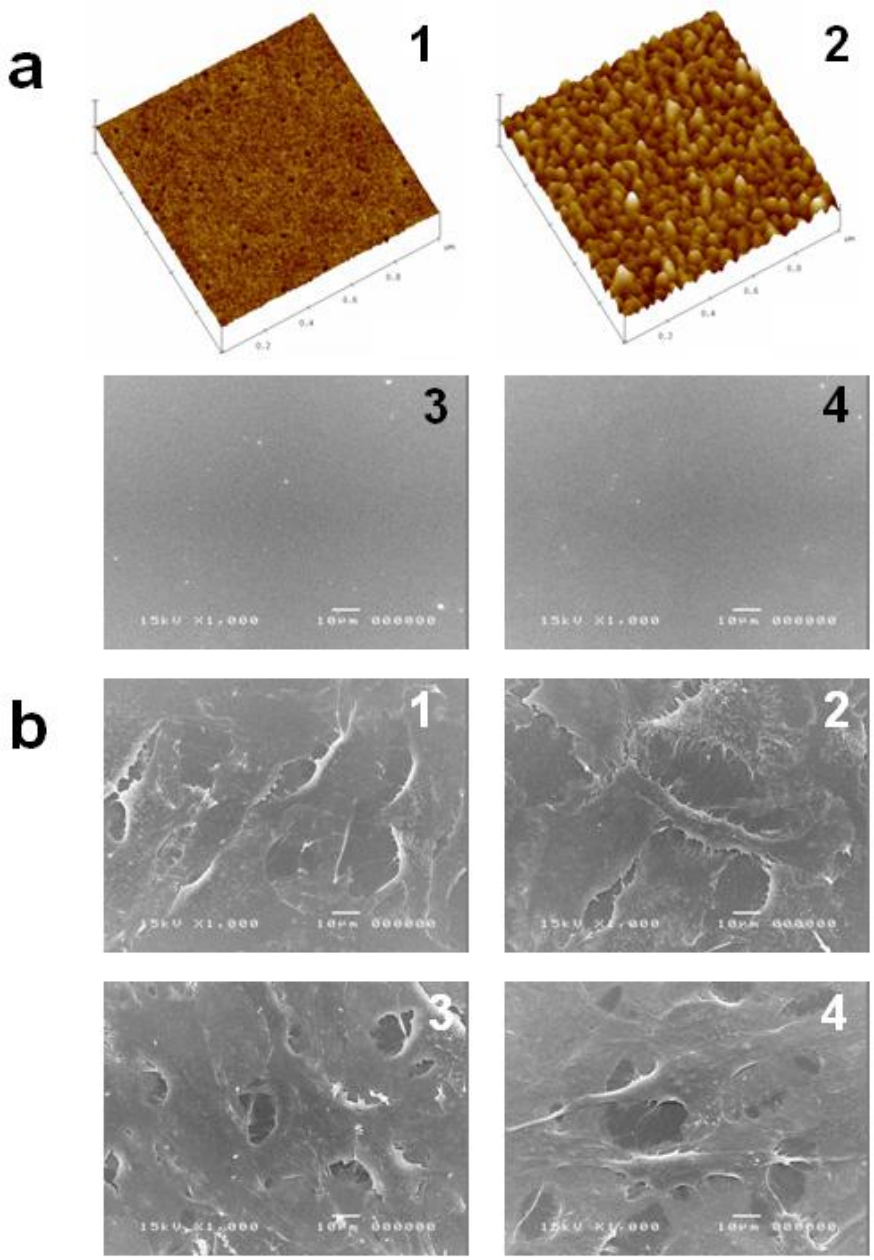

Figure 4.3 Surface characterization of glass and PSS-co-MA PEM film and morphology of MC3T3-E1 cells cultured on both surfaces

(a) Surface characteristics of the glasses cover slip surface (a1, a3) and PSS-co-MA PEM coated surfaces (a2, a4) analyzed by atomic force microscopy (a1, a2) and scanning electron microscopy (a3, a4). Adhesion of MC3T3-E1 cells on glass (b1, b3) and PSS-co-MA PEM surfaces (b2, b4) at 4 (b1, b2) and 16 hours (b3, b4).

Cell morphology

The morphology of MC3T3-E1 on both surfaces was analyzed after seeding for 4 and 16 hours. Cells on both surfaces appeared to be well spread at both time points. At 4 hours, cells appeared flattened and started to form contacts with the adjacent cells (Figure 4.3b1, 4.3b2). At 16 hours, a tightly packed cell layer was observed (Figure 4.3b3, 4.3b4).

Cell adhesion

The number of the cells increased during the culture period (from 4-16 hours) on both surfaces. Although the number of cells was slightly less on PSS-co-MA PEM compared to the uncoated glass, no statistically significant differences between the two groups were detected (p=0.226 for 4 hours and p=0.159 for 16 hours) as shown in Figure 4.4.

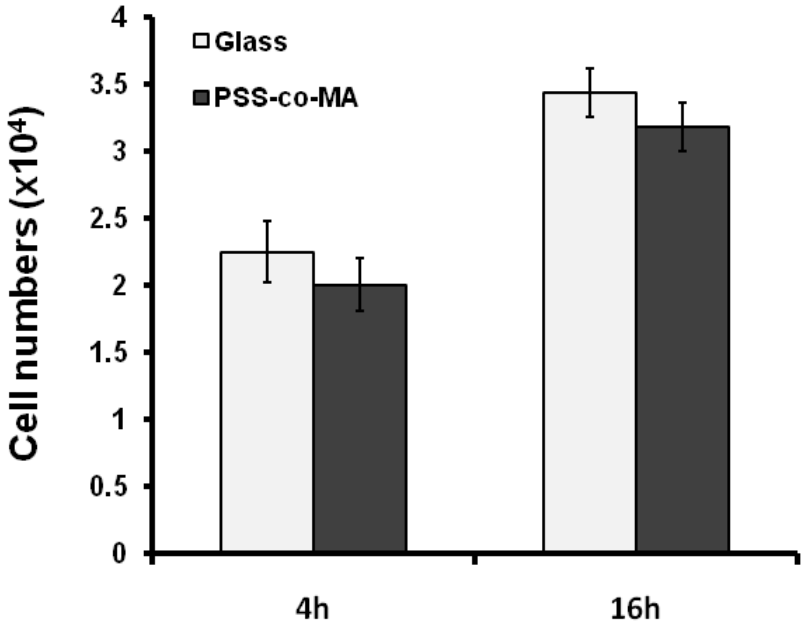

Figure 4.4 Adhesion of MC3T3-E1 cells on glass and PSS-co-MA PEM film

The cell number was estimated by the MTT assay after 4 and 16 hours incubation. Data were shown as the mean±SD.

ALP Activity

The ALP activity, an early marker of osteoblast differentiation, of MC3T3-E1 cultured on both surfaces was monitored on days 3, 5 and 7 after seeding (Figure 4.5). The ALP activity of cells seeded on PSS-co-MA PEM was higher than that on uncoated glass at day-5 with a significant difference at day-7 (p=0.027).

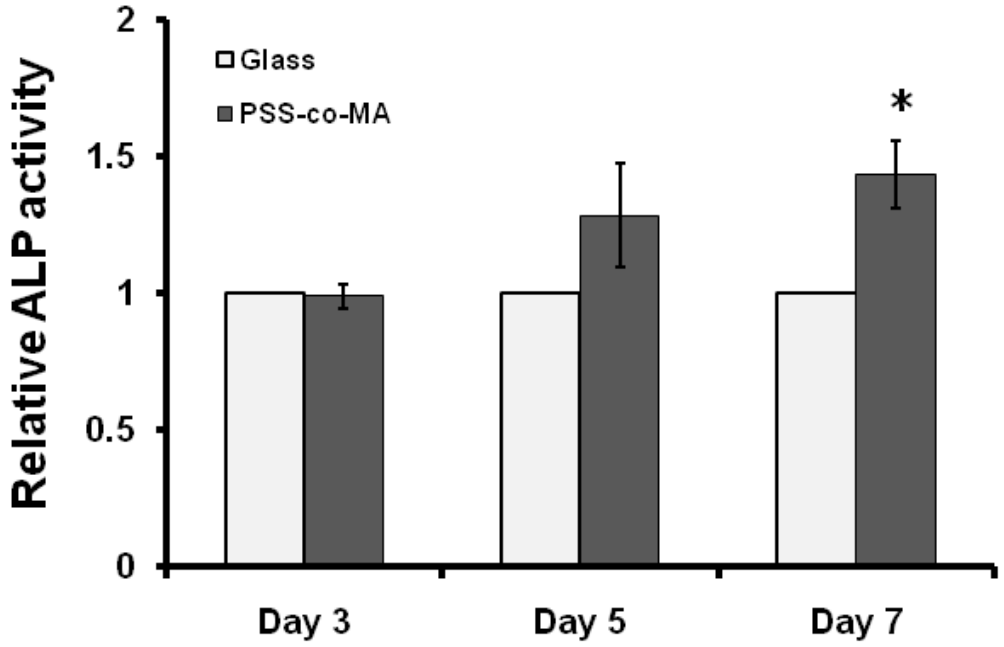

Figure 4.5 Alkaline phosphatase (ALP) activity of MC3T3-E1 cells

ALP activity of MC3T3-E1 cells after 3, 5 and 7 days culture on PSS-co-MA coated surfaces or glass. Data were shown as the mean±SD. * denoted the statistically significant, p<0.05

Osteoblastic gene expression

The differentiation of osteoblast was further indicated by the expression of Col I, OPN, BSP, and OC at day 13 (Figure 4.6a). Results from qRT-PCR revealed the 6-fold increase on the expression of BSP and OC in cell cultured on PSS-co-MA coated surface compared to glass cover slip control, while the expression of Col I and OPN were slightly increased (2 fold). To confirm the increase in OC expression, ELISA analysis of OC was also performed at day-13. Significantly increased of OC synthesis was observed in PSS-co-MA coated films compared to glass surfaces (Figure 4.6b).

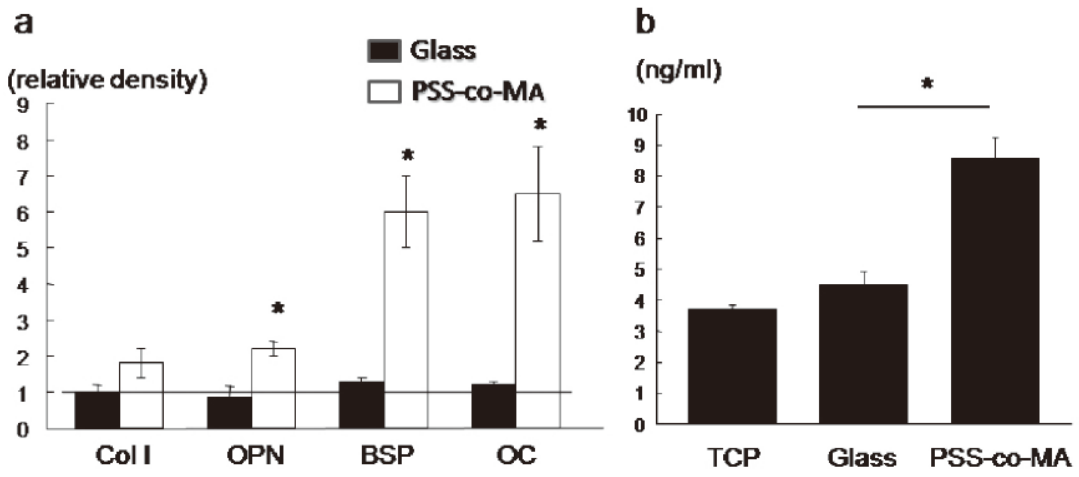

Figure 4.6 Osteoblastic gene expressions

a) The expression of Col I, OPN, BSP, and OC in MC3T3-E1 cells cultured on glass cover slip and PSS-co-MA surface at day 13 were examined using qRT-PCR analysis. Results for gene expression were normalized to GAPDH expression. Data were shown as the mean±SD from three separated experiments. * denoted the statistically significant, $p<0.05$

b) The protein synthesis of OC in MC3T3-E1 cells cultured on TCP, glass cover slip and PSS-co-MA surface at day 13 was examined by ELISA analysis. Data were shown as the mean±SD from three separated experiments. * denoted the statistically significant, $p<0.05$

***In vitro* calcification**

Cells were cultured in the presence of ascorbic acid and β-glycerophosphate for 15 days. The cultures were fixed and stained with Alizarin red-S to evaluate the presence of *in vitro* calcification. Macroscopically and microscopically observations revealed more reddish deposition in cultures on PSS-co-MA coated surfaces than on glass surfaces, (Figure 4.7a). Figure 4.7b showed a higher magnification of cells in Figure 4.7a (on PSS-co-MA coated surface).

The amount of calcium deposition on each surface was quantified colorimetricaly using 10% cetylpyridinium chloride monohydrate. The result showed that the amount of calcium deposition on PSS-co-MA coated surfaces was significantly greater than the control groups (p=0.003) (Figure 4.7c).

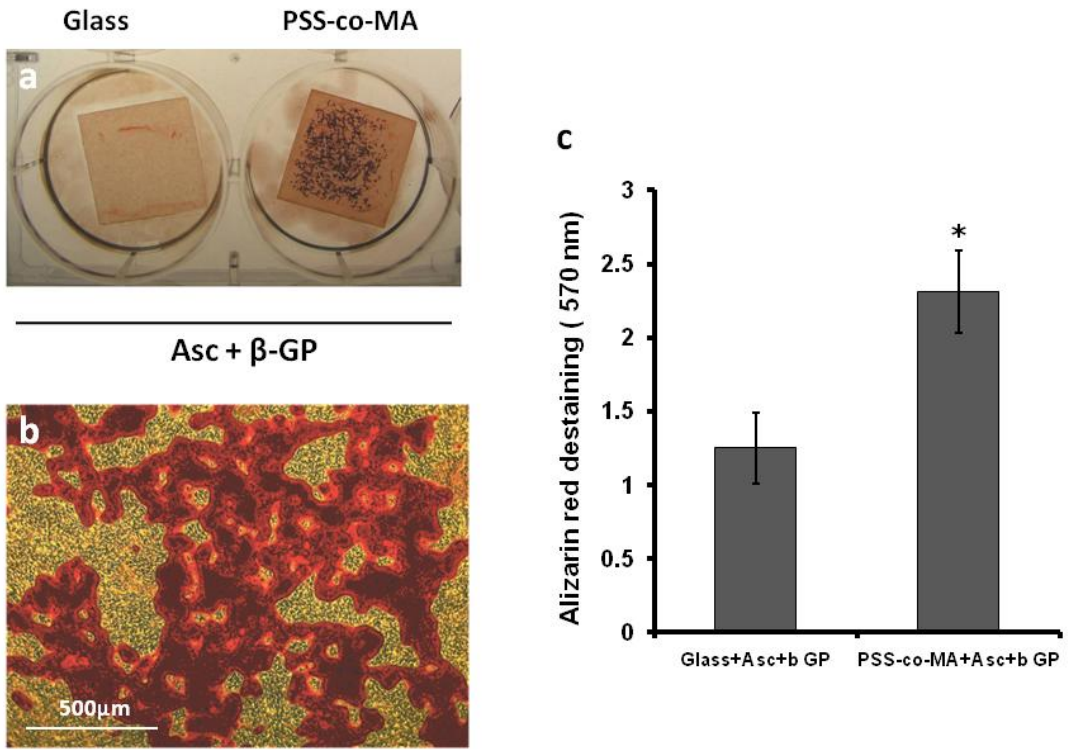

Figure 4.7 *In vitro* calcification

(a) Alizarin red-S staining indicating calcification in cells cultured at days 15 on glass and PSS-co-MA coated surfaces. Higher magnification of PSS-co-MA coated surfaces was showed in (b). (c) Graph showed the amount of calcium deposition of glass and PSS-co-MA coated surfaces.

Part II: Fabrication and analysis of the (PDADMAC/PSS)$_4$/PDADMAC+PSS-co-MA coated PEM films on cpTi discs and examination of the function and behavior of osteoblasts grown on PSS-co-MA coated on Ti surface

In part I results, PSS-co-MA coated on glass promote ALP activity and up-regulation of Col I, OPN, BSP and OC mRNA as well as OC protein than glass control. In addition, MC3T3-E1 cells cultured on PSS-co-MA film developed faster rate of *in vitro* calcium deposition compared to the control. However, the question remain whether PSS-co-MA PEM coating Ti could improve osteoblast function and differentiation, when compared to the bare Ti surface. Therefore, PSS-co-MA coated Ti surface was fabricated in this part, and human primary osteoblast function and differentiation were examined.

Surface characterization analysis

The roughness of glasses, Ti discs and PSS-co-MA coated Ti discs were examined by profilometer. The R_a of glass, Ti disc and PSS-co-MA coated surfaces were presented in Table 4.2. Results revealed no significantly difference in surface roughness between the Ti discs and PSS-co-MA coated surfaces. Although significant difference of surface roughness between glass and Ti or PSS-co-MA coated Ti discs was observed.

Table 4.2 Surface roughness determination

Materials	R_a (μm)
Glass	0.014±0.002
Ti	0.104±0.019*
Ti_PSS-co-MA	0.090±0.019*

Data were shown as the mean±SD. * Statistically significant, $p<0.05$

The hydrophilicity

The wettability of the glass, uncoated Ti and PSS-co-MA coated Ti was determined using water contact angle. Results showed that the PSS-co-MA coated surfaces has the lowest contact angle (28.66±0.74°) followed by glass (36.84±1.24°) and Ti disc (51.54±0.63°) as showed in Figure 4.8, indicated PSS-co-MA coated surface has more wettability than the other two.

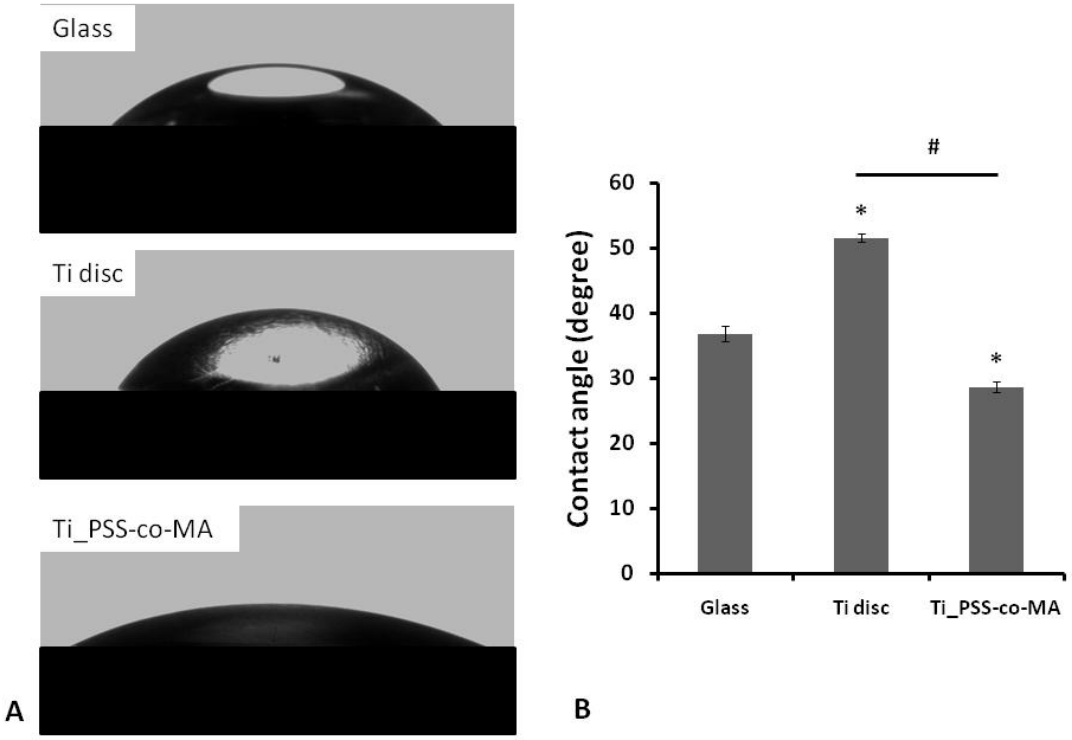

Figure 4.8 The wettability of the glass, Ti and PSS-co-MA coated Ti surfaces

Photographs (A) of water dropped and graphs (B) showed the water contact angle on glass, Ti and PSS-co-MA coated Ti surface. Data were shown as the mean±SD. *****indicates statistically difference between glass cover slips and Ti discs or PSS-co-MA coated Ti disc; # indicates statistically difference between Ti disc and PSS-co-MA coated Ti disc, $p<0.05$.

Cell morphology

Scanning electron microscopy study showed the attachment and morphology of human primary bone cells on all surfaces after seeding for 1 hour (Figure 4.9). Cell began to adhere and spread on the material surfaces within the short time after being seeded. Cells on both Ti and PSS-co-MA surfaces showed slightly higher numbers than glass surfaces. Cells on all surfaces were adherent with a heterogeneous morphology: some cells were rounded, other slightly spreaded (Figure 4.9A, B, C). At higher magnification, cells cultured on PSS-co-MA coated surfaces (Figure 4.9F) appeared more flattened and started to form contact with the adjacent cells, while cells cultured on bear Ti showed less activity (Figure 4.9E).

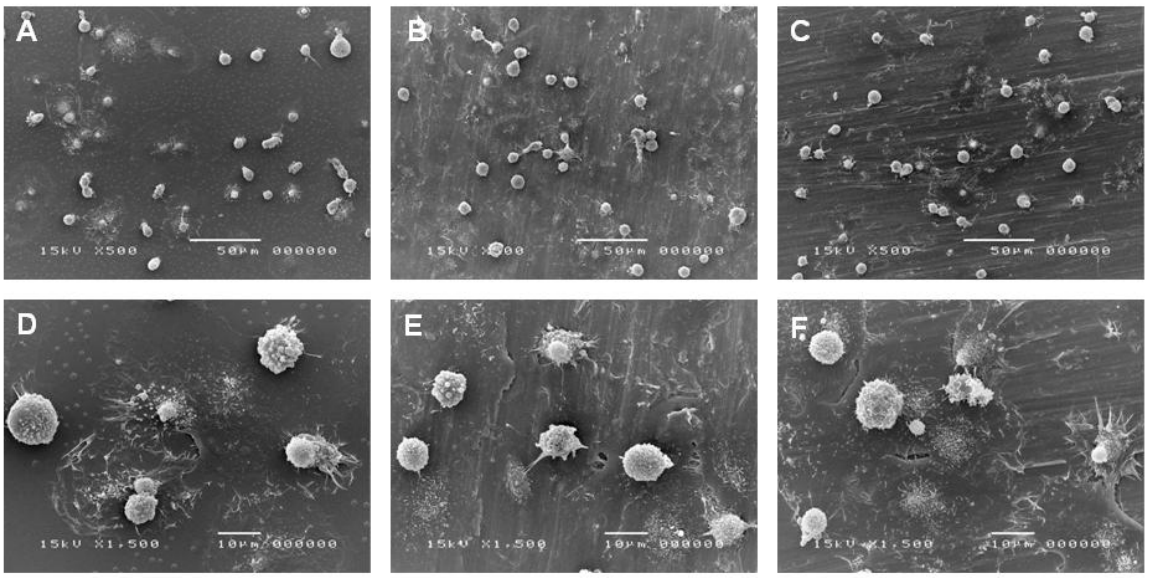

Figure 4.9 Cell morphology on glass, Ti and PSS-co-MA coated Ti surfaces

Human primary osteoblast cells adhesion on glass (A, D), Ti disc (B,E) and PSS-co-MA (C, F) after 1 hour incubation was determined using SEM at magnification of 500x (A, B, C) and 1,500x (D, E, F).

Cell adhesion

MTT assay was used to determined cell adhesion and proliferation. Results showed that the number of the cells increased in according to the culture period (from 4-24 hours) on all surfaces. Although no significant difference of cell numbers between Ti and PSS-co-MA coated Ti discs was observed at 4 hour incubation period. However, PSS-co-MA coating disc yield significant higher cell number at 24 hours as shown in Figure 4.10.

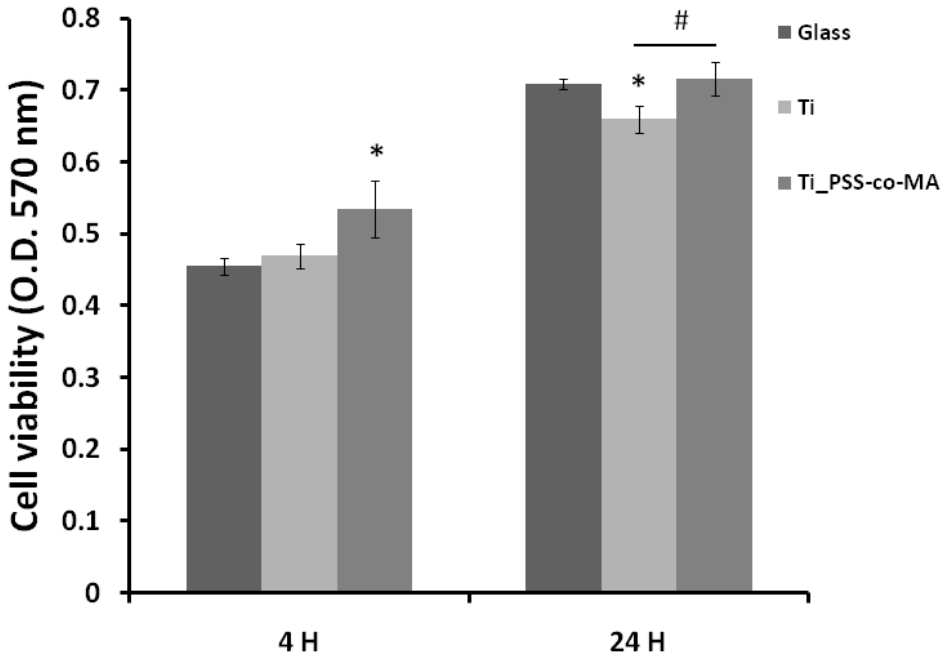

Figure 4.10 Cell viability analysis

The cell number of human primary osteoblast cells cultured on glass, Ti disc and PSS-co-MA coated Ti PEM surfaces was estimated by the MTT assay after 4 and 24 hours incubation. Data were shown as the mean±SD. * indicates statistically difference between glass cover slips and Ti discs or PSS-co-MA coated Ti disc; # indicates statistically difference between Ti disc and PSS-co-MA coated Ti disc, $p<0.05$.

ALP Activity

The ALP activity of human primary bone cells cultured on all surfaces was monitored on days 3, 5 and 7 after seeding (Figure 4.11). Apparently, enzyme activity increased from day 3 to day 7 on both surfaces. The ALP activity of cells seeded on PSS-co-MA PEM was higher than that on bare Ti discs at day 3 with a significant difference at day 5 and 7.

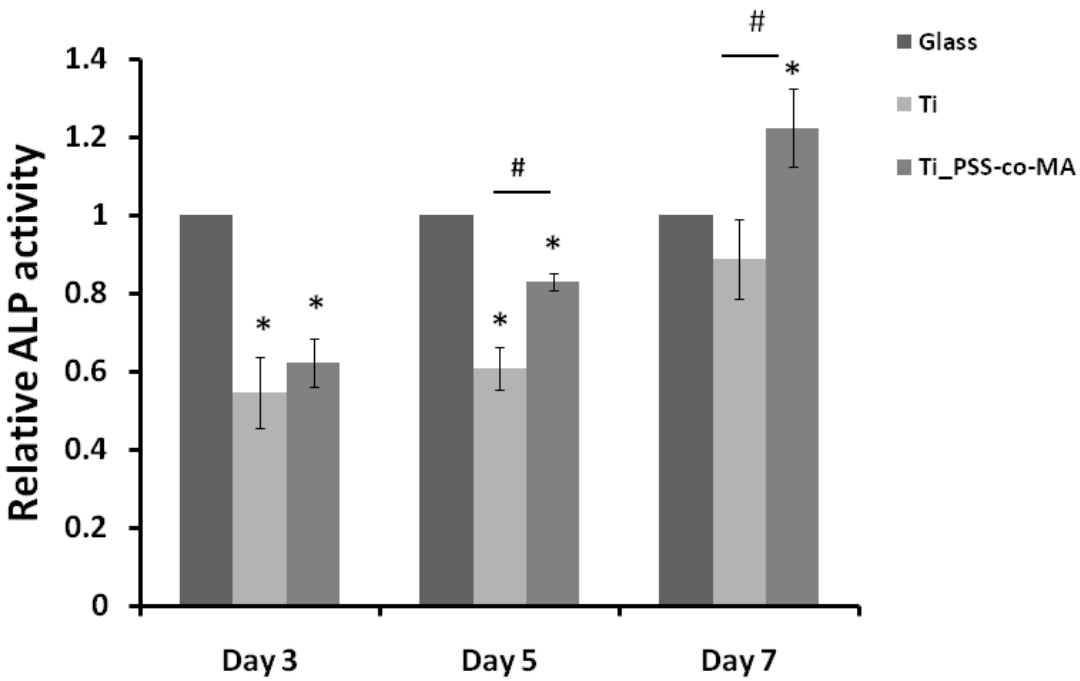

Figure 4.11 Alkaline phosphatase activity

Relative ALP activity after 3, 5 and 7 days of human primary osteoblast cultured on glass, Ti and PSS-co-MA coated surfaces. Data were shown as the mean±SD. * indicates statistically difference between glass cover slips and Ti discs or PSS-co-MA coated Ti disc; # indicates statistically difference between Ti disc and PSS-co-MA coated Ti disc, $p<0.05$.

Osteoblastic gene expression

The expressions of osteoblastic related genes were examined by RT-PCR at day 14 (Figure 4.12). Expression of BSP, OC, and DMP1 mRNA was significantly increased in osteoblasts seeded on PSS-co-MA coated Ti surfaces, when compared to bear Ti discs and glass cover slips. Graphs showed relative band intensity normalized to GAPDH.

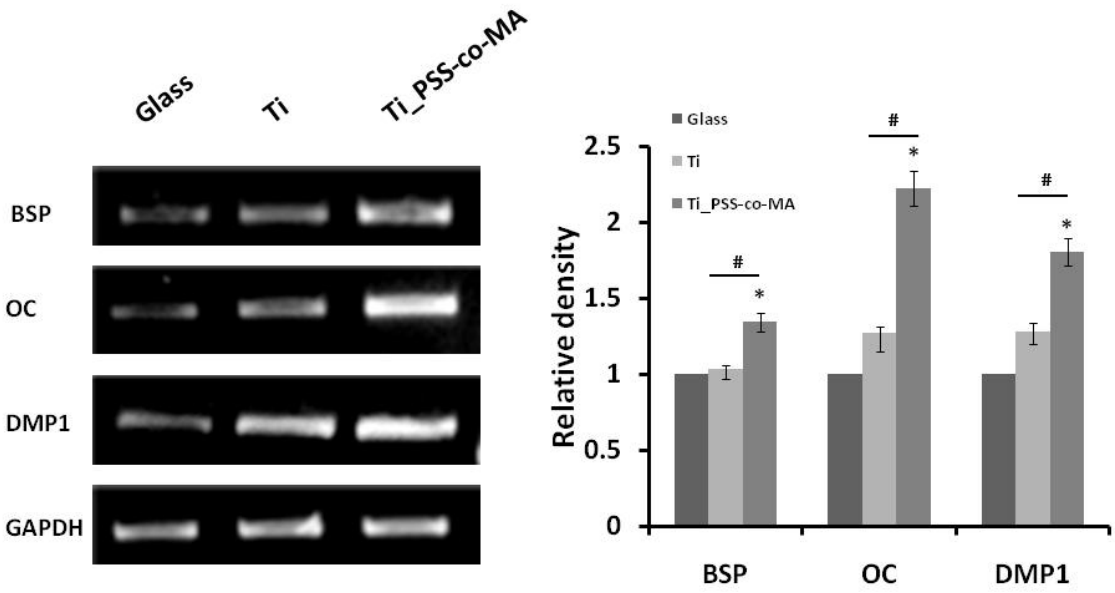

Figure 4.12 The mRNA expression of osteoblast marker genes

The expressions of BSP, OC, DMP1 were examined by RT-PCR analysis at day 14. Graph showed the band intensity normalized to GAPDH. Data were shown as the mean±SD. * indicates statistically difference between glass cover slips and PSS-co-MA coated Ti disc; # indicates statistically difference between Ti disc and PSS-co-MA coated Ti disc, $p<0.05$.

Osteocalcin analysis using ELISA

To confirm the change in OC expression, the OC level of human primary osteoblast was examined using ELISA at day 14 as showed in Figure 4.13. Significant increase of OC synthesis was observed in cells grown on PSS-co-MA coated Ti surface compared to the other two.

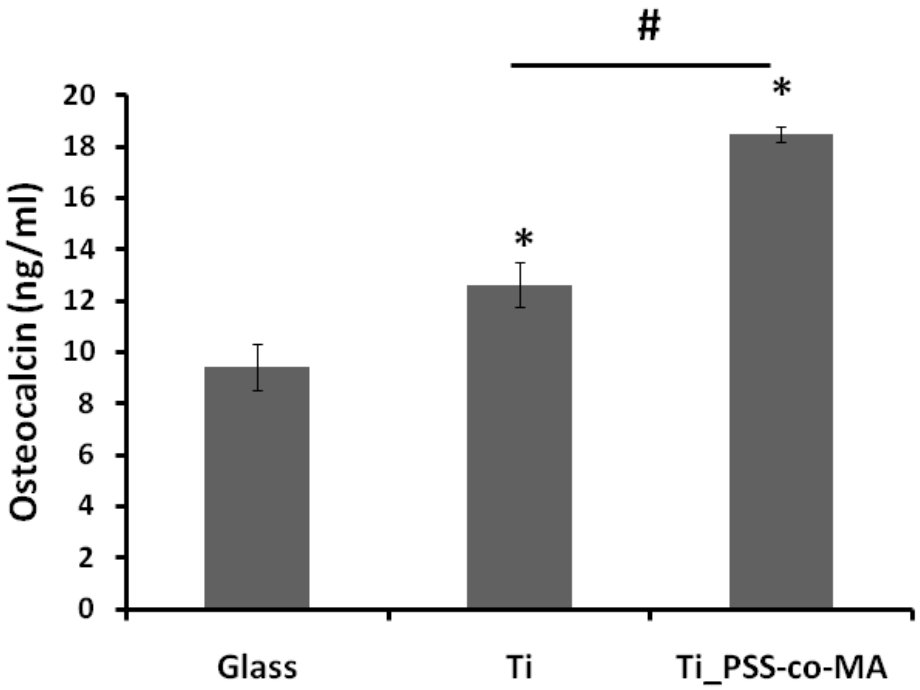

Figure 4.13 Osteocalcin analysis

The protein synthesis of OC human osteoblast cells cultured on glass, Ti and PSS-co-MA surface at day 14 was examined by ELISA analysis. Data were shown as the mean±SD. * indicates statistically difference between glass cover slips and Ti discs or PSS-co-MA coated Ti disc; # indicates statistically difference between Ti disc and PSS-co-MA coated Ti disc, $p<0.05$.

***In vitro* bone nodule formation**

In addition to studying osteoblast differentiation, *in vitro* calcification was also examined. Cells were cultured in the presence of ascorbic acid, β-glycerophosphate and dexamethazole for 15 days. The culture was fixed and stained with Alizarin red-S to evaluate the presence of *in vitro* calcification. Results showed more reddish deposition in cultured on PSS-co-MA coated Ti surfaces than on the glass and uncoated Ti surfaces (Figure 4.14A).

The amount of calcium deposition on each surface was quantified colorimetrical using 10% cetylpyridinium chloride monohydrate. The result showed that the amount of calcium deposition of the PSS-co-MA coated surfaces was significantly greater than the glass and Ti discs (Figure 1.14B).

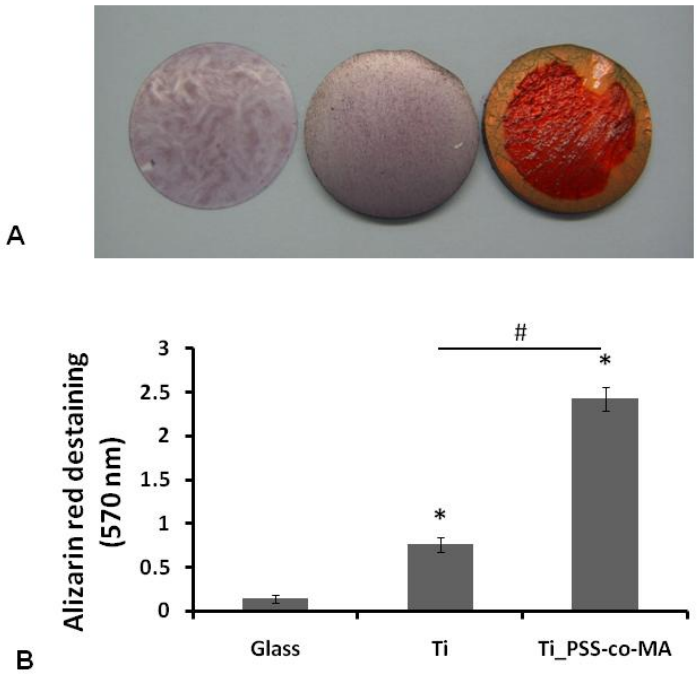

Fig. 4.14 *In vitro* bone nodule formation

Alizarin red-S staining showed the calcification in cells cultured on glasses, Ti and PSS-co-MA coated Ti surfaces (A) with the presence of ascorbic acid, β-glycerophosphate and dexamethazole at days 15. The amount of calcium deposition of the PSS-co-MA coated surfaces was determined by eluting with 10% cetylpyridinium chloride monohydrate (B).

Part III: Analysis of *in vivo* bone formation after implantation of PCL and PSS-co-MA coated PCL films in mouse model

PCL are biodegradable and biocompatible material and has been approved by FDA to use in human. In Part III, the ability of PSS-co-MA coated PCL films for supporting bone formation was evaluated in calvarial defects of mice, compared to PCL films.

The sections of calvarial after 6-week implantation were showed in Figure 4.15. After dissection, the images of calvarial skulls were taken with under stereomicroscopes to determine gross structure of bone formation (Figure 4.15A, 4.15B). The results showed that the implanted sites with PSS-co-MA coated PCL films had the amount of new bone formation greater than the sites implanted with PCL films.

Form Masson's Trichrome staining section (Figure 4.15C), the calvarial defect implanted with PCL film was filled with a thin, loose connective tissue with minimal mineralization around space of PCL films. On the contrary, the sited implanted with PSS-co-MA coated PCL contained obviously new bone formation at the outer side of defect. However, on the inner side of defect, which contact to the brain, loose fibrous connective tissue was formed with minimal bone formation. Histomorphometric analysis indicated an increased amount of new bone formation in PSS-co-MA coated PCL films as compared to the PCL films.

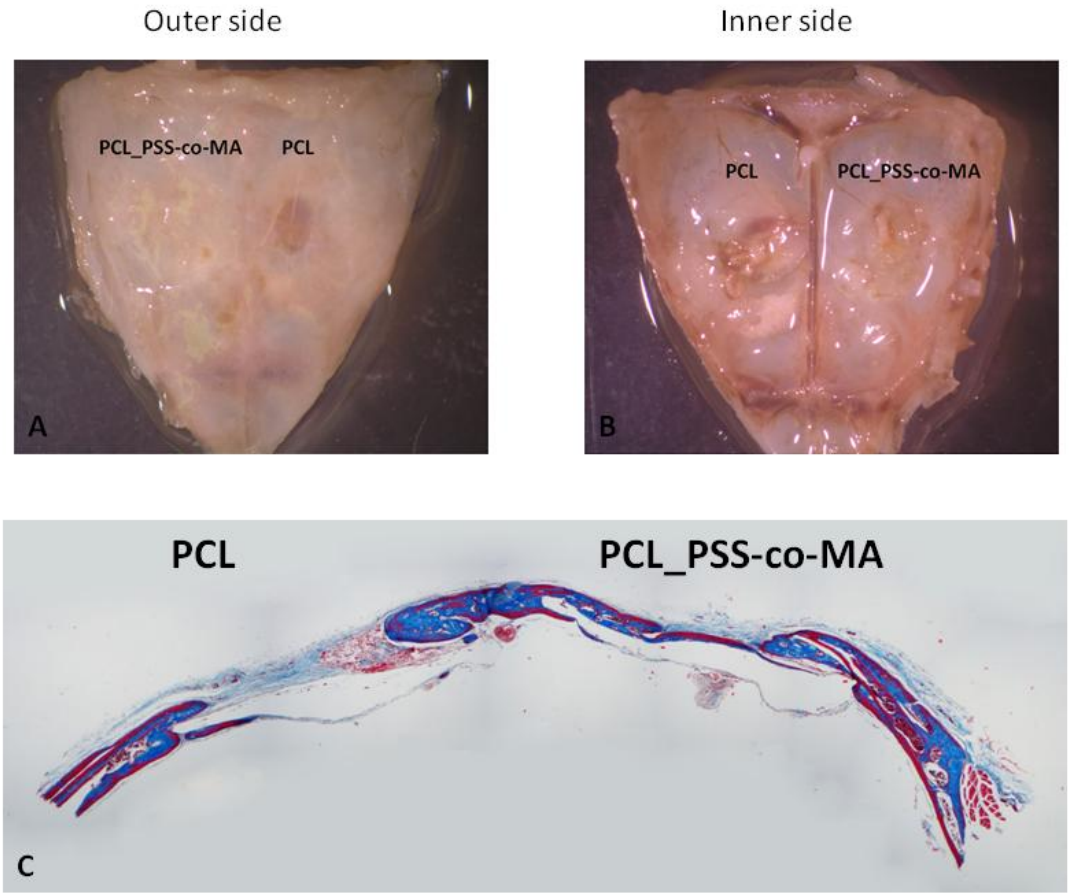

Figure 4.15 *In vivo* bone formation by implantation of PCL and PSS-co-MA coated PCL films

Stereomicroscopy images of outer (A) and inner sides (B) mice calvarial skull. Histological analysis of the sections stained with Masson's Trichrome staining was shown in (C) after 6-week implantation with PCL and PSS-co-MA coated PCL films.

CHAPTER V

DISCUSSION AND CONCLUSION

DISCUSSION

In this study, a surface modification was created by LbL technique. The PSS-co-MA PEM surface was generated by alternately exposing a substrate to positively (PDADMAC) and negatively (PSS or PSS-co-MA) charged polyelectrolyte solution under the controlled concentration of polymer and salt, pH of the solution and time of deposition.

Surface modification using PEM technique, a technique in which nanoscale layers of polyanion and polycations dipped onto a charged surface, has attracted an interest in the fields of implantable biomaterials and tissue engineering in recent years. The major reasons for this interest are their ease of processing, variety of materials which can be incorporated into their assembly (such as inorganics[73], proteins[20, 68, 69], DNA[72], polysaccharides[19, 20, 56], hormones[70], bioactive molecule[61, 64], biopolymer[16, 63]), capability of coating on a variety of materials (i.e. metal, ceramic, polymer and glass), tunable film thickness depending on the number of layers deposited and the solution conditions (i.e. pH, ionic strength, salt concentration[74]) used during fabrication, and the versatility of the technique.

Early studies of multilayer systems focused on the use of strong polyelectrolytes, where the charge density is effectively constant over a broad pH range[27]. In these systems, electrostatic interactions dominate, and it has been demonstrated that the film assembly and film properties are influenced by the charge density and molecular weight of the adsorbing species, and the ionic strength of the adsorption solutions. Positively charged PDADMAC and negatively charged PSS, which are strong polyelectrolytes, were used as a pair of polyelectrolytes in several studies to investigate the PEM properties such as influence of charge density, ionic strength, salt concentration, salt type, solvent quality, deposition time, polymer concentration and type of film deposition on the thickness, morphology, roughness and electrokinetic property of PEM films[23, 49, 74, 75]. For example, McAloney *et al.*[74] studied the influence of the salt concentration on the deposition of PDADMAC/PSS pair PEM films and showed that increased thickness and roughness of films were found to increase with the concentration of added salt. Study of

Schlenoff *et al.*[75] PADMAC/PSS film buildup for sprayed and dipped silicon wafers is compared and no significance of film thickness and chemical composition between two methods was observed. Dubas and Schlenoff[23] fabricated PDADMAC/PSS with varied salt and polymer concentration, type of salt and deposition times and demonstrated the influence of these factors on PEM films. Their results revealed the correlation between an increase of polymer concentration, salt concentration or deposition times with increasing layer number. Moreover, different type of salt also affected the thickness of PEM films.

PDADMAC and PSS were selected to form the base of PEM films before coating with different type of polyion[76-78]. These two polyelectrolytes have been chosen for PEM preparation due to their strong polyelectrolyte characteristic, which are independent of pH condition. The hydrophobic ring structure of PDADMAC polycations is stiff and consequently difficult to rotate, both in water and in the air, therefore, the outer layer containing the quaternary ammonium end groups can maintain hydrophilic property both in water and in the air and help supporting the outer PSS layer[26]. The success of PDADMAC and PSS forming PEM film was demonstrated. Ai *et al.*[76] successfully produced organized nanoshells on platelets by the LbL technique. Platelets were first coated with precursor layers of PDADMAC/PSS/PDADMAC and followed by one of the three ways including, $(FN/PDADMAC)_2$, $(silica/PDADMAC)_2$ and $(PSS/IgG)_2$. In another report, Grant *et al.*[77] had fabricated the PDADMAC$(PSS/Col\ I)_2$ coated PEM films for neural prosthesis and found that PEM film terminated with Col I can support the attachment and growth of C2C12 myoblast cells and PC12 pheochromocytoma cells. Moreover, Ladhari *et al.*[78] prepared PEM films from $(PSS/PDADMAC)_{20}$ with the presence of 1 M NaCl and subsequently imprinted with polydimethylsiloxane stamps and demonstrated that the depth of the initially imprinted channels did not significantly change over at least 9 months of storage in the dry state. When immersed these imprinted PEM films into a 0.15 M NaCl solution, mimicking biological fluids, the imprinted film shape and channel depth did not change. On the other hand, when the imprinted PEM films were put in presence of 4 M NaCl solutions, partial desorption of the film occurred and the imprinted shape practically disappeared. They proposed that these modified imprinted PEM films should offer large opportunities for the use of the imprinted PEM films as microfluidic channels.

Recently, weak polyelectrolytes had become more preferable in multilayer thin films fabrication. By varying the ionization of the weakly charged groups through pH adjustments, the properties of PEM film could be adjusted easier. Several weak polyelctrolytes, such as PAH, PAA and PSS-co-MA, were used to study the influence of pH change on PEM films properties[28, 79-81]. PSS-co-MA is a copolymer, containing strong sulfonate group in PSS, which expected to form electrostatic linkages (to enhance film stability), and weak carboxylic group from maleic acid (MA) segment. Report from Tjipto *et al.*[28] showed that PEM films could be produced from PSS-co-MA and PAH with varied several assembly conditions such as pH, PSS/MA ratio in PSS-co-MA, and the ionic strength of the polyelectrolyte solutions. The thickness of PSS-co-MA/PAH films decreased with increasing pH of PSS-co-MA solutions (pH 2-11). In addition, PEM films without salt were thinner, smoother, and grow less regularly than the presence of salt in polyelectrolyte solutions. Analysis of PSS/MA ratio revealed that the 3:1 ratio of PSS:MA in PSS-co-MA produced the thinner and rougher film compared to the 1:1 ratio[28, 80]. It has been shown that PSS-co-MA/PDADMAC films are significantly more stable than PSS-co-MA/PAH multilayers after post-assembly pH treatment (i.e. the films remain intact when exposed to pH extremes)[80]. From these results, they mentioned that by careful choice of the assembly conditions, stable and pH-responsive films can be obtained from PSS-co-MA/PDADMAC films. These films can find application in areas where fine control over the film morphology, and rearrangement with variation in pH are desirable, such as in the controlled release of therapeutics. For clinical application, PSS-co-MA has been recently used as an cation-exchange membranes, since the maleic acid has two ion-exchangable sites and exhibits lower water uptake than sulfonic acid[29]. However, it was never been applied in order to influence osteoblast behavior.

In this study, PDADMAC and PSS were used to fabricate the base of PEM films {(PDADMAC/PSS)$_4$/PDADMAC} before finally deposited with several polyelectrolytes, including PSS, PAA, GEL, SiO_2, and PSS-co-MA (as showed in Appendix A) in order to find the suitable morphology, thickness and roughness of PEM based films prior to the final layer coating. The appropriate film thickness was 9 layers of PDADMAC and PSS, as less film thickness resulted in unconstant polyelectrolytes distribution on substrate surfaces (data not showed) with high variation of PDADMAC and PSS absorbance observed by US-vis spectroscopy. The

preliminary results using MC3T3-E1, an osteoblast cell-line, seeded on $(PDADMAC/PSS)_4$/PDADMAC, indicated that PDADMAC coated surface could not support cell adhesion (data not showed), whereas, PSS-co-MA coated surface showed a good support for osteoblast adhesion and differentiation (determined by ALP activity as showed in Appendix A). Therefore, PSS-co-MA was selected to use as a final layer on the $(PDADMAC/PSS)_4$/PDADMAC base.

The results from this study direactly demonstrated the ability of PSS-co-MA PEM surface for supporting an *in vitro* osteoblast functions and differentiation for the first time. Results indicated that the PSS-co-MA PEM films enhanced the osteoblast differentiation by means of ALP activity, osteoblastic gene expression (Col I, OPN, BSP, OC and DMP1) and OC protein synthesis as well as *in vitro* calcification. Moreover, PSS-co-MA PEM coated on PCL films could support *in vivo* bone formation in calvarial defects of mice.

The terms osteoinduction and osteoconduction are frequently, but not always correctly, used in bone tissue engineering papers. Suggested definitions of osteoinduction and osteoconduction were described[42]. Osteoinduction means that primitive, undifferentiated and pluripotent cells are somehow stimulated to develop into the bone-forming cell lineage. One proposed definition is the process by which osteogenesis is induced. While osteoconduction means that bone grows on a surface. An osteoconductive surface is one that permits bone growth on its surface or down into pores, channels or pipes. From these definitions, our results suggested osteoconductive, but not osteoinductive properties of PSS-co-MA coated PEM surface.

The use of osteoblast cell lines, such as SaOS-2, MG63 and MC3T3-E1, to examine the osteoblast-biomaterials interaction *in vitro* is favorable due to their immortalization. Therefore, the phenotype expression of these cells will be maintained without senescence over a long period of time and after many passages. In this study, mouse MC3T3-E1 cell line was chosen in part I of the study. However, evidence suggested the variable pattern of growth control and gene differentiation expression[82], while primary cells is believed to be much more correlated to the *in vivo* condition[83]. Therefore, human primary osteoblast cells were used in part II of the study.

Generally, the process of osteoblast differentiation can be divided into proliferation period, extracellular matrix deposition, maturation and mineralization[84]. Specific pattern of gene expression were found correlated with certain stage of osteoblast differentiation and could be used to represent each stage of differentiation. Col I and ALP are highly expressed start at the end of the proliferative period to the period of extracellular matrix deposition and maturation, while OPN, BSP and OC are highly expressed at or near the time of mineralization[85]. Col I is the most abundant protein in bone matrix serves as a template for mineralization[86]. Moreover, Col I is an essential matrix protein that plays a fundamental role in the maintenance of osteoblastic phenotype making the matrix competent for mineralization[87]. ALP, a membrane bound enzyme, is abundant by expressed in early stages of bone formation and has been considered as an early marker of osteoblast differentiation. Increased ALP levels correlated with increased bone formation histomorphometrically[88]. OPN is a phosphorylated glycoprotein which contains a string of polyaspartic acid residues as well as RGD sequence. OPN is believed to facilitate the attachment of osteoblasts and osteoclasts to the extracellular matrix, allowing them to perform their respective functions during osteogenesis[89]. BSP is a highly glycosylated and sulphated phosphoprotein that is almost exclusively found in mineralized connective tissues such as bone and cementum. BSP contains large stretches of poly(glutamic acids) as well as the RGD sequence at its carboxy terminus with the ability to bind hydroxyapatite and cell-surface integrins and act as a nucleator of the initial apatite crystal[86, 90]. OC or γ-carboxyglutamic acid or Gla protein, an abundant Ca^{2+} binding protein commonly found in the organic matrix of mineralized tissues such as bone, dentin, and cementum[91], is highly expressed at or near the time of mineralization and has been considered as the late-stage marker of osteoblast differentiation. DMP1 is an acidic phosphoprotein, which is predominantly expressed in dentine and bone. It has been reported that DMP1 promotes cell attachment through the RGD motif in a cell- and tissue-specific manner as well as the expression of DMP1 was closely associated with bone nodule formation and mineralization through an unusually large number of acidic domains[92]. In present study, it well demonstrated that the PSS-co-MA films can induce an increase the ALP activity, expression of osteogenic marker genes including Col I, OPN, BSP, OC and DMP1.

In addition, higher calcium deposition level was found in cell cultured on PSS-co-MA coated surfaces compared to the control when examined by using Alizarin red-S staining, which is commonly used to detect and quantify calcium within the deposited mineral. Since bone nodule formation, is considered a functional *in vitro* endpoint reflecting advanced osteoblast differentiation, the increase of *in vitro* mineralization support the potential of PEM film in osteogenic differentiation. Taken together, the *in vitro* data suggests that PSS-co-MA PEM film may be able to support or accerelate the osteogenic differentiation.

It has been proposed that the influence of PEM film on cellular behaviors depended on the coated surface regardless of the substrate used[71, 93]. Elbert *et al.* demonstrated that when bioactive surface, i.e. TCP, gelatin adsorbed TCP or fibroblast extracellular matrix, was coated with PLL/ALG PEM film, the decrease of cell spreading was observed in all modified surfaces[94], suggesting the influence of PLL/ALG PEM coated surface, not substrate materials, on cellular response. In addition, it has also been reported that fibroblast cells response differently depended on the type and nature of coated PEM film, supporting the crucial role of material's surface properties on biological interaction[67]. Therefore, to rule out the effect of titanium from $(PDADMAC/PSS)_4$/PDADMAC+PSS-co-MA film, glass has been chosen instead of titanium disk. Although the data supports the potential of $(PDADMAC/PSS)_4$/ PDADMAC+PSS-co-MA PEM, the PEM film on titanium surface should be investigated. From the part II results, the similar trends of osteoblast response were observed on $(PDADMAC/PSS)_4$/PDADMAC+PSS-co-MA coated Ti surface compared to those on Ti surface. These may lead to potential application of $(PDADMAC/PSS)_4$/PDADMAC+PSS-co-MA coated film for endosseous Ti implants.

In part I, AFM analysis showed the existence of uniform and homogeneous polyelectrolyte deposition on the glass surface. The thickness of PSS-co-MA film could be measured, confirming the presence of PSS-co-MA film on glass surface. It is well established that surface characteristics of biomaterials have direct influence on cellular response by affecting protein adsorption and by modulating cell proliferation and differentiation[95, 96]. Among these characteristics, surface roughness is one of the important parameters that influence protein adsorption and cellular behavior. The effect of microscale surface topography on cellular responses has long been recognized[97-99]. However, nanoscale modification of an implant

surface could also provide the suitable environment that favored the process of rapid bone formation/remodeling. Surface feature as small as 10 nm could influence cell adhesion and differentiation[100, 101]. However, it is still controversial depending upon the degree of the roughness. For example, Washburn *et al.* fabricated the gradients of polymer crystallinity on poly(l-lactic acid) films to form roughness values ranging from 0.5 to 13nm. They found that the rate of proliferation on the smooth regions of the films is much greater than that on the rough regions[102]. In contrast, several investigations showed that surface roughness in the range of 20-85 nm promote better adhesion, proliferation and differentiation of osteoblastic cells[103-105]. Similarly, the effect of surface nanoscale features on protein adsorption is still unclear. While some report showed no influence of nanoscale level on protein adsorption[106, 107], several reports revealed an increase amount of adsorbed proteins when nanoscale surface roughness increased[108, 109]. For example, Rechendroff *et al.* fabricated nanoscale Ti surface by etching and glancing angle deposition technique and reported the increased FN adsorption correlated with the increase surface roughness (12-44 nm). Moreover, study of Scopelliti *et al*.[110] also showed that the increase of nanoscale roughness (from 15 nm to 30 nm) induces a relevant increase in adsorbed FN and albumin (ALB). In contrast, Cai *et al*.[106] found that the amount of fibrinogen and ALB adsorbed onto nano-rough Ti surfaces (2-21 nm) was unaltered compared to flat control Ti.

The increase of surface roughness in this study may not directly correlate to osteoblast differentiation. Although the roughness of PSS-co-MA coated on glass was significantly higher than glass surfaces, no significant difference in roughness between the Ti discs and PSS-co-MA coated Ti surface in a micrometer range was observed. Since the PSS-co-MA on both Glass and Ti gave the similar results, the micro roughness might not account for the phenomena. Moreover, when glass surfaces were coated with only PSS-co-MA alone, and produce the same roughness as the PEM, no favorable effect on osteoblast behavior was found (data not shown).

Furthermore, PSS-co-MA coated surfaces had better wettability as compared to control uncoated glass and Ti discs. It is well documented that hydrophilic/hydrophobic balance of a given surface is a major parameter affecting cellular behavior at the cell-materials interface. However, effects of surface wettability on cellular behavior are reported to be inconsistent and

controversial. For example, it had been shown that hydrophobic materials effected greater cell attachment than hydrophilic materials[111]. In contrast, there were studies demonstrating the positive effects of hydrophilic surfaces on cell adhesion for various cell types whereas moderately hydrophobic surfaces often inhibited cell-material interaction[112-114].

Despite the better hydrophilicity, the number of cells adhering on PSS-co-MA coated films was comparable to glass surfaces, suggesting hydrophilicity may not be the sole factor involved in cell attachment. The results of this study are in agreement with a report from Faucheux and coworkers[112], comparing the attachment of human fibroblasts on various modified surfaces, using different terminating functional groups. Weak interaction was observed when cells were grown on self-assembling monolayers (SAMs) terminating with methyl (CH_3) groups, which is considered a hydrophobic surface. In contrast, strong cell attachment, spreading, and growth were found in cells cultured on moderate hydrophilic COOH terminated SAMs[112]. Therefore, cell attachment and spreading might also depend on the different terminal functional groups on the material's surface.

Surface wettability was also accounted for protein adsorption property. It has been reported that protein absorbed on hydrophobic surface better than on hydrophilic surfaces[114-116]. However, surface wettability, is not solely determined by the micro- or nanostructure of surfaces, but also by the chemical composition, *i.e.* by the presence of hydroxyl, carboxyl, amine and other organic or inorganic chemical groups[37, 112]. These different chemical groups on the surface might support different type of protein interaction. Therefore, different type of protein might showed the different amount of absorption on the surface. For example, FN absorbed better on the hydrophilic surface, whereas ALB predominantly adsorbed on the hydrophobic surfaces[117-119].

During the process of surface modification, it is extremely difficult to control one factor from the others. Modification of surface composition could also changed other surface properties such as surface topography, roughness and wettability and thus preventing the identification of the genuine effect of one factor[36]. Evidence indicated that modification of Ti implant surfaces altered surface roughness, wettability and chemical composition that generated the better biosystem-material interface[37].

In terms of surface chemistry, studies suggested that nature and chemical composition of PEM films could affect adhesion and proliferation of cells cultured on the films[67, 71, 93, 120, 121]. Various cell types such as fibroblasts[67], osteoblast-like cells (SaOS-2, MC3T3-E1)[71, 93], human periodontal ligament (PDL) cells[93], endothelial cells[120] and various hepatocytes (human hepatocellular carcinoma cells, adult rat hepatocytes and human fetal hepatoblasts)[121] have been studied. For example, Tryoen-TÓth *et al*. suggested that a good cell adhesion, proliferation and stability of osteoblast phenotype of PSS- and PGA-ending films for PDL cells and of PSS-, PGA-, and PLL-terminating films for SaOS-2. On the other hand, the PEI-terminating layers was cytotoxic for both cells[93]. Furthermore, results of Chua *et al*. showed that CHI-graft Ti substrates better support MC3T3E-1 cell adhesion than HA-graft Ti and HA/CHI PEM functionalized Ti. Moreover, the immobilization of RGD peptide on the HA/CHI PEM functionalized Ti had a significant effect on osteoblast proliferation and ALP activity while retaining high antibacterial efficacy[71]. These results indicated the importance of chemical composition on the modified surfaces on cell behavior.

Evidences indicated that differentiation of osteoblasts on the material surface depend on material surface chemistry and topography. Previously we and others showed that different type of Ti (cpTi and Ti alloys) showed different effect on function and differentiation of osteoblast[122, 123]. It has been proposed that the different may due to the surface chemistry. Report from Scopelliti *et al.* showed that surface nanostructure affect cell behavior through the ability and type of protein adsorption[110]. They suggested that different types of protein that aggregated on the materials surface provide the environment for cell adhesion and subsequently differentiation[110]. Furthermore, the works of Keselowsky *et al.* revealed that different form of chemical groups adsorbed on the surface affected the cellular behavior differently[124-126]. These data supported the importance of surface chemistry compatibility on protein adsorption, attachment and differentiation of osteoblast on the implant materials.

The effect of surface chemistry on cell-material interactions might be considered as secondary effects. The type and amount of proteins adsorbed on the surface may act as a primary factor governing the cell-surface interactions. This hypothesis is in agreement with the work reported by Ma *et al*., who showed the hydrophilic and hydrophobic surface did not directly govern cell attachment. Rather, the ability of moderate wettable surfaces in adsorbing a proper

amount of protein is the key for improving cell-materials interactions[114]. In this study, the upper surface of PEM contained maleic acid. Maleic has been used in several studies to prepare the materials surface for protein adsorption such as FN[127, 128]. Renner *et al*. indicated that maleic anhydride coating was suitable for FN adsorption[128]. FN is a multifunctional glycoprotein that plays an important role in osteoblast differentiation. Moursi *et al*. used a polyclonal anti-FN antibody to study the role of FN in the progressive differentiation of osteoblast[129]. They found that osteoblast interactions with the central cell-binding domain of FN (integrin-mediated mechanism) are required for *in vitro* nodule formation. Moreover, they reported that the disruption of osteoblast-FN interactions suppressed expression of ALP and OC mRNA but had no significant effect on Col I and OPN mRNA expression. In addition, Jimbo *et al.* studied the effects of plasma FN (pFN) on the osseointegration process in the mice femur[6]. They showed the increased OC mRNA expression at bone-implant interface and found the faster rate of bone formation on the pFN-coated implant surface compared to the control. It is possible that the mechanism of PSS-co-MA on the induction of osteoblast differentiation is due to the rapidly adsorbed proteins on the films. The ability of PSS-co-MA surface on the amount and type of protein absorption needs further investigation.

Due to the fact that nanoscale PSS-co-MA coated surface is hydrophilic, it was interesting to investigate the amount and type of protein adsorbed on the sureface such as vitronectin, which involved in osteoblast cell adhesion, spreading and differentiation[130, 131]. Webster *et al*. showed greater concentrations of vitronectin and FN adsorption on nanophase ceramics, compared to conventional surface, resulted in enhanced osteoblast adhesion[103, 132]. In addition, Faucheu *et al.* showed greater protein adsorption, especially vitronectin, on hydropillic surfaces terminated with COOH group[112], which also presented in maleic acid.

Despite the surface property on protein adsorption, the increased differentiation and mineralization observed in this study may result from the direct interaction of cells to the PEM film. PSS-co-MA contains certain amount of carboxyl group from maleic acid which may interact with osteoblast cell surface. Formation of ionic bonds between the carboxyl group of maleic acid and the calcium of hydroxyapatite and enamel has been reported[133-135]. The direct interaction between maleic acid and osteoblast participates in the induction ability of PSS-co-MA film remain to be elucidated.

Although the *in vitro* results are promising, *in vivo* study is still required to confirm the potential of PSS-co-MA PEM film. Synthetic polymer has been approved to use in bone tissue engineering. In this study, we modified the synthetic polymer, PCL, with PSS-co-MA PEM film and implanted in calvarial defect of mice. PCL is semi-crystalline linear resorbable aliphatic elastomeric polyester, rubbery characteristics, low melting point ~ 58-60°C, high thermal stability, good solubility in most solvent, hydrophobic, biodegradable, biocompatible and FDA-approval[136-138]. PCL has been recently suggested several clinical applications, including ureteral substitution, urethral catheters, drug delivery systems, resorbable sutures, temporary joint spacer, as well as bone and cartilage tissue engineering [137, 139]. Besides, many studies reported that PCL could support cell attachment, proliferation, differentiation and *in vitro* mineralization of osteoblast cells[140-142]. Moreover, the study of Bhattacharya *et al*, PCL sheets were used as substrate to fabricate carbon nanotube (CNT)-comp {[(polydimethyldiallylammonium/PSS)$_2$(PEI/single-welled CNT)$_6$]$_{10}$PEI on the PCL} using LbL technique and were implanted in the calvarial defect of Sprague-Dawley rats for 6 weeks. They showed that CNT-comp permitted bone formation and bone repair without signs of rejection or inflammation[143].

PCL is generally considered as a nontoxic and tissue compatible polymer. After PSS-co-MA coated PCL implantation, PCL films will be degrade within 2-3 years by hydrolysis of ester linkage, while its degradation products caproic acid will be resorbed through the metabolic pathways [144]. The degradation mechanisms and metabolic products of PDADMAC, PSS and PSS-co-MA are still unknown, but might occur through hydrolysis or enzymatic degradation. Therefore the degradation mechanisms and products of these synthetic polymers should be investigated before clinical used.

To evaluate the *in vivo* effect of PSS-co-MA PEM surface, PSS-co-MA coated PCL films were implanted in calvarial of mice with naive PCL sheet as a positive control. Results from histomorphometric analysis revealed the greater amount of new bone formation in PSS-co-MA coated PCL films compare to naive PCL films. Taken altogether, results from both *in vitro* and *in vivo* studies suggested the significant potential of PSS-co-MA coated PEM films to be used in bone tissue engineering.

CONCLUSION

In the present study, the formation of PSS-co-MA PEM films had been fabricated in order to improve the properties of Ti surface. Cell adhesion, proliferation, differentiation and *in vitro* calcium deposition of MC3T3-E1 and human primary bone cells cultured on PSS-co-MA films were investigated. The results showed that PEM films terminating with PSS-co-MA promoted osteoblast differentiation as shown by increasing in ALP activity, expression of OC mRNA/protein and faster rate of calcification. Furthermore, *in vivo* study showed that PSS-co-MA coated PCL films can accelerate new bone formation in calvarial defects of mice. The results suggested the ability of PSS-co-MA coated PEM surfaces in the enhancement of osteoblast differentiation.

FUTURE STUDY

Although the present study support the role of PSS-co-MA PEM films in osteoblast differentiation and bone formation and its possible clinical application in implantation, the exact mechanism of interaction between PSS-co-MA and osteoblast is still unknown. It is possible that increase in osteoblast differentiation and mineralization observed in this study may result from the rapidly adsorbed proteins, especially FN, on the PSS-co-MA coated films, as well as a direct interaction between maleic acid and osteoblast cell surface. Moreover, formation of ionic bonds between carboxyl group of maleic acid and calcium ion of hydroxyapatite and enamel has also been reported. Therefore, it is important to investigate the detailed underlying mechanism of PSS-co-MA coated PEM films on the induction of osteoblast differentiation. Importantly, the effect of PSS-co-MA coated Ti implant along with the degradation mechanisms and by-products of PDADMAC, PSS and PSS-co-MA need further investigation both *in vitro* and in animal models such as rat, rabbit, dog or monkey before clinical trial in human.

REFERENCES

[1] Puleo, D. A. and Nanci, A. Understanding and controlling the bone-implant interface. Biomaterials 1999;20:2311-2321.

[2] Boyan, B. D., Hummert, T. W., Dean, D. D. and Schwartz, Z. Role of material surfaces in regulating bone and cartilage cell response. Biomaterials 1996;17:137-146.

[3] Marco, F., Milena, F., Gianluca, G. and Vittoria, O. Peri-implant osteogenesis in health and osteoporosis. Micron 2005;36:630-644.

[4] Sato, M. and Webster, T. J. Nanobiotechnology: implications for the future of nanotechnology in orthopedic applications. Expert Rev Med Devices 2004;1:105-114.

[5] Hench, L. L. and Polak, J. M. Third-generation biomedical materials. Science 2002; 295:1014-1017.

[6] Jimbo, R., et at. Enhanced osseointegration by the chemotactic activity of plasma fibronectin for cellular fibronectin positive cells. Biomaterials 2007;28:3469-3477.

[7] Huang, H., et al. Enhanced osteoblast functions on RGD immobilized surface. J Oral Implantol 2003;29:73-79.

[8] Jonasova, L., Muller, F. A., Helebrant, A., Strnad, J. and Greil, P. Biomimetic apatite formation on chemically treated titanium. Biomaterials 2004;25:1187-1194.

[9] de Oliveira, P. T., Zalzal, S. F., Beloti, M. M., Rosa, A. L. and Nanci, A. Enhancement of in vitro osteogenesis on titanium by chemically produced nanotopography. J Biomed Mater Res A 2007;80:554-564.

[10] Fujibayashi, S., Neo, M., Kim, H. M., Kokubo, T. and Nakamura, T. Osteoinduction of porous bioactive titanium metal. Biomaterials 2004;25:443-450.

[11] Yang, B., Uchida, M., Kim, H. M., Zhang, X. and Kokubo, T. Preparation of bioactive titanium metal via anodic oxidation treatment. Biomaterials 2004;25:1003-1010.

[12] Li, L. H., et al. Improved biological performance of Ti implants due to surface modification by micro-arc oxidation. Biomaterials 2004;25:2867-2875.

[13] Tsukimura, N., et al. The effect of superficial chemistry of titanium on osteoblastic function. J Biomed Mater Res A 2008;84:108-116.

[14] Decher, G. Fuzzy Nanoassemblies: Toward Layered Polymeric Multicomposites Science 1997;277:1232 - 1237.

[15] Richert, L., et al. Layer by layer buildup of polysaccharide films: physical chemistry and cellular adhesion aspects. Langmuir 2004;20:448-458.

[16] Etienne, O., et al. Polyelectrolyte multilayer film coating and stability at the surfaces of oral prosthesis base polymers: an in vitro and in vivo study. J Dent Res 2006;85:44-48.

[17] Schultz, P., et al. Polyelectrolyte multilayers functionalized by a synthetic analogue of an anti-inflammatory peptide, alpha-MSH, for coating a tracheal prosthesis. Biomaterials 2005;26:2621-2630.

[18] Etienne, O., et al. Multilayer polyelectrolyte films functionalized by insertion of defensin: a new approach to protection of implants from bacterial colonization. Antimicrob Agents Chemother 2004;48:3662-3669.

[19] Cai, K., Hu, Y., Jandt, K. D. and Wang, Y. Surface modification of titanium thin film with chitosan via electrostatic self-assembly technique and its influence on osteoblast growth behavior. J Mater Sci Mater Med 2008;19:499-506.

[20] Cai, K., Rechtenbach, A., Hao, J., Bossert, J. and Jandt, K. D. Polysaccharide-protein surface modification of titanium via a layer-by-layer technique: characterization and cell behaviour aspects. Biomaterials 2005;26:5960-5971.

[21] Kreke, M. R., Badami, A. S., Brady, J. B., Akers, R. M. and Goldstein, A. S. Modulation of protein adsorption and cell adhesion by poly(allylamine hydrochloride) heparin films. Biomaterials 2005;26:2975-2981.

[22] Klitzing, R. V., Wong, J. E., Jaeger, W. and Steitz, R. Short range interactions in polyelectrolyte multilayers. Curr Opin Colloid Interface Sci 2004;9:158-162.

[23] Dubas, S. T. and Schlenoff, J. B. Factors controlling the growth of polyelectrolyte multilayers. Macromolecules 1999;32:8153-8160.

[24] Kostler, S., Ribitsch, V., Stana-Kleinschek, K., Jakopic, G. and Strnad, S. Electrokinetic investigation of polyelectrolyte adsorption and multilayer formation on a polymer surface. Colloids and Surfaces A: Physicochem. Eng. Aspects 2005;270-271:107-114.

[25] Schoeler, B., Kumaraswamy, G. and Caruso, F. Investigation of the influence of polyelectrolyte charge density on the growth of multilayer thin films prepared by the Layer-by-Layer technique. Macromolecules 2002;35:889-897.

[26] Chen, J., Luo, G. and Cao, W. The Study of Layer-by-Layer Ultrathin Films by the Dynamic Contact Angle Method. J Colloid Interface Sci 2001;238:62-69.

[27] Baba, A., Kaneko, F. and Advincula, R. C. Polyelectrolyte adsorption processes characterized in situ using the quartz crystal microbalance technique: alternate adsorption properties in ultrathin polymer films. Colloids and Surfaces A: Physicochem. Eng. Aspects 2000;173:39-49.

[28] Tjipto, E., Quinn, J. F. and Caruso, F. Assembly of multilayer films from polyelectrolytes containing weak and strong acid moieties. Langmuir 2005;21:8785-8792.

[29] Kang, M., Choi, Y. and Moon, S. Water-swollen cation-exchange membranes prepared using poly(vinyl alcohol) (PVA)/poly(styrene sulfonic acid-co-maleic acid) (PSSA-MA) J. Membr. Sci. 2002;207:157-170.

[30] Balazic, M., Kopac, J., Jackson, J. and Ahmed, W. Review: titanium and titanium alloy applications in medicine. Int. J. Nano Biomater. 2007;1:3-34.

[31] de Jonge, L. T., Leeuwenburgh, S. C., Wolke, J. G. and Jansen, J. A. Organic-inorganic surface modifications for titanium implant surfaces. Pharm Res 2008;25:2357-2369.

[32] Albrektsson, T., et al. The Interface Zone of Inorganic Implants In vivo – Titanium Implants in Bone. Annals of Biomedical Engineering 1983;11:1-27.

[33] Long, M. and Rack, H. J. Titanium alloys in total joint replacement--a materials science perspective. Biomaterials 1998;19:1621-1639.

[34] Martin, J. Y., et al. Effect of titanium surface roughness on proliferation, differentiation, and protein synthesis of human osteoblast-like cells (MG63). J Biomed Mater Res 1995;29:389-401.

[35] Eisenbarth, E., et al. Interactions between cells and titanium surfaces. Biomol Eng 2002;19:243-249.

[36] Zhu, X., Chen, J., Scheideler, L., Reichl, R. and Geis-Gerstorfer, J. Effects of topography and composition of titanium surface oxides on osteoblast responses. Biomaterials 2004;25:4087-4103.

[37] Ochsenbein, A., Chai, F., Winter, S., Traisnel, M., Breme, J. and Hildebrand, H. F. Osteoblast responses to different oxide coatings produced by the sol-gel process on titanium substrates. Acta Biomater 2008;4:1506-1517.

[38] Singhatanadgit, W. Biological Responses to New Advanced Surface Modifications of Endosseous Medical Implants. Bone and Tissue Regeneration Insights 2009;2 1-11.

[39] Roach, P., Eglin, D., Rohde, K. and Perry, C. C. Modern biomaterials: a review - bulk properties and implications of surface modifications. J Mater Sci Mater Med 2007;18:1263-1277.

[40] Branemark, P. I., et al. Osseointegrated implants in the treatment of the edentulous jaw. Experience from a 10-year period. Scand J Plast Reconstr Surg Suppl 1977;16:1-132.

[41] Albrektsson, T., Branemark, P. I., Hansson, H. A. and Lindstrom, J. Osseointegrated titanium implants. Requirements for ensuring a long-lasting, direct bone-to-implant anchorage in man. Acta Orthop Scand 1981;52:155-170.

[42] Albrektsson, T. and Johansson, C. Osteoinduction, osteoconduction and osseointegration. *Eur Spine J* 2001;10 Suppl 2:S96-101.

[43] Davies, J. E. Understanding peri-implant endosseous healing. J Dent Educ 2003;67:932-949.

[44] Advincula, M. C., Rahemtulla, F. G., Advincula, R. C., Ada, E. T., Lemons, J. E. and Bellis, S. L. Osteoblast adhesion and matrix mineralization on sol-gel-derived titanium oxide. Biomaterials 2006;27:2201-2212.

[45] Harle, J., Kim, H. W., Mordan, N., Knowles, J. C. and Salih, V. Initial responses of human osteoblasts to sol-gel modified titanium with hydroxyapatite and titania composition. Acta Biomater 2006;2:547-556.

[46] Kim, H. W., Koh, Y. H., Li, L. H., Lee, S. and Kim, H. E. Hydroxyapatite coating on titanium substrate with titania buffer layer processed by sol-gel method. Biomaterials 2004;25:2533-2538.

[47] Salloum, D. S. Surfaces modified with polyelectrolyte multilayers for bio-interface applications. In: Department of Chemistry and Biochemistry The florida state university college of arts and sciences, Florida, 2004:p.191.

[48] Boudou, T., Crouzier, T., Ren, K., Blin, G. and Picart, C. Multiple functionalities of polyelectrolyte multilayer films: new biomedical applications. Adv Mater 2010;22:441-467.

[49] Klitzing, R. Internal structure of polyelectrolyte multilayer assemblies Phys. Chem. Chem. Phys. 2006;8:5012-5033.

[50] Zhu, H., Ji, J., Barbosa, M. A. and Shen, J. Protein electrostatic self-assembly on poly(DL-lactide) scaffold to promote osteoblast growth. J Biomed Mater Res B Appl Biomater 2004;71:159-165.

[51] Mehta, G., Kiel, M., Lee, J., Kotov, N., Linderman, J. and Takayama, S. Polyelectrolyte-Clay-Protein Layer Films on Microfluidic PDMS Bioreactor Surfaces for Primary Murine Bone Marrow Culture. Adv. Funct. Mater. 2007;17:2701–2709.

[52] Nichols, J. E., et al. In vitro analog of human bone marrow from 3D scaffolds with biomimetic inverted colloidal crystal geometry. Biomaterials 2009;30:1071-1079.

[53] Rinckenbach, S., et al. Characterization of polyelectrolyte multilayer films on polyethylene terephtalate vascular prostheses under mechanical stretching. J Biomed Mater Res A 2008;84:576-588.

[54] Liu, M., Yue, X., Dai, Z., Xing, L., Ma, F. and Ren, N. Stabilized hemocompatible coating of nitinol devices based on photo-cross-linked alginate/heparin multilayer. Langmuir 2007;23:9378-9385.

[55] Moby, V., et al. Poly(styrenesulfonate)/poly(allylamine) multilayers: a route to favor endothelial cell growth on expanded poly(tetrafluoroethylene) vascular grafts. Biomacromolecules 2007;8:2156-2160.

[56] Thierry, B., Winnik, F. M., Merhi, Y., Silver, J. and Tabrizian, M. Bioactive coatings of endovascular stents based on polyelectrolyte multilayers. Biomacromolecules 2003;4:1564-1571.

[57] Kerdjoudj, H., et al. Re-endothelialization of Human Umbilical Arteries Treated with Polyelectrolyte Multilayers: A Tool for Damaged Vessel Replacement. Adv. Funct. Mater. 2007;17:2667–2673.

[58] Huang, L. Y. and Yang, M. C. Surface immobilization of chondroitin 6-sulfate/heparin multilayer on stainless steel for developing drug-eluting coronary stents. Colloids Surf B Biointerfaces 2008;61:43-52.

[59] Sperling, C., Houska, M., Brynda, E., Streller, U. and Werner, C. In vitro hemocompatibility of albumin-heparin multilayer coatings on polyethersulfone prepared by the layer-by-layer technique. J Biomed Mater Res A 2006;76:681-689.

[60] Fu, J., Ji, J., Yuan, W. and Shen, J. Construction of anti-adhesive and antibacterial multilayer films via layer-by-layer assembly of heparin and chitosan. Biomaterials 2005;26:6684-6692.

[61] Pastorino, L., Caneva Soumetz, F. and Ruggiero, C. Nanofunctionalisation for the treatment of peripheral nervous system injuries. Conf Proc IEEE Eng Med Biol Soc 2005;6:5854-5857.

[62] Gheith, M., Sinani, V., Wicksted, J., Matts, R. and Kotov, N. Single-Walled Carbon Nanotube Polyelectrolyte Multilayers and Freestanding Films as a Biocompatible Platform for Neuroprosthetic Implants. Adv. Mater. 2005;17:2663–2670.

[63] Vautier, D., et al. 3-D surface charges modulate protrusive and contractile contacts of chondrosarcoma cells. Cell Motil Cytoskeleton 2003;56:147-158.

[64] Muller, S., et al. VEGF-Functionalized Polyelectrolyte Multilayers as Proangiogenic Prosthetic Coatings. Adv. Funct. Mater. 2008;18:1767–1775.

[65] Etienne, O., et al. Antifungal coating by biofunctionalized polyelectrolyte multilayered films. Biomaterials 2005;26:6704-6712.

[66] Werner, S., et al. The effect of microstructured surfaces and laminin-derived peptide coatings on soft tissue interactions with titanium dental implants. Biomaterials 2009;30:2291-2301.

[67] Brunot, C., Grosgogeat, B., Picart, C., Lagneau, C., Jaffrezic-Renault, N. and Ponsonnet, L. Response of fibroblast activity and polyelectrolyte multilayer films coating titanium. Dent Mater 2008;24:1025-1035.

[68] Halthur, T. J., Claesson, P. M. and Elofsson, U. M. Immobilization of enamel matrix derivate protein onto polypeptide multilayers. Comparative in situ measurements using ellipsometry, quartz crystal microbalance with dissipation, and dual-polarization interferometry. Langmuir 2006;22:11065-11071.

[69] Cai, K., Hu, Y. and Jandt, K. D. Surface engineering of titanium thin films with silk fibroin via layer-by-layer technique and its effects on osteoblast growth behavior. J Biomed Mater Res A 2007;82:927-935.

[70] Hu, Y., Cai, K., Luo, Z. and Jandt, K. D. Layer-by-layer assembly of beta-estradiol loaded mesoporous silica nanoparticles on titanium substrates and its implication for bone homeostasis. Adv Mater 2010;22:4146-4150.

[71] Chua, P. H., Neoh, K. G., Kang, E. T. and Wang, W. Surface functionalization of titanium with hyaluronic acid/chitosan polyelectrolyte multilayers and RGD for promoting osteoblast functions and inhibiting bacterial adhesion. Biomaterials 2008;29:1412-1421.

[72] van den Beucken, J. J., et al. A. Multilayered DNA coatings: in vitro bioactivity studies and effects on osteoblast-like cell behavior. Acta Biomater 2007;3:587-596.

[73] Kommireddy, D. S., Sriram, S. M., Lvov, Y. M. and Mills, D. K. Stem cell attachment to layer-by-layer assembled TiO2 nanoparticle thin films. Biomaterials 2006;27:4296-4303.

[74] McAloney, R., Sinyor, M., Dudnik, V. and Goh, M. Atomic force microscopy studies of salt effects on polyelectrolyte multilayer film morphology. Langmuir 2001;17:6655-6663.

[75] Schlenoff, J., Dubas, S. and Farhat, T. Sprayed polyelectrolyte multilayers. Langmuir 2000;16: 9968-9969.

[76] Ai, H., Fang, M., Jones, S. A. and Lvov, Y. M. Electrostatic layer-by-layer nanoassembly on biological microtemplates: platelets. Biomacromolecules 2002;3:560-564.

[77] Grant, G., Koktysh, D., Yun, B., Matts, R. and Kotov, N. Layer-By-Layer assembly of collagen thin films: controlled thickness and biocompatibility. Biomedical Microdevices 2001;3:301-306.

[78] Ladhari, N., Hemmerle, J., Haikel, Y., Voegel, J., Schaaf, P. and Ball, V. Stability of embossed PEI-(PSS–PDADMAC)20 multilayer films versus storage time and versus a change in ionic strength. Applied Surface Science 2008;255 1988–1995.

[79] Yoo, D., Shiratori, S. and Rubner, M. Controlling bilayer composition and surface wettability of sequentially adsorbed multilayers of weak polyelectrolytes. Macromolecules 1998;31:4309–4318.

[80] Tjipto, E., Quinn, J. and Caruso, F. Layer-by-layer assembly of weak-strong copolymer polyelectrolytes: A route to morphological control of thin films. J Polym Sci Part A: Polym Chem 2007;45:4341–4351,.

[81] Shiratori, S. and Rubner, M. pH-Dependent thickness behavior of sequentially adsorbed layers of weak polyelectrolytes. Macromolecules 2000;33:4213-4219.

[82] Stein, G. S., Lian, J. B. and Owen, T. A. Relationship of cell growth to the regulation of tissue-specific gene expression during osteoblast differentiation. Faseb J 1990;4:3111-3123.

[83] Kartsogiannis, V. and Ng, K. W. Cell lines and primary cell cultures in the study of bone cell biology. Mol Cell Endocrinol 2004;228:79-102.

[84] Owen, T. A., et al. Progressive development of the rat osteoblast phenotype in vitro: reciprocal relationships in expression of genes associated with osteoblast proliferation and differentiation during formation of the bone extracellular matrix. J Cell Physiol 1990; 143:420-430.

[85] Enomoto, H., et al. Cbfa1 is a positive regulatory factor in chondrocyte maturation. J Biol Chem 2000;275:8695-8702.

[86] Palmer, L. C., Newcomb, C. J., Kaltz, S. R., Spoerke, E. D. and Stupp, S. I. Biomimetic systems for hydroxyapatite mineralization inspired by bone and enamel. Chem Rev 2008; 108:4754-4783.

[87] Lynch, M. P., Stein, J. L., Stein, G. S. and Lian, J. B. The influence of type I collagen on the development and maintenance of the osteoblast phenotype in primary and passaged rat calvarial osteoblasts: modification of expression of genes supporting cell growth, adhesion, and extracellular matrix mineralization. Exp Cell Res 1995;216:35-45.

[88] Lee, J. H., Rhie, J. W., Oh, D. Y. and Ahn, S. T. Osteogenic differentiation of human adipose tissue-derived stromal cells (hASCs) in a porous three-dimensional scaffold. Biochem Biophys Res Commun 2008;370:456-460.

[89] Beck, G. R., Jr., Zerler, B. and Moran, E. Phosphate is a specific signal for induction of osteopontin gene expression. Proc Natl Acad Sci U S A 2000;97:8352-8357.

[90] Chen, S., et al. Expression and processing of small integrin-binding ligand N-linked glycoproteins in mouse odontoblastic cells. Arch Oral Biol 2008;53:879-889.

[91] Hauschka, P. V., Lian, J. B., Cole, D. E. and Gundberg, C. M. Osteocalcin and matrix Gla protein: vitamin K-dependent proteins in bone. Physiol Rev 1989;69:990-1047.

[92] Qin, C., D'Souza, R. and Feng, J. Q. Dentin matrix protein 1 (DMP1): new and important roles for biomineralization and phosphate homeostasis. J Dent Res 2007;86:1134-1141.

[93] Tryoen-Toth, P., et al. Viability, adhesion, and bone phenotype of osteoblast-like cells on polyelectrolyte multilayer films. J Biomed Mater Res 2002;60:657-667.

[94] Elbert, D., Herbert, C. and Hubbell, J. Thin Polymer Layers Formed by Polyelectrolyte Multilayer Techniques on Biological Surfaces. Langmuir 1999;15:5355-5362.

[95] Kieswetter, K., Schwartz, Z., Dean, D. and Boyan, B. The role of implant surface characteristics in the healing of bone. Crit Rev Oral Biol Med 1996;7:329-345.

[96] Schwartz, Z. and Boyan, B. Underlying mechanisms at the bone-biomaterialinterface. J Cell Biochem 1994;56:340-347.

[97] Curtis, A. S. and Varde, M. Control of Cell Behavior: Topological Factors. J Natl Cancer Inst 1964;33:15-26.

[98] Rosenberg, M. D. Cell guidance by alterations in monomolecular films. Science 1963;139:411-412.

[99] Wojciak-Stothard, B., Madeja, Z., Korohoda, W., Curtis, A. and Wilkinson, C. Activation of macrophage-like cells by multiple grooved substrata. Topographical control of cell behaviour. Cell Biol Int 1995;19:485-490.

[100] Dalby, M., Riehle, M., Johnstone, H., Affrossman, S. and Curtis, A. Investigating the limits of filopodial sensing: A brief report using SEM to image the interaction between 10 nm

high nano-topography and fibroblast filopodia. Cell Biology International 2004;28:229-236.

[101] Mendonca, G., Mendonca, D. B., Aragao, F. J. and Cooper, L. F. Advancing dental implant surface technology--from micron- to nanotopography. Biomaterials 2008;29:3822-3835.

[102] Washburn, N. R., Yamada, K. M., Simon, C. G., Jr., Kennedy, S. B. and Amis, E. J. High-throughput investigation of osteoblast response to polymer crystallinity: influence of nanometer-scale roughness on proliferation. Biomaterials 2004;25:1215-1224.

[103] Webster, T. J., Ergun, C., Doremus, R. H., Siegel, R. W. and Bizios, R. Specific proteins mediate enhanced osteoblast adhesion on nanophase ceramics. J Biomed Mater Res 2000;51:475-483.

[104] Lim, J. Y., Hansen, J. C., Siedlecki, C. A., Runt, J. and Donahue, H. J. Human foetal osteoblastic cell response to polymer-demixed nanotopographic interfaces. J R Soc Interface 2005;2:97-108.

[105] Liu, H., Slamovich, E. B. and Webster, T. J. Increased osteoblast functions among nanophase titania/poly(lactide-co-glycolide) composites of the highest nanometer surface roughness. J Biomed Mater Res A 2006;78:798-807.

[106] Cai, K., Bossert, J. and Jandt, K. Does the nanometre scale topography of titanium influence protein adsorption and cell proliferation? Colloids Surf B Biointerfaces 2006; 49:136-144.

[107] Han, M., Sethuraman, A., Kane, R. and Belfort, G. Nanometer-scale roughness having little effect on the amount or structure of adsorbed protein. Langmuir 2003;19:9868–9872.

[108] Rechendorff, K., Hovgaard, M., Foss, M., Zhdanov, V. and Besenbacher, F. Enhancement of protein adsorption induced by surface roughness. Langmuir 2006;22:10885–10888.

[109] Riedel, M., Muller, B. and Wintermantel, E. Protein adsorption and monocyte activation on germanium nanopyramids. Biomaterials 2001;22:2307-2316.

[110] Scopelliti, P. E., et al. The effect of surface nanometre-scale morphology on protein adsorption. PLoS One 2010; **5**:e11862.

[111] Vogler, E. A. Structure and reactivity of water at biomaterial surfaces. Adv Colloid Interface Sci 1998;74:69-117.

[112] Faucheux, N., Schweiss, R., Lutzow, K., Werner, C. and Groth, T. Self-assembled monolayers with different terminating groups as model substrates for cell adhesion studies. Biomaterials 2004;25:2721-2730.

[113] Webb, K., Hlady, V. and Tresco, P. A. Relative importance of surface wettability and charged functional groups on NIH 3T3 fibroblast attachment, spreading, and cytoskeletal organization. J Biomed Mater Res 1998;41:422-430.

[114] Ma, Z., Mao, Z. and Gao, C. Surface modification and property analysis of biomedical polymers used for tissue engineering. Colloids Surf B Biointerfaces 2007;60:137-157.

[115] Tangpasuthadol, V., Pongchaisirikul, N. and Hoven, V. P. Surface modification of chitosan films. Effects of hydrophobicity on protein adsorption. Carbohydr Res 2003;338:937-942.

[116] Tilton, R., Robertson, C. and Gast, A. Manipulation of hydrophobic interactions in protein adsorption. Langmuir 1991;7:2710-2718.

[117] Wei, J., et al. Influence of surface wettability on competitive protein adsorption and initial attachment of osteoblasts. Biomed Mater 2009;4:045002.

[118] Wei, J., et al. Adhesion of mouse fibroblasts on hexamethyldisiloxane surfaces with wide range of wettability. J Biomed Mater Res B Appl Biomater 2007;81:66-75.

[119] Yoshinari, M., Wei, J., Matsuzaka, K. and Takashi Inoue, T. Effect of cold plasma-surface modification on surface wettability and initial cell attachment. World Academy of Science, Engineering and Technology 2009;58:171-175.

[120] Boura, C., et al. Endothelial cells grown on thin polyelectrolyte mutlilayered films: an evaluation of a new versatile surface modification. Biomaterials 2003;24:3521-3530.

[121] Wittmer, C. R., Phelps, J. A., Lepus, C. M., Saltzman, W. M., Harding, M. J. and Van Tassel, P. R. Multilayer nanofilms as substrates for hepatocellular applications. Biomaterials 2008;29:4082-4090.

[122] Osathanon, T., Bespinyowong, K., Arksornnukit, M., Takahashi, H. and Pavasant, P. Ti-6Al-7Nb promotes cell spreading and fibronectin and osteopontin synthesis in osteoblast-like cells. J Mater Sci Mater Med 2006;17:619-625.

[123] Park, J. W., Kim, H. K., Kim, Y. J., Jang, J. H., Song, H. and Hanawa, T. Osteoblast response and osseointegration of a Ti-6Al-4V alloy implant incorporating strontium. Acta Biomater 2010;6:2843-2851.

[124] Keselowsky, B. G., Collard, D. M. and Garcia, A. J. Integrin binding specificity regulates biomaterial surface chemistry effects on cell differentiation. Proc Natl Acad Sci U S A 2005;102:5953-5957.

[125] Keselowsky, B. G., Collard, D. M. and Garcia, A. J. Surface chemistry modulates fibronectin conformation and directs integrin binding and specificity to control cell adhesion. J Biomed Mater Res A 2003;66:247-259.

[126] Keselowsky, B. G., Collard, D. M. and Garcia, A. J. Surface chemistry modulates focal adhesion composition and signaling through changes in integrin binding. Biomaterials 2004;25:5947-5954.

[127] Pompe, T., et al. Maleic anhydride copolymers--a versatile platform for molecular biosurface engineering. Biomacromolecules 2003;4:1072-1079.

[128] Renner, L., Pompe, T., Salchert, K. and Werner, C. Dynamic alterations of fibronectin layers on copolymer substrates with graded physicochemical characteristics. Langmuir 2004;20:2928-2933.

[129] Moursi, A. M., et al. Fibronectin regulates calvarial osteoblast differentiation. J Cell Sci 1996;109:1369-1380.

[130] Li, J., et al. Impact of vitronectin concentration and surface properties on the stable propagation of human embryonic stem cells. Biointerphases 2010;5:FA132-142.

[131] Salasznyk, R. M., Williams, W. A., Boskey, A., Batorsky, A. and Plopper, G. E. Adhesion to Vitronectin and Collagen I Promotes Osteogenic Differentiation of Human Mesenchymal Stem Cells. J Biomed Biotechnol 2004;2004:24-34.

[132] Webster, T. J., Schadler, L. S., Siegel, R. W. and Bizios, R. Mechanisms of enhanced osteoblast adhesion on nanophase alumina involve vitronectin. Tissue Eng 2001;7:291-301.

[133] Fu, B., Yuan, J., Qian, W., Shen, Q., Sun, X. and Hannig, M. Evidence of chemisorption of maleic acid to enamel and hydroxyapatite. Eur J Oral Sci 2004;112:362-367.

[134] Yoshida, Y., et al. Adhesion to and decalcification of hydroxyapatite by carboxylic acids. *J* Dent Res 2001;80:1565-1569.

[135] Yoshioka, M., et al. Adhesion/decalcification mechanisms of acid interactions with human hard tissues. J Biomed Mater Res 2002;59:56-62.

[136] Coombes, A. G., Rizzi, S. C., Williamson, M., Barralet, J. E., Downes, S. and Wallace, W. A. Precipitation casting of polycaprolactone for applications in tissue engineering and drug delivery. Biomaterials 2004;25:315-325.

[137] Lebourg, M., Sabater Serra, R., Mas Estelles, J., Hernandez Sanchez, F., Gomez Ribelles, J. L. and Suay Anton, J. Biodegradable polycaprolactone scaffold with controlled porosity obtained by modified particle-leaching technique. J Mater Sci Mater Med 2008;19:2047-2053.

[138] Shor, L., Guceri, S., Wen, X., Gandhi, M. and Sun, W. Fabrication of three-dimensional polycaprolactone/hydroxyapatite tissue scaffolds and osteoblast-scaffold interactions in vitro. Biomaterials 2007;28:5291-5297.

[139] Ciapetti, G., et al. Osteoblast growth and function in porous poly epsilon -caprolactone matrices for bone repair: a preliminary study. Biomaterials 2003;24:3815-3824.

[140] Pham, Q. P., Sharma, U. and Mikos, A. G. Electrospun poly(epsilon-caprolactone) microfiber and multilayer nanofiber/microfiber scaffolds: characterization of scaffolds and measurement of cellular infiltration. Biomacromolecules 2006;7:2796-2805.

[141] Yoshimoto, H., Shin, Y. M., Terai, H. and Vacanti, J. P. A biodegradable nanofiber scaffold by electrospinning and its potential for bone tissue engineering. Biomaterials 2003;24:2077-2082.

[142] Ruckh, T. T., Kumar, K., Kipper, M. J. and Popat, K. C. Osteogenic differentiation of bone marrow stromal cells on poly(epsilon-caprolactone) nanofiber scaffolds. Acta Biomater 2010;6:2949-2959.

[143] Bhattacharya, M., et al. Bone formation on carbon nanotube composite. J Biomed Mater Res A 2011;96:75-82.

[144] Gunatillake, P. A. and Adhikari, R. Biodegradable synthetic polymers for tissue engineering. Eur Cell Mater 2003;5:1-16.

APPENDICES

APPENDIX A

APPENDIX A

Selection of polyelectrolyte to be used in the study

For chosen polyelectrolyte in this study, many polyelectrolytes as PDADMAC, PSS, PSS-co-MA, PAA, GEL and SiO_2 were used to fabricate PEM film (Chemical structures of the each polyelectrolytes used are showed in Figure A1). Then each PEM coated surface was examined in term of cell viability, cell morphology and ALP activity.

Fabrication of Polyelectrolyte Multilayer films on glass coverslip

For substrate preparation, 12 mm round glass coverslips were pretreated with freshly prepared piranha solution (30:70 vol.% mixture of 40 wt.% hydrogen peroxide and 98 wt.% sulfuric acid), then immersed in 1% ammonia for 10 minutes. The pre-treated glass coverslips were thoroughly rinsed three times with distilled water and dried.

Polyelectrolyte multilayer films were constructed from 9 layers of PDADMAC and PSS with stop layer of a one of negative charge polyelectrolyte (PSS-co-MA, PSS, PAA, GEl or SiO_2) onto glass cover slips. Briefly, the pre-treated glass cover slips were alternatively immersed in 10mM PDADMAC containing 0.1M NaCl or 10mM PSS containing 0.1M NaCl for 5 min with intermediate triple rinses using distilled water until the ninth layer. For the final layer, the glass cover slips were immersed in 10mM of PSS-co-MA, PSS, PAA or GEL containing 0.1M NaCl or SiO_2 0.1 wt% at pH10 for 30 min , then rinsed three times with distilled water (pH 10) and dried (The fabrication method diagram is showed in Figure A2).

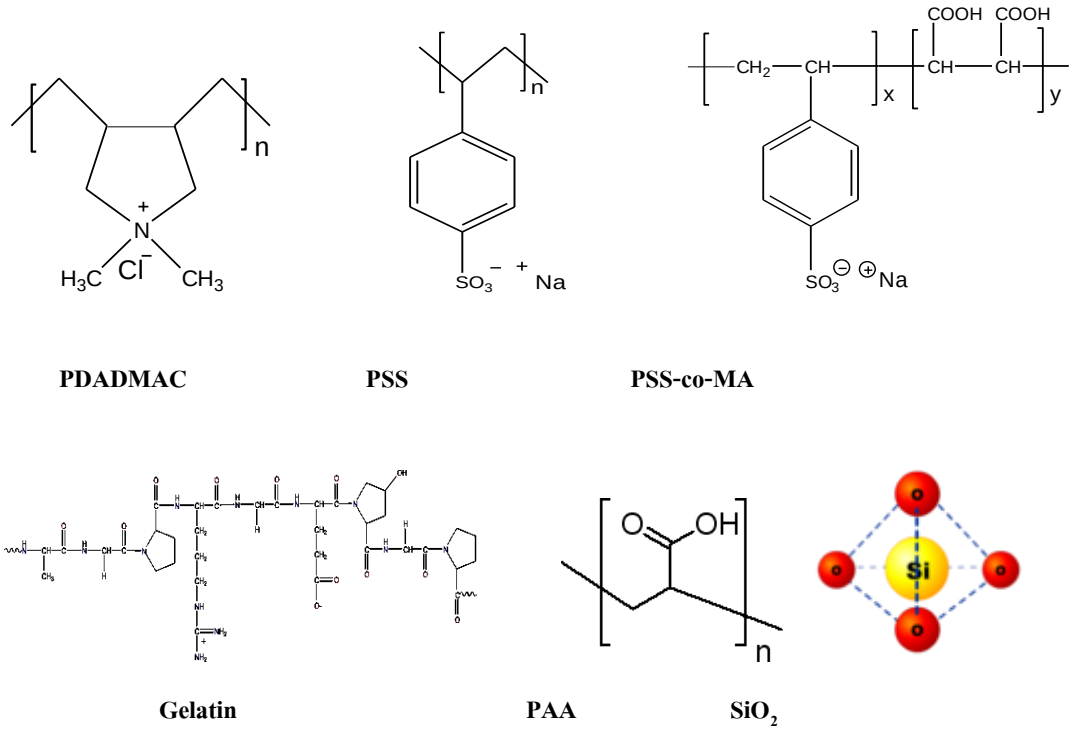

FigureA1 Chemical structure of polyelectrolytes used in this research

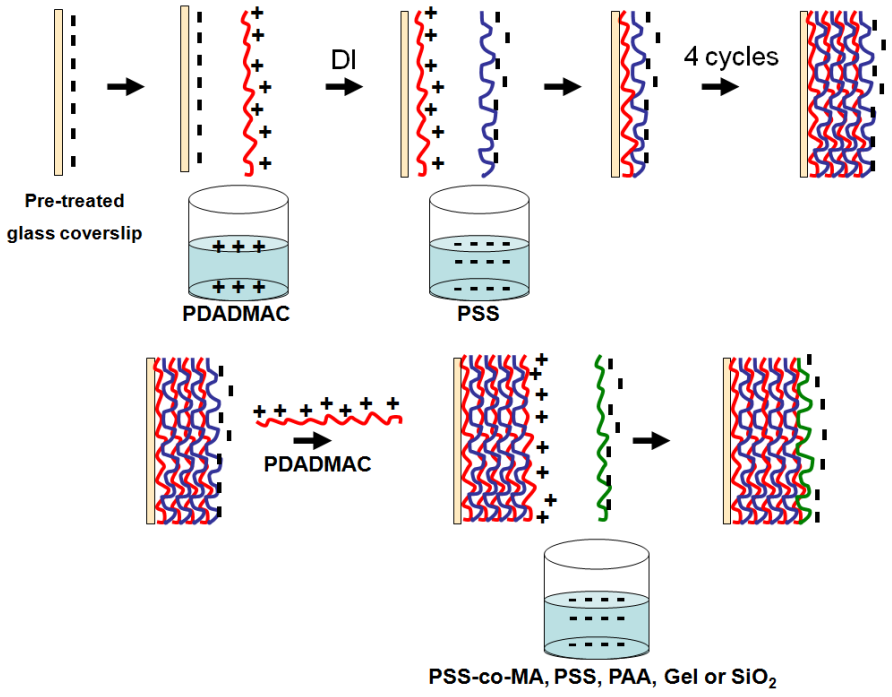

Figure A2 Fabrication of polyelectrolyte multilayer films (PEMs)

Cell culture

The specimens were put into 24 well culture plates and were sterilized by washing with 70% ethanol for 10 min, two times rinsing with PBS followed by culture medium and air dried.

MC3T3-E1 cells (ATCC CRL-2593), the immortalized cell line derived from mouse calvarium tissue, at 18 to 22 passages were seeded on 12 mm in a diameter glass coverslip at density of 40,000 cells per well in minimum essential medium (HyQ® MEM/EBSS, Hycone, Logan, Ultah, USA) supplemented with 10% fetal bovine serum (FBS, ICP biologicals, Henderson, Auckland, New Zeland), 2 mM L-glutamine, 100 unit ml^{-1} penicillin, 100 μg ml^{-1} streptomycin and 0.25 μg ml^{-1} amphotericin B (Gibco,Grand Island, New York, USA) under standard condition (at 37°C in 100% humidity and 5% CO_2). The medium was changed every other day.

MTT assay

Cell viability was determined by MTT assay. An MTT (USB Corporation, Cleveland, OH, USA) solution of 5 mg ml^{-1} was prepared by dissolving MTT in 10% serum culture medium without phenol red. After 4 and 16 hours of culture, the specimens were washed with PBS. MTT solution was added to each well and incubated for 30 min at 37°C. At the end of assay, the blue formazan reaction product was dissolved by 1 ml mixing of glycine buffer (pH = 10) (125 μl/well) and DMSO (Sigma-Aldrich, Seelze,Germany) (900 μl/well). The optical density of this colored solution in each well was measured using Thermospectronic Genesis10 UV-vis spectrophotometer at a wavelength of 570 nm. The data represented the number of viable cells.

Before stating MTT assay at 16 hours of incubation, cell morphology was also analyzed by using light microscope.

The result showed increase cell numbers in correlation with culture time on all surface, although the number of cell was slightly less on PAA coated and SiO_2 coated PEM than the others (Figure A3).

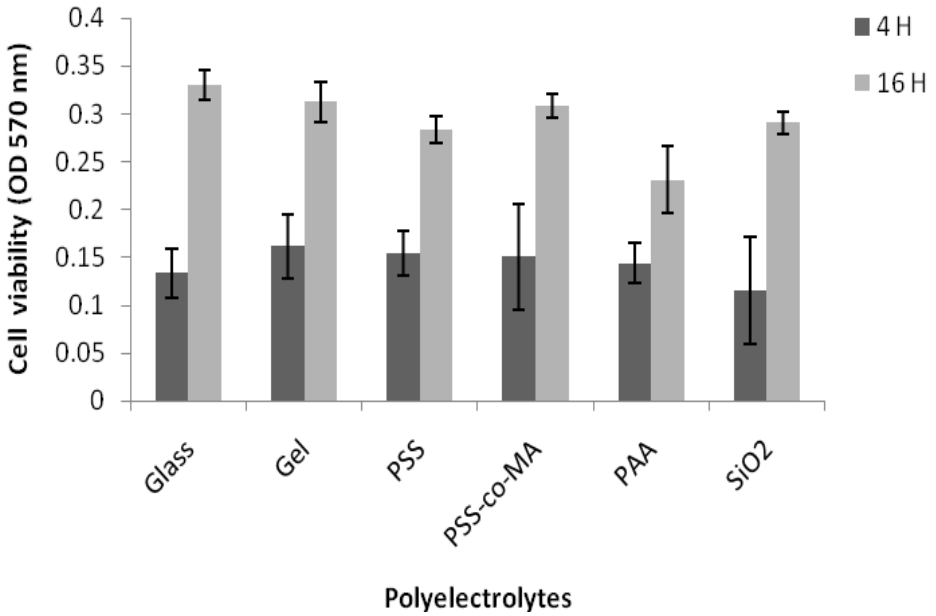

Figure A3 Cell viability of MC3T3-E1 cells cultured on glass cover slips with each PEM coated surface estimated by the MTT assay after 4 and 16 hours incubation. Data showed show as the mean ± SD (n=3).

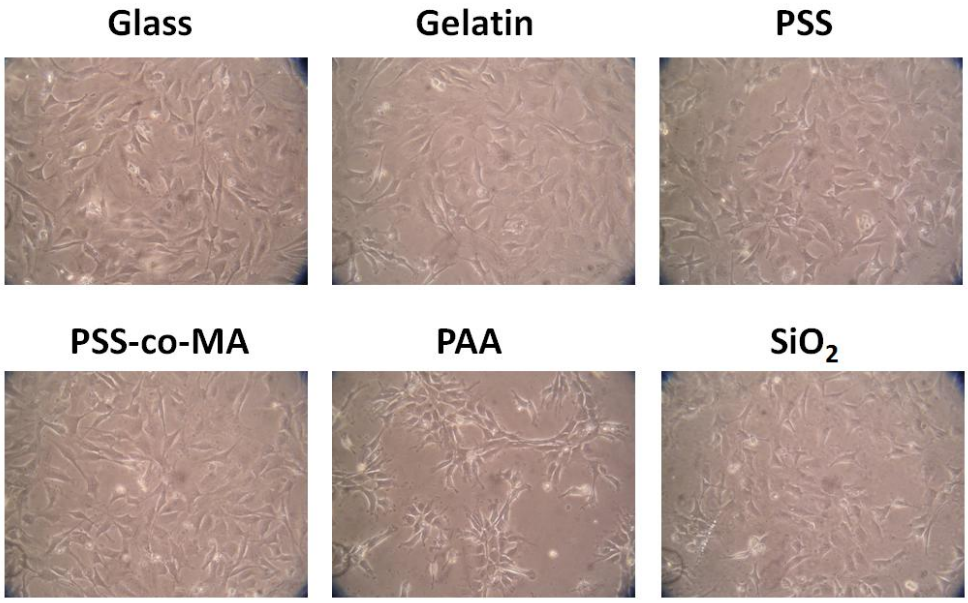

Figure A4 The morphology of MC3T3-E1 cells on the different outermost layers after 16 hours by light microscope (the magnification is 40x).

Cell morphology and cell number were also examined using light microscope. Results showed similar cell morphology as well as cell numbers in most groups, except PAA coated surface group. Cell culture on PAA coated PEM films were smaller both in size and number, and not constantly distributed (Figure A4).

From cell viability and cell morphology results analysis, PAA and SiO_2 PEM coated surface were excluded from experiment. Next, ALP activity was used to examine the remaining PEM coated surface.

Alkaline phosphatase activity (ALP activity)

MC3T3-E1 were cultured for 3, 5 and 7 days to observe ALP activity. Each specimen was rinsed with PBS after removal of the culture medium. Alkaline lysis buffer (10 mM Tris-HCl, 2 mM $MgCl_2$, 0.1% Triton-X100, pH 10) was added, removed the cell with a cell scraper and then frozen up at -20 ^{o} c. After freezing, an aqueous solution prepare from p-nitrophenyl phosphate (PNPP substrate; Zymed, Invitrogen ,Carlsbad ,CA ,USA) and 0.1M aminopropanol in 2mM $MgCl_2$ was added into the substrates. After incubated at 37 ºC for 15 min, the above mixture was added with 0.1 M NaOH to stop the reaction and the absorbance at 410 nm was measured using UV-vis spectrophotometer. The amount of ALP was then calculated against a standard curve.

To determine the ALP activity, the amount of ALP must be normalized by the amount of total proteins synthesized. In the protein assay, the cell lysis was mixed with a bicinchoninic acid (BCA^{TM} Protein assay, Thermo Scientific, Rockford, IL, USA) solution, and incubated at 37 °C for 15 min. The absorbance of the medium solution was then measured at 562 nm by the UV-vis spectrophotometer, and the amount of the total proteins was calculated against a standard curve.

From ALP activity, MC3T3-E1 cultured on PSS-co-MA coated surface showed highest relative ALP activity when compared to others (Figure A5). Thus, PSS-co-MA coated PEM surface were chosen to be use in the latter experiments.

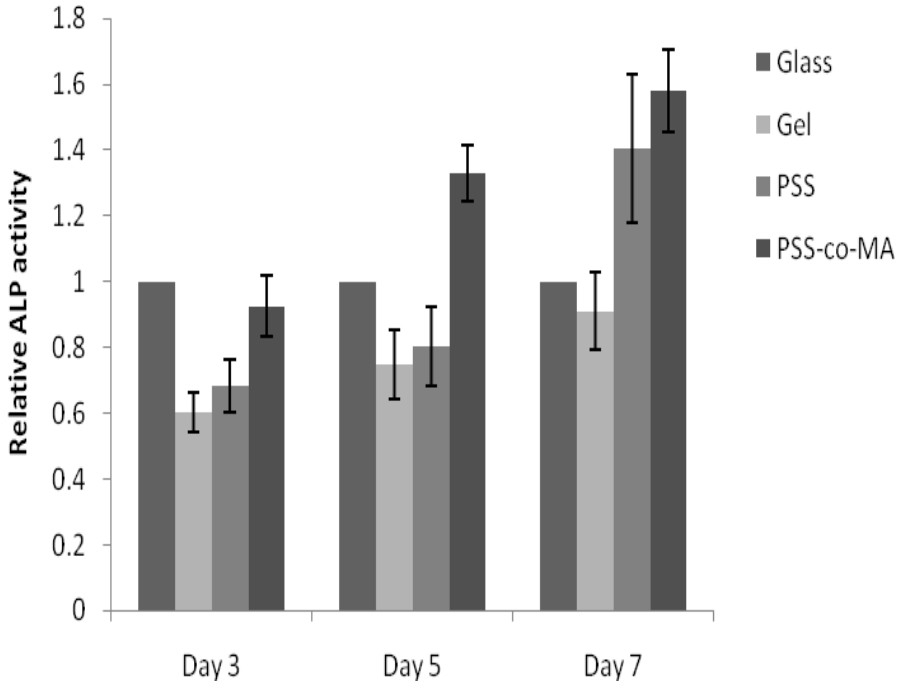

Figure A5 Alkaline phosphatase activity after 3, 5 and 7 days of MC3T3-E1 cultured on glass cover slips, GEL, PSS, and PSS-co-MA coated surfaces as well as control glass cover slips.

APPENDIX B

APPENDIX B

Characterization of osteoblastic cells

In Part II study, cells were obtained from bone chips, which were harvested form alveoloplasty, torus palatinus or torus mandibularis removal for prosthodontic reasons or residual iliac bone in procedure of cleft palate reconstruction. All patients gave informed consent and the protocol has been approved by the Ethical Committee, Faculty of Dentistry, Chulalongkorn University. Bone chip was washed extensively in sterile phosphate buffer saline (PBS, pH 7.4) and cut into pieces of approximately 2x2 mm^2. The bone pieces were digested with 0.25% trypsin-EDTA to remove residual adipose and hematopoietic tissue. The bone pieces were harvested in 35 mm × 10 mm culture dish (Coring, NY, USA) and grown in DMEM (GIBBCO, Grand Island, NY, USA), containing 15% FBS (ICP biologicals, Henderson, Auckland, New Zealand), 2mM L-glutamine, 100 units/ml penicillin, 100 µg/ml streptomycin, and 5 µg/ml amphotericin B (Gibco, Grand Island, New York, USA) in a humidified incubator at 37°C with 5% (v/v) CO_2. Cells were subcultured at a 1:3 ratio after cells become confluent. To confirm the characteristic of osteoblast cells, the expression of osteoblastic gene including Col I, ALP, OPN, BSP, OC and DMP1, ALP staining and *in vitro* calcification were examined.

Reverse-transcription polymerase chain reaction (RT-PCR)

Expressions of osteogenic marker gene were assessed using RT-PCR. After 5 days of cells cultured on 12 wells plate, the RNA was extracted with 1 ml of TriPure Isolation Reagent (Roche Diagnostics, Indianapolis, IN, USA) according to the manufacturer protocol. RNA yields were evaluated with a NanoDrop 2000 UV-Vis spectrophotometer (Thermo Fisher Scientific Inc., Wilmington, DE, USA) based on the absorbance ratio at 260/280 nm. First strand DNA was reverse transcribed from 1 µg of total RNA using reverse transcriptase enzyme (ImProm-II Reserve Transcription System, Promega, Madison, WI, USA).

The PCR was performed with Tag DNA Polymerase (Tag DNA Polymerase, Recombinant, Invitrogen, Sao Paulo Brazil) using PCR oligonucleotide sequences of the primers as showed in Table B1. The primer was designed from the sequence in GenBank database. The

PCR products were analyzed by separation on 1.8% agarose (Usb, Cleveland, OH, USA) gel using electrophoresis (Power Pac Junior, Bio-Rad, Hercules, CA, USA) and visualized with ethidium bromide solution (EtBr; Bio-Rad, Hercules, CA, USA) staining. The stained bands were photographed under UV light, and the intensity was quantified with Scion Image Software (Scion Corporation, Walkersville, MD, USA).

Table B1 Oligonucleotide primers for PCR amplication

Target cDNA	Primer sequence (5′-3′)	Product size (bp)	GenBank database
Col I	sense 5' CTG GCA AAG AAG GCG GCA AA 3'	500	MN_000088.3
	antisense 5' CTC ACC ACG ATC ACC ACT CT 3'		
ALP	sense5'CGA GAT ACA AGC ACT CCC ACT TC3'	120	NM_000478.3
	antisense5'CTG TTC AGC TCG TAC TGC ATG TC3'		
OPN	sense 5′CCA ACG GCC GAG GTG ATA3'	320	MN_001040060.1
	antisense 5′CAG GCT GGC TTT GGA ACT TG3'		
BSP	sense 5'GAT GAA GAC TCT GAG GCT GAG A3'	517	NM_004967.3
	antisense 5'TTG ACG CCC GTG TAT TCG TA 3'		
OC	sense 5'ATG AGA GCC CTC ACA CTC CTC 3'	293	NM_199173.3
	antisense 5'GCC GTA GAA GCG CCG ATA GGC 3'		
DMP1	sense 5' CAG GAG CAC AGG AAA AGG AG 3'	213	NM 004407.3
	antisense 5' CTG GTG GTA TCT TGG GCA CT 3'		
GAPDH	sense 5′TGA AGG TCG GAG TCA ACG GAT 3′	395	MN_002046.3
	antisense 5′TCA CAC CCA TGA CGA ACA TGG 3′		

Alkaline phosphatase staining

For ALP staining, cells were seed on 24-well TCP for 7 days. Media was changed every other day. After culture for 7 days, cells were rinsed with PBS, followed by fixing and staining with ALP staining kit (TRACP & ALP double-stain kit; TAKARA BIO INC., Shiga, Japan) according to manufacturer's instruction.

Alizarin red-S staining

In vitro calcium deposition was quantified by Alizarin red-S staining (Alizarin Red S –certified, Sigma, St. Louis, MO, USA). Cells were cultured overnight on 12 well plate until confluent. The media was changed to osteogenic medium medium (containing 5 mM β-glycerophosphate (Sigma, St. Louis, MO, USA), 50 μg ml^{-1} l-ascorbic acid sodium salt (Sigma, St. Louis, MO, USA) and dexamethazole (Sigma, St. Louis, MO, USA)) for culture for 10, 14 and 21 days. The cells were rinsed with PBS and fixed with cold methanol for 10 minutes, washed with de-ionized water, followed by staining with 1% Alizarin Red in 1:100 (v/v) ammonium hydroxide/water (pH 4.2) into each well for 3 minutes.

It has been reported that of Col I, ALP, OPN, BSP OC and DMP1 highly expressed in stage of osteoblast differentiation and could be used as the specific markers at each stage of differentiation. Therefore, these genes were chosen to confirm the characteristic of osteoblast cells. Results from RT-PCR showed the expression of Col I, ALP, OPN, BSP OC and DMP1 in cells cultured on TCP at day 5 (Figure B1A). Moreover, ALP staining at culture day 7 revealed the ALP positive area on TCP (Figure B1B). In addition, bone nodule formation, which is considered a functional *in vitro* endpoint reflect advanced osteoblast differentiation, was determined by Alizarin res-S staining. Macroscopically observation revealed reddish deposition in cultures on TCP and the color increased in according the culture period (Figure B1C).

Results from RT-PCR analysis, ALP staining and *in vitro* calcification indicated that cells explanted from bone chips, which were obtained from alveoloplasty, torus palatinus or torus mandibularis removal for prosthodontic reasons or residual iliac bone in procedure of cleft palate reconstruction, revealed the characteristic of osteoblast cells and can be used in this study.

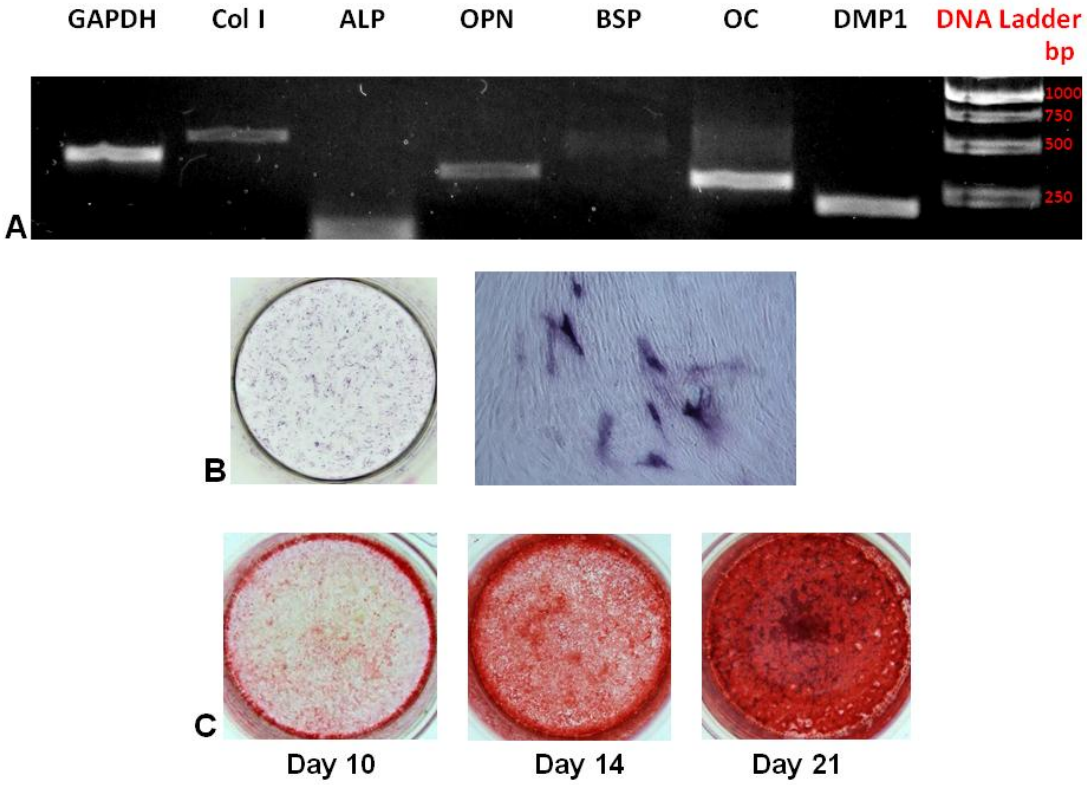

Figure B1 Osteoblastic cell characterization

The expression of GAPDH, Col I, ALP, OPN, BSP OC and DMP1 were examined by RT-PCR at day 5 (A). Alkaline phosphatase (ALP) activity was measured by the ALP staining (B). In vitro calcification was determined by Alizarin red-S staining at day 10, 14 and 21 (C).

VITA

Miss Thidarat Angwarawong was born in Khon Kaen, Thailand on December 15, 1978. In 2001, she was conferred the Degree of Doctor of Dental Surgery (D.S.S.), which first class honors from Faculty of Dentistry, Mahidol University . After graduation, she worked as a lecturer in Phosthodontics Department, Faculty of Dentistry, Khonkaen University. In 2004, she started her post-graduated study for the Master of Science in Prosthodontics Program at the Faculty of Dentistry, Chulalongkorn University. After finished her Master of Science Program (M.Sc.), she started her study for the Doctor of Philosophy in Oral Biology Ph.D Program at the Faculty of Dentistry, Chulalongkorn University in 2007. The research component of this degree was performed at the Research Unit of Mineralized Tissue, Faculty of Dentistry, Chulalongkorn University. At present, she works at the Department of Prosthodontics, Faculty of Dentistry, Khonkaen University.